Volume 8, Number 2, 2008 ISSN 1562-8353

NONLINEAR DYNAMICS AND SYSTEMS THEORY
An International Journal of Research and Surveys

Volume 8 Number 2 2008

CONTENTS

 ISSN 1562-8353 Printed in Ukraine
To receive contents and abstracts by e-mail, visit our Website at: **http://www.e-ndst.kiev.ua**

NONLINEAR DYNAMICS & SYSTEMS THEORY

Volume 8, No. 2, 2008

Nonlinear Dynamics and Systems Theory

An International Journal of Research and Surveys

InforMath Publishing Group
http://www.sciencearea.com.ua

Nonlinear Dynamics and Systems Theory

An International Journal of Research and Surveys

NONLINEAR DYNAMICS AND SYSTEMS THEORY

An International Journal of Research and Surveys

INSTRUCTIONS FOR CONTRIBUTORS

(1) General. The Journal will publish original carefully refereed papers, brief notes and reviews on a wide range of nonlinear dynamics and systems theory problems. Contributions will be considered for publication in ND&ST if they have not been published previously. Before preparing your submission, it is essential that you consult our style guide; please visit our website: http://www.e-ndst.kiev.ua

(2) Manuscript and Correspondence. Contributions are welcome from all countries and should be written in English. Two copies of the manuscript, double spaced one column format, and the electronic version by AMSTEX, TEX or LATEX program (on diskette) should be sent directly to

Professor A.A. Martynyuk
Institute of Mechanics,
Nesterov str.3, 03057, MSP 680
Kiev-57, Ukraine
(e-mail: anmart@stability.kiev.ua
e-mail: amartynyuk@voliacable.com)

or to one of the Editors or to a member of the Editorial Board.

The title of the article must include: author(s) name, name of institution, department, address, FAX, and e-mail; an Abstract of 50-100 words should not include any formulas and citations; key words, and AMS subject classifications number(s). The size for regular paper should be 10-14 pages, survey (up to 24 pages), short papers, letter to the editor and book reviews (2-3 pages).

(3) Tables, Graphs and Illustrations. All figures must be suitable for reproduction without being retouched or redrawn and must include a title. Line drawings should include all relevant details and should be drawn in black ink on plain white drawing paper. In addition to a hard copy of the artwork, it is necessary to attach a PC diskette with files of the artwork (preferably in PCX format).

(4) References. Each entry must be cited in the text by author(s) and number or by number alone. All references should be listed in their alphabetic order. Use please the following style:

Journal: [1] Poincaré, H. Title of the article. *Title of the Journal* **Vol.1**(No.1) (year) pages. [Language].
Book: [2] Liapunov, A.M. *Title of the book.* Name of the Publishers, Town, year.
Proceeding: [3] Bellman, R. Title of the article. In: *Title of the book.* (Eds.). Name of the Publishers, Town, year, pages. [Language].

(5) Proofs and Reprints. Proofs sent to authors should be returned to the Editor with corrections within three days after receipt. Acceptance of the paper entitles the author to 10 free reprints.

(6) Editorial Policy. Every paper is reviewed by the regional editor, and/or a referee, and it may be returned for revision or rejected if considered unsuitable for publication.

(7) Copyright Assignment. When a paper is accepted for publication, author(s) will be requested to sign a form assigning copyright to InforMath Publishing Group. Failure to do it promptly may delay the publication.

NONLINEAR DYNAMICS AND SYSTEMS THEORY
An International Journal of Research and Surveys
Published by InforMath Publishing Group since 2001

Volume 8 Number 2 2008

CONTENTS

Founded by A.A. Martynyuk in 2001.
Registered in Ukraine Number: КВ № 5267 / 04.07.2001.

NONLINEAR DYNAMICS AND SYSTEMS THEORY

An International Journal of Research and Surveys

Nonlinear Dynamics and Systems Theory (ISSN 1562-8353 (Print), ISSN 1813-7385 (Online)) is an international journal published under the auspices of the S.P.Timoshenko Institute of Mechanics of National Academy of Sciences of Ukraine and the Laboratory for Industrial and Applied Mathematics (LIAM) at York University (Toronto, Canada). It is aimed at publishing high quality original scientific papers and surveys in area of nonlinear dynamics and systems theory and technical reports on solving practical problems. The scope of the journal is very broad covering:

SCOPE OF THE JOURNAL

Analysis of uncertain systems • Bifurcations and instability in dynamical behaviors • Celestial mechanics, variable mass processes, rockets • Control of chaotic systems • Controllability, observability, and structural properties • Deterministic and random vibrations • Differential games • Dynamical systems on manifolds • Dynamics of systems of particles • Hamilton and Lagrange equations • Hysteresis • Identification and adaptive control of stochastic systems • Modeling of real phenomena by ODE, FDE and PDE • Nonlinear boundary problems • Nonlinear control systems, guided systems • Nonlinear dynamics in biological systems • Nonlinear fluid dynamics • Nonlinear oscillations and waves • Nonlinear stability in continuum mechanics • Non-smooth dynamical systems with impacts or discontinuities • Numerical methods and simulation • Optimal control and applications • Qualitative analysis of systems with aftereffect • Robustness, sensitivity and disturbance rejection • Soft computing: artificial intelligence, neural networks, fuzzy logic, genetic algorithms, etc. • Stability of discrete systems • Stability of impulsive systems • Stability of large-scale power systems • Stability of linear and nonlinear control systems • Stochastic approximation and optimization • Symmetries and conservation laws

PUBLICATION AND SUBSCRIPTION INFORMATION

The **Nonlinear Dynamics and Systems Theory** is published four times per year in 2008. Base list subscription price per volume: US$180.00. This price is available only to individuals whose library subscribes to the journal OR who warrant that the Journal is for their own use and provide a home address for mailing. Separate rates apply to academic and corporate/government institutions. Our charge includes postage, packing, handling and airmail delivery of all issues. Mail order and inquires to: Department of Processes Stability, S.P.Timoshenko Institute of Mechanics NAS of Ukraine, Nesterov str., 3, 03057, Kiev-57, MSP 680, Ukraine, Tel: ++38-044-456-6140, Fax: ++38-044-456-0319, E-mail: amartynyuk@voliacable.com, http://www.sciencearea.com.ua; http://www.e-ndst.kiev.ua

ABSTRACTING AND INDEXING SERVICES

EBSCO Database, PASCAL Database, SCOPUS Database, Swets Information Services, Mathematical Reviews/ MathSciNet, Zentralblatt MATH/Mathematics Abstracts.

Nonlinear Dynamics and Systems Theory, 8 (2) (2008) 109–122

Conditions of Ultimate Boundedness of Solutions for a Class of Nonlinear Systems

A.Yu. Aleksandrov * and A.V. Platonov

Saint Petersburg State University,
198504, Universitetskij ave., 35, Petrodvorets, St. Petersburg, Russia

Received: May 12, 2007; Revised: March 13, 2008

Abstract: A class of nonlinear differential equations systems is considered. An approach for the construction of Lyapunov's functions for these systems is suggested. By the use of functions constructed the conditions of ultimate boundedness of solutions for systems investigated are obtained.

Keywords: *Nonlinear systems; Lyapunov's functions; ultimate boundedness; large scale systems.*

Mathematics Subject Classification (2000): 34D20, 93D20, 93D30.

1 Introduction

In a variety of control systems design problems it is often required not only to stabilize given programmed motions but to ensure also boundedness for every solution of system investigated. Of great practical interest is the case when all the solutions enter a neighborhood of the origin and remain within it thereafter. Generally the time period needed for the solution to enter this neighborhood depends on the initial values of the solution. In this case solutions are called ultimately bounded [14].

The main approach for finding the conditions of boundedness of solutions for nonlinear systems is the Lyapunov direct method. Using this method, numerous results on various types of boundedness are obtained [6, 11, 12, 14, 16]. However, there are still no general constructive approaches for the construction of Lyapunov's functions.

In the present paper, a certain class of differential equations systems is considered. An approach for the construction of Lyapunov's functions for these systems is suggested. The conditions for the existence of Lyapunov's functions in the given form, satisfying the assumptions of the Yoshizawa ultimate boundedness theorem [14] are investigated. The results obtained are used for the analysis of the asymptotic behavior of solutions of essentially nonlinear complex systems.

* Corresponding author: alex@vrm.apmath.spbu.ru

2 Statement of the Problem

Consider the system of differential equations

$$\dot{x}_s = a_s f_s(x_s) + \sum_{j=1}^{k_s} b_{sj} f_1^{\alpha_{s1}^{(j)}}(x_1) \dots f_n^{\alpha_{sn}^{(j)}}(x_n), \quad s = 1, \dots, n. \tag{2.1}$$

Here a_s and b_{sj} are constant coefficients, $\alpha_{si}^{(j)}$ are nonnegative rationals with odd denominators, functions $f_s(x_s)$ are defined and continuous for $x_s \in (-\infty, +\infty)$ and possess the following properties: $x_s f_s(x_s) > 0$ for $x_s \neq 0$, $f_s(x_s) \to -\infty$ as $x_s \to -\infty$, $f_s(x_s) \to +\infty$ as $x_s \to +\infty$.

System (2.1) is a generalization of this one

$$\dot{x}_s = \sum_{j=1}^{n} b_{sj} f_j(x_j), \quad s = 1, \dots, n,$$

which is widely used in automatic control systems design [3, 7, 9].

In this paper we shall assume that coefficients a_s and b_{sj} in (2.1) satisfy the conditions

$$a_s < 0, \quad b_{sj} > 0, \quad j = 1, \dots, k_s, \quad s = 1, \dots, n. \tag{2.2}$$

For instance, inequalities (2.2) are valid if (2.1) is obtained as comparison system for a complex system [4, 13].

Consider, at first, the case where

$$\sum_{i=1}^{n} \alpha_{si}^{(j)} > 0, \quad j = 1, \dots, k_s, \quad s = 1, \dots, n. \tag{2.3}$$

Then system (2.1) has the zero solution.

Definition 2.1 [2] System (2.1) is called absolutely stable if the zero solution of this system is asymptotically stable for any admissible functions $f_1(x_1), \dots, f_n(x_n)$.

The criterion of absolute stability for (2.1) was established in [2].

Definition 2.2 [2] System (2.1) satisfies the Martynyuk–Obolenskij condition [8] (MO-condition) if for any $\delta > 0$ there exists solution $\tilde{\theta}_1, \dots, \tilde{\theta}_n$ of the system

$$a_s \theta_s + \sum_{j=1}^{k_s} b_{sj} \theta_1^{\alpha_{s1}^{(j)}} \dots \theta_n^{\alpha_{sn}^{(j)}} < 0, \quad s = 1, \dots, n, \tag{2.4}$$

such that $0 < \tilde{\theta}_s < \delta$, $s = 1, \dots, n$.

It was proved [2] that (2.1) is absolutely stable if and only if it satisfies the MO-condition.

The proof of necessity of this criterion is based on the fact, that for the special choice of admissible functions $f_1(x_1), \dots, f_n(x_n)$ system (2.1) is Wazewskij's one, and for it the general criterion of asymptotic stability of autonomous Wazewskij's systems [8] is applicable.

To prove the sufficiency, it was suggested [2] to construct Lyapunov's function for (2.1) in the form

$$V(x) = \sum_{s=1}^{n} \lambda_s \int_0^{x_s} f_s^{\mu_s}(\tau)d\tau, \tag{2.5}$$

where $x = (x_1, \dots, x_n)^*$, $\lambda_s > 0$ are constant coefficients, $\mu_s > 0$ are rationals with odd numerators and denominators. It was shown that (2.1) is absolutely stable if and only if for this system there exists Lyapunov's function in the form (2.5), satisfying the assumptions of the Lyapunov asymptotic stability theorem.

Definition 2.3 We call (2.1) absolutely ultimately bounded if solutions of this system are ultimately bounded for any admissible functions $f_1(x_1), \dots, f_n(x_n)$.

The main goal of the present paper is to obtain the criterion of absolute ultimate boundedness for (2.1). To solve this problem, let us determine the conditions under which for system investigated there exists Lyapunov's function in the form (2.5), satisfying the assumptions of the Yoshizawa ultimate boundedness theorem [14].

Remark 2.1 In what follows, we do not assume the fulfilment of inequalities (2.3).

3 Conditions of Ultimate Boundedness for Wazewskij's Systems

Let us note, just as in [2], that in the case where $f_1(x_1), \dots, f_n(x_n)$ are nondecreasing functions, system (2.1) is Wazewskij's one. Therefore, we shall investigate, first, conditions of ultimate boundedness of solutions for autonomous Wazewskij's systems of the general form.

Consider the system

$$\dot{x} = g(x), \tag{3.1}$$

where $x = (x_1, \dots, x_n)^*$ and vector function $g(x)$ is defined and continuous for all $x \in R^n$.

Assume that system (3.1) possesses the following properties:

(a) for any $t_0 \in (-\infty, +\infty)$ and any $x_0 \in R^n$ the initial value problem for (3.1) has unique solution $x(t, x_0, t_0)$;

(b) system (2.1) is Wazewskij's one;

(c) there exists a number $D > 0$ such that in the region $\|x\| \geq D$ there is no equilibrium position of (3.1).

Here $\|\cdot\|$ is the Euclidean norm of the vector.

Remark 3.1 Condition (c) is a necessary one for the solutions of (3.1) to be ultimately bounded.

Furthermore, we shall assume that nonnegative cone $K^+ = \{x \in R^n : \, x_s \geq 0, \, s = 1, \dots, n\}$ is an invariant set for (3.1).

Definition 3.1 The solutions of (3.1) are ultimately bounded in K^+ if there exists a $H > 0$ and if, corresponding to every $Q > 0$, one can choose a $T > 0$ such that for any $t_0 \in (-\infty, +\infty)$ and for any $x_0 \in K^+$, $\|x_0\| < Q$, the inequality $\|x(t, x_0, t_0)\| < H$ holds for all $t \geq t_0 + T$.

Definition 3.2 We shall say that (3.1) satisfies the $\widetilde{MO}$-condition if for any $\Delta > 0$ there exists vector $\theta = (\theta_1, \dots, \theta_n)^*$, $\|\theta\| > \Delta$, such that $\theta > 0$ and $g(\theta) < 0$ (the inequalities are componentwise).

By the use of Lemmas 3.1 and 3.2 from [8], we get the validity of the following

Theorem 3.1 (necessary condition of ultimate boundedness) *If the solutions of (3.1) are ultimately bounded in K^+, then this system satisfies the $\widetilde{MO}$-condition.*

Remark 3.2 The $\widetilde{MO}$-condition is a necessary one for the ultimate boundedness of solutions. However, it is not, generally, the sufficient condition.

Example 3.1 Let system (3.1) be of the form

$$\begin{aligned} \dot{x}_1 &= -x_1 + x_1^2 x_2, \\ \dot{x}_2 &= -x_2. \end{aligned} \tag{3.2}$$

This system possesses properties (a) – (c) and K^+ is an invariant set for it.

Consider the inequalities

$$-\theta_1 + \theta_1^2\theta_2 < 0, \qquad -\theta_2 < 0. \tag{3.3}$$

For given $\Delta > 0$ there exists positive vector $\tilde{\theta} = (1/(2\Delta), \Delta)^*$, satisfying (3.3), such that $\|\tilde{\theta}\| > \Delta$. Thus, for system (3.2) the $\widetilde{MO}$-condition is fulfilled.

At the same time, (3.2) has the solution $x(t) = (2e^t, e^{-t})^*$. Hence, solutions of this system are not ultimately bounded in K^+.

Definition 3.3 We shall say that (3.1) satisfies the $\overline{MO}$-condition if for any $\Delta > 0$ there exists vector $\theta = (\theta_1, \ldots, \theta_n)^*$ such that $\theta_s > \Delta$, $s = 1, \ldots, n$, and $g(\theta) < 0$.

Using Lemma 3.3 from [8], it is easy to show the validity of the following

Theorem 3.2 (sufficient condition of ultimate boundedness) *If system (3.1) satisfies the $\overline{MO}$-condition, then its solutions are ultimately bounded in K^+.*

Remark 3.3 The $\overline{MO}$-condition is a sufficient one for the ultimate boundedness of solutions. However, it is not, generally, the necessary condition.

Example 3.2 Let the system

$$\begin{aligned} \dot{x}_1 &= -x_1 + x_1 x_2, \\ \dot{x}_2 &= -x_2 \end{aligned} \tag{3.4}$$

be given. This system satisfies all the above assumptions (properties (a)–(c) and invariance of K^+).

By the direct integration, one can verify that solutions of (3.4) are ultimately bounded.

On the other hand, if for a positive vector $\theta = (\theta_1, \theta_2)^*$ the inequalities

$$-\theta_1 + \theta_1\theta_2 < 0, \qquad -\theta_2 < 0,$$

are valid, then $\theta_2 < 1$. Hence, for (3.4) the $\overline{MO}$-condition is not fulfilled.

4 Construction of Lyapunov's Functions

Now, let us investigate the problem of absolute ultimate boundedness for system (2.1).

Construct Lyapunov's function for this system in the form (2.5), where, as before, $\lambda_s > 0$ are constant coefficients and $\mu_s > 0$ are rationals with odd numerators and denominators.

Function $V(x)$ is positive for all $x \neq 0$, and $V(x) \to +\infty$ as $\|x\| \to \infty$. On differentiating this function with respect to (2.1), one arrives at

$$\left.\frac{dV}{dt}\right|_{(2.1)} = \sum_{s=1}^{n} \lambda_s a_s f_s^{\mu_s+1}(x_s) + \sum_{s=1}^{n} \lambda_s f_s^{\mu_s}(x_s) \sum_{j=1}^{k_s} b_{sj} f_1^{\alpha_{s1}^{(j)}}(x_1) \dots f_n^{\alpha_{sn}^{(j)}}(x_n).$$

Hence, $V(x)$ satisfies the assumptions of the Yoshizawa ultimate boundedness theorem for any admissible functions $f_1(x_1), \dots, f_n(x_n)$, if coefficients λ_s and exponents μ_s, $s = 1, \dots, n$, are chosen for the function

$$W(y) = \sum_{s=1}^{n} \lambda_s a_s y_s^{\mu_s+1} + \sum_{s=1}^{n} \lambda_s y_s^{\mu_s} \sum_{j=1}^{k_s} b_{sj} y_1^{\alpha_{s1}^{(j)}} \dots y_n^{\alpha_{sn}^{(j)}} \tag{4.1}$$

to be negative in a region $\|y\| > R$. Here $y = (y_1, \dots, y_n)^*$, while $R > 0$ is a constant.

Let us denote $h_s = 1/(\mu_s + 1)$, $s = 1, \dots, n$. By the use of generally-homogeneous functions properties [15], we get that $W(y)$ might be negative for all $\|y\| > R$ only in the case, where following inequalities are valid:

$$-h_s + \sum_{i=1}^{n} \alpha_{si}^{(j)} h_i \leq 0, \quad j = 1, \dots, k_s, \quad s = 1, \dots, n, \tag{4.2}$$

Remark 4.1 If there exist positive rationals $h_1, \dots, h_n$ for which all the inequalities in (4.2) are strict, i.e.

$$-h_s + \sum_{i=1}^{n} \alpha_{si}^{(j)} h_i < 0, \quad j = 1, \dots, k_s, \quad s = 1, \dots, n, \tag{4.3}$$

then for corresponding values of μ_s and for any admissible values of a_s, b_{sj} and λ_s, $j = 1, \dots, k_s$, $s = 1, \dots, n$, one can choose a constant $R > 0$ such that $W(y) < 0$ for $\|y\| > R$.

5 Auxiliary Results

Let us determine the conditions of the existence of positive solutions for systems (4.2) and (4.3).

Remark 5.1 It is known [4, 13], that in the case where $k_s = 1$, $s = 1, \dots, n$, for the existence of a positive solution for (4.3) it is necessary and sufficient for the matrix

$$A = \begin{pmatrix} \alpha_{11}^{(1)} - 1 & \alpha_{12}^{(1)} & \dots & \alpha_{1n}^{(1)} \\ \alpha_{21}^{(1)} & \alpha_{22}^{(1)} - 1 & \dots & \alpha_{2n}^{(1)} \\ \dots & \dots & \dots & \dots \\ \alpha_{n1}^{(1)} & \alpha_{n2}^{(1)} & \dots & \alpha_{nn}^{(1)} - 1 \end{pmatrix}$$

to satisfy the Sevast'yanov–Kotelyanskij conditions.

Lemma 5.1 *If there exists a positive solution for (4.3), then for system (2.1) the $\overline{MO}$-condition is fulfilled.*

Proof Let inequalities (4.3) be valid for positive constants $\tilde{h}_1, \dots, \tilde{h}_n$. Then for given number $\Delta > 0$, one can choose $\tau > 0$ so large that the constants $\tilde{\theta}_s = \tau^{\tilde{h}_s}$, $s = 1, \dots, n$, satisfy inequalities (2.4), and $\tilde{\theta}_s > \Delta$ for $s = 1, \dots, n$. □

Along with (4.2), consider the system

$$-h_s + \sum_{i=1}^{n} \alpha_{si}^{(j)} h_i = c_s^{(j)}, \quad j = 1, \dots, k_s, \quad s = 1, \dots, n,$$

where $c_s^{(j)}$ are nonpositive constants. This system can be splitted into n subsystems

$$A_s h = c_s, \quad s = 1, \dots, n. \tag{5.1}$$

Here $h = (h_1, \dots, h_n)^*$, $c_s = (c_s^{(1)}, \dots, c_s^{(k_s)})^*$,

$$A_1 = \begin{pmatrix} \alpha_{11}^{(1)} - 1 & \alpha_{12}^{(1)} & \dots & \alpha_{1n}^{(1)} \\ \dots & \dots & \dots & \dots \\ \alpha_{11}^{(k_1)} - 1 & \alpha_{12}^{(k_1)} & \dots & \alpha_{1n}^{(k_1)} \end{pmatrix}, \quad \dots \quad , \quad A_n = \begin{pmatrix} \alpha_{n1}^{(1)} & \alpha_{n2}^{(1)} & \dots & \alpha_{nn}^{(1)} - 1 \\ \dots & \dots & \dots & \dots \\ \alpha_{n1}^{(k_n)} & \alpha_{n2}^{(k_n)} & \dots & \alpha_{nn}^{(k_n)} - 1 \end{pmatrix}.$$

Let us apply to (5.1) the modified Gaussian elimination procedure. On the s-th step of this procedure each of the equations with negative coefficient of h_s is used for the elimination of h_s from the $(s+1)$-th, etc., and n-th subsystems. This results in a new set of subsystems with (generally) the other number of equations than in the initial system.

Lemma 5.2 *System (4.2) possesses a positive solution if and only if the above modified Gaussian elimination procedure reduces system (5.1) to the form*

$$B_s h = \tilde{c}_s, \quad s = 1, \dots, n,$$

where

$$B_1 = \begin{pmatrix} \beta_{11}^{(1)} & \dots & \beta_{1n}^{(1)} \\ \dots & \dots & \dots \\ \beta_{11}^{(q_1)} & \dots & \beta_{1n}^{(q_1)} \end{pmatrix}, \; B_2 = \begin{pmatrix} 0 & \beta_{22}^{(1)} & \dots & \beta_{2n}^{(1)} \\ \dots & \dots & \dots & \dots \\ 0 & \beta_{22}^{(q_2)} & \dots & \beta_{2n}^{(q_2)} \end{pmatrix}, \; \dots, B_n = \begin{pmatrix} 0 & \dots & 0 & \beta_{nn}^{(1)} \\ \dots & \dots & \dots & \dots \\ 0 & \dots & 0 & \beta_{nn}^{(q_n)} \end{pmatrix},$$

$$\tilde{c}_1 = \left(\tilde{c}_1^{(1)}, \dots, \tilde{c}_1^{(q_1)}\right)^*, \quad \dots, \quad \tilde{c}_n = \left(\tilde{c}_n^{(1)}, \dots, \tilde{c}_n^{(q_n)}\right)^*,$$

$\tilde{c}_s^{(j)} \le 0$, $\beta_{ss}^{(j)} \le 0$, $\beta_{si}^{(j)} \ge 0$ for $j = 1, \dots, q_s$, $i = s+1, \dots, n$, $s = 1, \dots, n$, and if $\beta_{ss}^{(j)} = 0$ for some values of indices s and j, then $\beta_{si}^{(j)} = 0$, $i = s+1, \dots, n$, for all such s and j.

Remark 5.2 In the case where $\beta_{ss}^{(j)} < 0$, $j = 1, \dots, q_s$, $s = 1, \dots, n$, there exist positive numbers $\tilde{h}_1, \dots, \tilde{h}_n$ satisfying strict inequalities (4.3).

Lemma 5.3 *If for (2.1) the $\overline{MO}$-condition is fulfilled, then there exists a positive solution for system (4.2).*

The proofs of Lemmas 5.2 and 5.3 are similar to those ones of Lemmas 4.2 and 4.3 from [2].

Remark 5.3 The proof of Lemma 5.2 contains a constructive algorithm for finding a positive solution $\tilde{h}_1, \dots, \tilde{h}_n$ for (4.2). Moreover, let us note that using this algorithm one may choose $\tilde{h}_1, \dots, \tilde{h}_n$ for the numbers $\mu_s = 1/\tilde{h}_s - 1$, $s = 1, \dots, n$, to be positive rationals with odd numerators and denominators.

6 Conditions of Absolute Ultimate Boundedness

Consider the necessary conditions of absolute ultimate boundedness for system (2.1).

Theorem 6.1 *If system (2.1) is absolutely ultimately bounded, then it satisfies the* $\widetilde{MO}$*-condition.*

Proof Suppose that (2.1) is absolutely ultimately bounded. Then its solutions are ultimately bounded for any admissible functions $f_1(x_1), \dots, f_n(x_n)$.

Let $f_s(x_s) = x_s^{m_s}$, $s = 1, \dots, n$, where m_s are odd positive integers such that $\alpha_{si}^{(j)} m_i \geq 1$ for $j = 1, \dots, k_s$, $i, s = 1, \dots, n$. For chosen admissible functions, system (2.1) possesses all the properties from Section 3 (properties (a)–(c) and invariance of K^+). Using Theorem 3.1, we get that (2.1) satisfies the $\widetilde{MO}$-condition. □

Theorem 6.2 *Let there exist positive constants* $\tilde{h}_1, \dots, \tilde{h}_n$*, and for every* $s = 1, \dots, n$ *there exists at least one value of* $j \in \{1, \dots, k_s\}$ *such that*

$$-\tilde{h}_s + \sum_{i=1}^{n} \alpha_{si}^{(j)} \tilde{h}_i > 0.$$

Then system (2.1) is not absolutely ultimately bounded.

Proof Choose, again, functions $f_1(x_1), \dots, f_n(x_n)$ for the obtained system to satisfy all the assumptions from Section 3.

Consider the numbers $\tilde{\theta}_s = \tau^{\tilde{h}_s}$, $\tau > 0$, $s = 1, \dots, n$. For all sufficiently large values of τ the inequalities

$$a_s \tilde{\theta}_s + \sum_{j=1}^{k_s} b_{sj} \tilde{\theta}_1^{\alpha_{s1}^{(j)}} \dots \tilde{\theta}_n^{\alpha_{sn}^{(j)}} > 0, \quad s = 1, \dots, n,$$

are fulfilled. Applying Lemma 3.4 from [8], we get that for chosen admissible functions, the solutions of system (2.1) are not ultimately bounded. □

Consider, next, the sufficient conditions of absolute ultimate boundedness.

Theorem 6.3 *If for system (2.1) the* $\overline{MO}$*-condition is fulfilled, then it is absolutely ultimately bounded.*

Proof Let us show that for system investigated there exists Lyapunov's function in the form (2.5), satisfying the assumptions of the Yoshizawa ultimate boundedness theorem.

According to Lemma 5.3, we obtain that if for (2.1) the $\overline{MO}$-condition is fulfilled, then one can choose positive rationals $\mu_1, \dots, \mu_n$ with odd numerators and denominators such that for the numbers $\tilde{h}_s = 1/(\mu_s + 1)$, $s = 1, \ldots, n$, inequalities (4.2) are valid. We shall take these values of $\mu_1, \ldots, \mu_n$ as exponents in Lyapunov's function (2.5).

Let us show the existence of positive coefficients $\lambda_1, \ldots, \lambda_n$ under which function (4.1) is negative in a region $\|y\| > R$, where $R > 0$ is a constant.

Consider inequalities (4.2) for $h_s = \tilde{h}_s$, $s = 1, \ldots, n$. It should be noted that in the case where for some values of indices j and s the corresponding inequalities are strict, one can construct, instead of (4.1), new function $\widehat{W}(y)$ by setting $b_{sj} = 0$ for all such j and s. If there exist positive coefficients $\lambda_1, \ldots, \lambda_n$ for which $\widehat{W}(y)$ is negative definite, then for these values of $\lambda_1, \ldots, \lambda_n$ and for some number $R > 0$, the inequality $W(y) < 0$ holds in the region $\|y\| > R$. Therefore, we may assume, without loss of generality, that for the numbers $\tilde{h}_1, \ldots, \tilde{h}_n$ all the inequalities in (4.2) turn to equalities.

The rest part of the proof is similar to that one of Theorem 5.1 from [2]. □

Remark 6.1 Theorem 6.3 looks similar to Theorem 3.2. However, in comparison with the conditions of ultimate boundedness of solutions for autonomous Wazewskij's systems obtained in Section 3, Theorem 6.3 states that the only $\overline{MO}$-condition is a sufficient one for the absolute ultimate boundedness of (2.1), i.e. the other assumptions from Section 3 (properties (a)–(c) and invariance of K^+) are redundant.

Corollary 6.1 *Let system (4.2) has a positive solution. Then (2.1) is absolutely ultimately bounded if and only if there exists at least one set of positive constants $\tilde{\theta}_1, \ldots, \tilde{\theta}_n$, satisfying inequalities (2.4).*

Proof The necessity follows from Theorem 6.1.

To prove the sufficiency, suppose that the positive vectors $\tilde{h} = (\tilde{h}_1, \ldots, \tilde{h}_n)^*$ and $\tilde{\theta} = (\tilde{\theta}_1, \ldots, \tilde{\theta}_n)^*$ are solutions of systems (4.2) and (2.4) correspondingly. Then the numbers $\hat{\theta}_s = \tau^{\tilde{h}_s}\tilde{\theta}_s$, $\tau > 0$, $s = 1, \ldots, n$, satisfy inequalities (2.4) for all sufficiently large values of τ. Hence, the $\overline{MO}$-condition is fulfilled for (2.1). □

Corollary 6.2 *For system (2.1) there exists Lyapunov's function in the form (2.5), satisfying the assumptions of the Yoshizawa ultimate boundedness theorem, if and only if the $\overline{MO}$-condition is fulfilled for this system.*

Proof The sufficiency follows from Theorem 6.3. Let us prove the necessity.

In Section 4 it was noted that if function (2.5) satisfies the assumptions of the Yoshizawa ultimate boundedness theorem, then system (4.2) possesses a positive solution. On the other hand, the existence of such Lyapunov's function provides the absolute ultimate boundedness for (2.1). Then, according to Theorem 6.1, there exists a positive solution for system (2.4). By analogy with the proof of Corollary 6.1, we get that for (2.1) the $\overline{MO}$-condition is fulfilled. □

Consider now, along with (2.1), the perturbed system

$$\dot{x}_s = a_s f_s(x_s) + \sum_{j=1}^{k_s} b_{sj} f_1^{\alpha_{s1}^{(j)}}(x_1) \ldots f_n^{\alpha_{sn}^{(j)}}(x_n) + \psi_s(t,x), \quad s = 1, \ldots, n. \tag{6.1}$$

Here functions $\psi_s(t,x)$ are continuous for all $t \in (-\infty, +\infty)$, $x \in R^n$, and satisfy the inequalities $|\psi_s(t,x)| \le \gamma_s + \varepsilon_s |f_s(x_s)|$, where γ_s and ε_s are positive constants, $s = 1, \ldots, n$.

Corollary 6.3 *Let for (2.1) the $\overline{MO}$-condition be fulfilled. Then solutions of (6.1) are uniformly ultimately bounded for sufficiently small values of $\varepsilon_1, \dots, \varepsilon_n$.*

Proof Construct for system (2.1) Lyapunov's function in the form (2.5), satisfying the assumptions of the Yoshizawa ultimate boundedness theorem. It is easily shown that for sufficiently large number $R > 0$ and for sufficiently small values of $\varepsilon_1, \dots, \varepsilon_n$ the derivative of Lyapunov's function constructed with respect to (6.1) is negative in the region $\|x\| > R$. □

Remark 6.2 In a similar way, the conditions of absolute ultimate boundedness can be obtained for the case when the inequalities $b_{sj} > 0$ in (2.2) are replaced by those connecting coefficients b_{sj} and a basis $\omega_1, \dots, \omega_n$: $b_{sj}\omega_s\omega_1^{\alpha_{s1}^{(j)}} \dots \omega_n^{\alpha_{sn}^{(j)}} > 0$ for $j = 1, \dots, k_s$, $s = 1, \dots, n$ [9]. Here every constant $\omega_1, \dots, \omega_n$ takes either of the values $+1$ or -1.

7 Systems with the Special Structure of Connections

In the previous section it was proved that for (2.1) to be absolutely ultimately bounded it is sufficient the fulfilment of the $\overline{MO}$-condition. Consider now some types of systems of the form (2.1) with the special structure of connections for which the $\overline{MO}$-condition is not only sufficient one but also a necessary one for absolute ultimate boundedness.

Example 7.1 Consider system (2.1) with $k_1 = 1, \dots, k_n = 1$:

$$\dot{x}_s = a_s f_s(x_s) + b_s f_1^{\alpha_{s1}}(x_1) \dots f_n^{\alpha_{sn}}(x_n), \quad s = 1, \dots, n. \tag{7.1}$$

Here $a_s < 0$ and $b_s > 0$ are constant coefficients, α_{si} are nonnegative rationals with odd denominators. For (7.1) the corresponding system of inequalities (4.2) is of the form

$$-h_s + \sum_{i=1}^{n} \alpha_{si} h_i \le 0, \quad s = 1, \dots, n. \tag{7.2}$$

According to Corollary 6.1, we get that if (7.2) possesses a positive solution, then for (7.1) to be absolutely ultimately bounded it is necessary and sufficient for this system to satisfy the $\overline{MO}$-condition.

On the other hand, if (7.2) has no positive solutions, and $\alpha_{si} > 0$ for $s \ne i$, then there exist positive constants $\tilde{h}_1, \dots, \tilde{h}_n$ such that

$$-\tilde{h}_s + \sum_{i=1}^{n} \alpha_{si} \tilde{h}_i > 0, \quad s = 1, \dots, n.$$

Hence (v. Theorem 6.2), system (7.1) is not absolutely ultimately bounded.

Thus, in the case where $\alpha_{si} > 0$ for $s \ne i$, $i, s = 1, \dots, n$, system (7.1) is absolutely ultimately bounded if and only if the $\overline{MO}$-condition is fulfilled for this system.

Example 7.2 Let system (2.1) be of the form

$$\begin{aligned} \dot{x}_1 &= a_1 f_1(x_1) + b_1 f_n^{\alpha_1}(x_n), \\ \dot{x}_i &= a_i f_i(x_i) + b_i f_{i-1}^{\alpha_i}(x_{i-1}), \quad i = 2, \dots, n-1, \\ \dot{x}_n &= a_n f_n(x_n) + b_n f_1^{\beta_1}(x_1) \dots f_{n-1}^{\beta_{n-1}}(x_{n-1}), \end{aligned} \tag{7.3}$$

where $a_s < 0$ and $b_s > 0$ are constant coefficients, $\alpha_j > 0$ and $\beta_j \geq 0$ are rationals with odd denominators, $j = 1, \dots, n-1$, $s = 1, \dots, n$.

Consider inequalities (2.4), corresponding to system (7.3). We get

$$\theta_1 > -\frac{b_1}{a_1}\,\theta_n^{\alpha_1}, \qquad \theta_i \quad > -\frac{b_i}{a_i}\,\theta_{i-1}^{\alpha_i},\ \ i = 2, \dots, n-1, \qquad \theta_n > -\frac{b_n}{a_n}\,\theta_1^{\beta_1} \dots \theta_{n-1}^{\beta_{n-1}}.$$

It is easily shown that (7.3) is absolutely ultimately bounded if and only if the inequality

$$\alpha_1\beta_1 + \alpha_1\alpha_2\beta_2 + \dots + \alpha_1 \dots \alpha_{n-1}\,\beta_{n-1} \leq 1 \tag{7.4}$$

holds, and in the case where (7.4) turns to equality, the condition

$$\left(-\frac{b_1}{a_1}\right)^{\xi_1}\left(-\frac{b_2}{a_2}\right)^{\xi_2} \dots \left(-\frac{b_{n-1}}{a_{n-1}}\right)^{\xi_{n-1}}\left(-\frac{b_n}{a_n}\right) < 1$$

is fulfilled. Here $\xi_i = \beta_i + \alpha_{i+1}\xi_{i+1},\ i = 1, \dots, n-2,\ \xi_{n-1} = \beta_{n-1}$. Hence, the absolute ultimate boundedness of system (7.3) implies that this system satisfies the $\overline{MO}$-condition.

Thus, for (7.3) the sufficient condition of absolute ultimate boundedness is also a necessary one.

Example 7.3 Consider the system

$$\begin{aligned} \dot{x}_i &= a_i f_i(x_i) + b_i f_n^{\alpha_i}(x_n), \quad i = 1, \dots, n-1, \\ \dot{x}_n &= a_n f_n(x_n) + b_n f_1^{\beta_1}(x_1) \dots f_{n-1}^{\beta_{n-1}}(x_{n-1}). \end{aligned} \tag{7.5}$$

Here parameters a_s, b_s, α_j and β_j, $j = 1, \dots, n-1$, $s = 1, \dots, n$, possess the same properties as in the previous example. We get, again, that if the system investigated is absolutely ultimately bounded, then it satisfies the $\overline{MO}$-condition.

It can be easily shown that for the absolute ultimate boundedness of (7.5) it is necessary and sufficient the validity of the inequality $\alpha_1\beta_1 + \alpha_2\beta_2 + \dots + \alpha_{n-1}\beta_{n-1} \leq 1$. If this inequality turns to equality, then for coefficients a_s and b_s the condition

$$\left(-\frac{b_1}{a_1}\right)^{\beta_1}\left(-\frac{b_2}{a_2}\right)^{\beta_2} \dots \left(-\frac{b_{n-1}}{a_{n-1}}\right)^{\beta_{n-1}}\left(-\frac{b_n}{a_n}\right) < 1$$

should be fulfilled.

8 Systems with Additive Connections

Let system (2.1) be of the form

$$\dot{x}_s = \sum_{j=1}^{n} p_{sj} f_j^{\alpha_{sj}}(x_j), \quad s = 1, \dots, n, \tag{8.1}$$

where $\alpha_{sj} > 0$ are rationals with odd denominators, $\alpha_{ss} = 1$, and p_{sj} are constant coefficients, $p_{ss} < 0$, $p_{sj} \geq 0$ for $j \neq s$, $j, s = 1, \dots, n$. Thus, connections in the equations considered are additive.

Theorem 8.1 *System (8.1) is absolutely ultimately bounded if and only if it satisfies the $\overline{MO}$-condition.*

Proof The sufficiency follows from Theorem 6.3. Let us prove the necessity.

Suppose that (8.1) is absolutely ultimately bounded. Then (v. Theorem 6.1) the $\widetilde{MO}$-condition is fulfilled for this system. Therefore, there exists a sequence of positive vectors $\tilde{\theta}^{(m)} = (\tilde{\theta}_{1m}, \dots, \tilde{\theta}_{nm})^*$ such that $\|\tilde{\theta}^{(m)}\| \to \infty$ as $m \to \infty$, and for every $m = 1, 2, \dots$ vector $\tilde{\theta}^{(m)}$ is a solution of the system

$$\sum_{j=1}^{n} p_{sj} \theta_j^{\alpha_{sj}} < 0, \quad s = 1, \dots, n. \tag{8.2}$$

One may assume, without loss of generality, that $\tilde{\theta}_{sm} \to +\infty$ as $m \to \infty$ for $s = 1, \dots, k$, where $1 \le k \le n$, and for $s > k$ the sequences $\{\tilde{\theta}_{sm}\}$ are bounded.

If $k = n$, then for system (8.1) the $\overline{MO}$-condition is fulfilled. Consider, further, the case where $k < n$. The inequalities

$$\sum_{j=1}^{n} p_{sj} \tilde{\theta}_{jm}^{\alpha_{sj}} < 0, \quad s = k+1, \dots, n,$$

are valid for $m = 1, 2, \dots$. Hence, (8.1) can be splitted into the following two subsystems:

$$\dot{x}_s = \sum_{j=1}^{k} p_{sj} f_j^{\alpha_{sj}}(x_j) + \sum_{j=k+1}^{n} p_{sj} f_j^{\alpha_{sj}}(x_j), \quad s = 1, \dots, k, \tag{8.3}$$

$$\dot{x}_s = \sum_{j=k+1}^{n} p_{sj} f_j^{\alpha_{sj}}(x_j), \quad s = k+1, \dots, n. \tag{8.4}$$

Since (8.1) is absolutely ultimately bounded, then subsystem (8.4) possesses the same property. For this subsystem, one can to repeat the above arguments. Continuing this process, we get that (8.1) can be splitted into a ordered set of subsystems such that every subsystem does not influence the subsequent ones.

The last subsystem satisfies the $\overline{MO}$-condition. Let us show that for the set of the last two, three, etc. subsystems the $\overline{MO}$-condition is also fulfilled.

We shall assume, without loss of generality, that (8.1) is splitted only into the two subsystems: (8.3) and (8.4).

System (8.4) and the system

$$\dot{x}_s = \sum_{j=1}^{k} p_{sj} f_j^{\alpha_{sj}}(x_j), \quad s = 1, \dots, k,$$

satisfy the $\overline{MO}$-condition. Hence, for every $\Delta > 0$ there exist numbers $\hat{\theta}_1, \dots, \hat{\theta}_n$ such that $\hat{\theta}_s > \Delta$, $s = 1, \dots, n$, and

$$\sum_{j=1}^{k} p_{sj} \hat{\theta}_j^{\alpha_{sj}} < 0, \ \ s = 1, \dots, k; \qquad \sum_{j=k+1}^{n} p_{sj} \hat{\theta}_j^{\alpha_{sj}} < 0, \ \ s = k+1, \dots, n.$$

By the use of Lemma 5.3, we get that the system

$$-h_s + \alpha_{sj} h_j \le 0, \quad j \ne s, \quad j, s = 1, \dots, k,$$

has a positive solution $\tilde{h}_1, \dots, \tilde{h}_k$. Then for the numbers $\bar{\theta}_j = \tau^{\tilde{h}_j} \hat{\theta}_j$, $j = 1, \dots, k$, $\tau > 1$, following inequalities are valid:

$$\sum_{j=1}^{k} p_{sj} \bar{\theta}_j^{\alpha_{sj}} < 0, \quad s = 1, \dots, k,$$

Thus, for sufficiently large values of τ the vector $(\bar{\theta}_1, \dots, \bar{\theta}_k, \hat{\theta}_{k+1}, \dots, \hat{\theta}_n)^*$ is a solution of system (8.2), and all the entries of this vector are greater than Δ. Hence, (8.1) satisfies the $\overline{MO}$-condition. □

Remark 8.1 Theorem 8.1 states that for systems with additive connections the $\overline{MO}$-condition is not only sufficient one but also a necessary condition for the absolute ultimate boundedness. On the other hand, the $\widetilde{MO}$-condition is a necessary one for (8.1) to be absolutely ultimately bounded. However, this condition is not a sufficient one.

Example 8.1 Let system (8.1) be of the form

$$\begin{aligned} \dot{x}_1 &= -f_1(x_1), \\ \dot{x}_2 &= -f_2(x_2) + f_3^2(x_3), \\ \dot{x}_3 &= -f_3(x_3) + f_2^2(x_2). \end{aligned} \tag{8.5}$$

It is easily verified that the $\widetilde{MO}$-condition is fulfilled for (8.5). At the same time, if $f_s(x_s) = x_s$, $s = 1, 2, 3$, then solutions of this system are not ultimately bounded.

9 Conditions of Ultimate Boundedness for Large Scale Systems

Let us show now that the results obtained in the present paper can be used for the determination of conditions of ultimate boundedness of solutions for essentially nonlinear complex systems.

Consider the system

$$\dot{x}_s = F_s(x_s) + \sum_{j=1}^{k_s} Q_{sj}(t, x), \quad s = 1, \dots, n, \tag{9.1}$$

where $x_s \in R^{m_s}$, $x = (x_1^*, \dots, x_n^*)^*$; the elements of the vectors $F_s(x_s)$ are continuous homogeneous functions of the orders $\sigma_s > 0$; the vector functions $Q_{sj}(t, x)$ are continuous for $t \geq 0$, $x \in R^m$ $(m = m_1 + \dots + m_n)$. We will assume that in the region $t \geq 0$, $\|x\| \geq H$ ($H > 0$ is a constant) functions $Q_{sj}(t, x)$ satisfy the inequalities

$$\|Q_{sj}(t, x)\| \leq c_{sj} \|x_1\|^{\beta_{s1}^{(j)}} \dots \|x_n\|^{\beta_{sn}^{(j)}}, \quad c_{sj} > 0, \quad \beta_{si}^{(j)} \geq 0.$$

System (9.1) describes the dynamics of complex system composed of n interconnected subsystems [4, 13]. Here x_s are state vectors, the functions $F_s(x_s)$ define the interior connections of subsystems while the functions $Q_{sj}(t, x)$ characterize the interaction between the subsystems.

Consider the isolated subsystems

$$\dot{x}_s = F_s(x_s), \quad s = 1, \dots, n. \tag{9.2}$$

Let the zero solutions of subsystems (9.2) be asymptotically stable. In [1, 2, 5, 10] the conditions are obtained under which asymptotic stability of the zero solutions of (9.2) implies that the zero solution of (9.1) is also asymptotically stable. In the present section, we will look for the conditions of ultimate boundedness of solutions for system (9.1).

Assume that for isolated subsystems there exist Lyapunov's functions $V_s(x_s)$, $s = 1, \dots, n$, with the following properties:

(a) $V_s(x_s)$ are positive definite;

(b) $V_s(x_s)$ are continuously differentiable for all $x_s \in R^{m_s}$;

(c) $V_s(x_s)$ are positive homogeneous functions of orders $\gamma_s - \sigma_s + 1$;

(d) the derivatives of $V_s(x_s)$ with respect to (9.2) are negative functions.

Remark 9.1 In the case where $F_1(x_1), \dots, F_n(x_n)$ are continuously differentiable functions, the existence of such Lyapunov's functions it was proved in [17].

Remark 9.2 In the capacity of $\gamma_1, \dots, \gamma_n$ one may choose arbitrary numbers such that $\gamma_s > \sigma_s$, $s = 1, \dots, n$.

By the use of the homogeneous functions properties [17], we get that functions $V_1(x_1), \dots, V_n(x_n)$ satisfy the inequalities $a_{1s}\|x_s\|^{\gamma_s - \sigma_s + 1} \le V_s(x_s) \le a_{2s}\|x_s\|^{\gamma_s - \sigma_s + 1}$,

$$\left\|\frac{\partial V_s}{\partial x_s}\right\| \le a_{3s}\|x_s\|^{\gamma_s - \sigma_s}, \qquad \left(\frac{\partial V_s}{\partial x_s}\right)^* F_s \le -a_{4s}\|x_s\|^{\gamma_s}$$

for all $x_s \in R^{m_s}$, where a_{1s}, a_{2s}, a_{3s}, a_{4s} are positive constants, $s = 1, \dots, n$.

On differentiating $V_s(x_s)$ with respect to (9.1), one can deduce that the estimations

$$\frac{dV_s}{dt}\Big|_{(9.1)} \le -a_{4s}\|x_s\|^{\gamma_s} + a_{3s}\|x_s\|^{\gamma_s - \sigma_s} \sum_{j=1}^{k_s} c_{sj}\|x_1\|^{\beta_{s1}^{(j)}} \dots \|x_n\|^{\beta_{sn}^{(j)}}$$

are valid for $t \ge 0$, $\|x\| \ge H$, $s = 1, \dots, n$.

Consider the function

$$V(x) = \sum_{s=1}^{n} \lambda_s V_s(x_s),$$

where $\lambda_1, \dots, \lambda_n$ are positive coefficients. For all $t \ge 0$ and $\|x\| \ge H$ we obtain

$$\frac{dV}{dt}\Big|_{(9.1)} \le -\sum_{s=1}^{n} \lambda_s a_{4s}\|x_s\|^{\gamma_s} + \sum_{s=1}^{n} \lambda_s a_{3s}\|x_s\|^{\gamma_s - \sigma_s} \sum_{j=1}^{k_s} c_{sj}\|x_1\|^{\beta_{s1}^{(j)}} \dots \|x_n\|^{\beta_{sn}^{(j)}}.$$

Hence, to prove the ultimate boundedness of solutions for (9.1) it is sufficient to show that one can choose coefficients $\lambda_1, \dots, \lambda_n$ for the function

$$W(y) = -\sum_{s=1}^{n} \lambda_s a_{4s} y_s^{\gamma_s} + \sum_{s=1}^{n} \lambda_s a_{3s} y_s^{\gamma_s - \sigma_s} \sum_{j=1}^{k_s} c_{sj}\, y_1^{\beta_{s1}^{(j)}} \dots y_n^{\beta_{sn}^{(j)}}$$

to be negative in a region $\|y\| > R$. Here $R > 0$ is a constant.

Suppose that parameters $\gamma_1, \dots, \gamma_n$ satisfy the inequalities

$$-\frac{\sigma_s}{\gamma_s} + \sum_{i=1}^{n} \frac{\beta_{si}^{(j)}}{\gamma_i} \le 0, \quad j = 1, \dots, k_s, \quad s = 1, \dots, n. \tag{9.3}$$

In this case, by analogy with the proof of Theorem 6.3, we get the validity of the following

Theorem 9.1 *If there exist positive numbers $\tilde{\theta}_1, \dots, \tilde{\theta}_n$ such that*

$$-a_{4s}\tilde{\theta}_s^{\sigma_s} + a_{3s}\sum_{j=1}^{k_s} c_{sj}\tilde{\theta}_1^{\beta_{s1}^{(j)}} \dots \tilde{\theta}_n^{\beta_{sn}^{(j)}} < 0, \quad s = 1, \dots, n, \tag{9.4}$$

then solutions of (9.1) are uniformly ultimately bounded.

Remark 9.3 Coefficients a_{3s}, a_{4s} in (9.4) depend, in general, on the chosen values of $\gamma_1, \dots, \gamma_n$.

Remark 9.4 If for chosen values of $\gamma_1, \dots, \gamma_n$ all the inequalities in (9.3) are strict, then solutions of (9.1) are uniformly ultimately bounded (the verification of the existence of the positive numbers $\tilde{\theta}_1, \dots, \tilde{\theta}_n$, satisfying the inequalities (9.4), in this case is redundant).

References

[1] Aleksandrov, A.Yu. On the stability of complex systems in critical cases. *Autom. i Telemekh* (9) (2001) 3–13. [Russian]

[2] Aleksandrov, A.Yu. and Platonov, A.V. Construction of Lyapunov's functions for a class of nonlinear systems. *Nonlinear Dynamics and Systems Theory* **6**(1) (2006) 17–29.

[3] Barbashin, Ye.A. *The Lyapunov Functions.* Nauka, Moscow, 1967. [Russian]

[4] Grujic, Lj.T., Martynyuk, A.A. and Ribbens-Pavella, M. *Stability of Large Scale Systems under Structural and Singular Perturbations.* Naukova Dumka, Kiev, 1984. [Russian]

[5] Kosov, A.A. On the stability of complex systems by the nonlinear approximation. *Differ. Uravn.* **33**(10) (1997) 1432–1434. [Russian]

[6] LaSalle, J.P. and Lefschetz, S. *Stability by Liapunov's Direct Method with Applications.* Academic Press, New York, London, 1961.

[7] Lur'e, A.I. *Certain Nonlinear Problems of Automatic Control Theory.* Gostekhizdat, Moscow, 1951. [Russian]

[8] Martynyuk, A.A. and Obolenskij, A.Yu. On the stability of solutions for the Wazewskij autonomous systems. *Differ. Uravn.* **16**(8) (1980) 1392–1407. [Russian]

[9] Persidsky, S.K. On the problem of absolute stability. *Autom. i Telemekh.* (12) (1969) 5–11. [Russian]

[10] Platonov, A.V. On stability of complex nonlinear systems. *Izv. RAN: Teoriya i Sistemy Upravleniya* (4) (2004) 41–46. [Russian]

[11] Pliss, V.A. *Nonlocal Problems of Oscillations Theory.* Nauka, Moscow, Leningrad, 1964. [Russian]

[12] Rouche, N., Habets, P. and Laloy, M. *Stability Theory by Liapunov's Direct Method.* Springer, New York etc., 1977.

[13] Siljak, D.D. *Decentralized Control of Complex Systems.* Academic Press, Cambridge, MA, 1991.

[14] Yoshizawa, T. *Stability Theory by Liapunov's Second Method.* The Math. Soc. of Japan, Tokyo, 1966.

[15] Zubov, V.I. *Mathematical Methods for the Study of Automatical Control Systems.* Sudostroenie, Leningrad, 1959. [Russian]

[16] Zubov, V.I. *Oscillations in Nonlinear and Controled Systems.* Sudostroenie, Leningrad, 1962. [Russian]

[17] Zubov, V.I. *Stability of Motion.* Vysshaya Shkola, Moscow, 1973. [Russian]

Nonlinear Dynamics and Systems Theory, 8 (2) (2008) 123–135

Adaptive Control of Nonlinear in Parameters Chaotic Systems

S.M. Ayati * and A. Khaki-Sedigh

Department of Electrical Engineering, K.N. Toosi University of Technology, Sayyed Khandan Bridge, Shariati Street, Tehran, Iran

Received: September 25, 2006; Revised: April 6, 2008

Abstract: This paper presents the adaptive control of chaotic systems, which are nonlinear in parameters (NLP). A method based on Lagrangian of an objective functional is used to identify the parameters of the system. Also this method is improved to result in better rate of convergence of the estimated parameters. Estimation results are used to calculate the Lyapunov exponents adaptively. Finally, the Lyapunov exponents placement method is used to assign the desired Lyapunov exponents of the closed loop system. Simulation results are provided to show the effectiveness of the results.

Keywords: *Chaotic system; nonlinear in parameter system identification; Lyapunov exponents placement; gradient method.*

Mathematics Subject Classification (2000): 93C10, 93C40, 34C28.

1 Introduction

Chaotic systems have been widely studied by many scientists and engineers from different viewpoints. The recent applications of chaotic systems have raised new questions regarding chaos control [1, 2, 3]. From a practical control system design point of view, an important issue in the analysis and control of chaotic systems can be the uncertainty associated with the system parameters. Equally important is the time varying nature of many system parameters. In [4, 5] an adaptive strategy is proposed for the on-line identification and control of chaotic systems. However, the method is restricted to chaotic systems that are linear in parameters. In this paper, the adaptive control of nonlinear in parameter chaotic systems is considered.

Parameter estimation methods for nonlinear chaotic systems, such as NARX (nonlinear autoregressive with exogenous inputs) [6], NARMAX (nonlinear autoregressive

* Corresponding author: ayati@dena.kntu.ac.ir

moving average with exogenous inputs) [7, 8] are employed for linear in parameter (LP) systems. For NLP systems, nonlinear programming methods can be used [9, 10]. In this paper, a proper local objective functional is defined and minimized based on the Lagrangian of an objective functional using the speed gradient (SG) method. The method results in fast convergence and estimated parameters are unbiased [11].

To achieve faster convergence rate of the estimated parameters, the SG method is improved. In the new improved SG (ISG) method, descent gradient method [9, 10] is used to optimize step length matrix of SG method in each iteration, to minimize another local objective functional.

Lyapunov exponents are commonly used for chaos identification in nonlinear dynamical systems. Lyapunov exponents show the average rate of growing or shrinking of a small volume of initial conditions. These exponents provide a quantitative measure for the sensitivity of the nonlinear system to the change of initial conditions. Also Lyapunov exponents demonstrate the chaotic behavior of the system [12, 13].

There are several methods for numerical calculation of Lyapunov exponents [14, 15]. Throughout this paper, we use a Jacobian approach with QR factorization to extract the Lyapunov exponents from long term product of the local Jacobian matrices.

Lyapunov exponents placement has been used for chaotization and anti-chaotization of a system [16]. It also could be used for the adaptive control of unknown or time varying LP chaotic systems [4]. This paper proposes an adaptive methodology for NLP chaotic systems.

The paper is organized as follows. Section 1 provides the introduction. In Section 2, the SG method for identification of NLP systems is described. In Section 3, we use descent gradient method to formulate the improved SG method. In Section 4, Lyapunov exponents of the system are determined. In Section 5, Lyapunov exponents placement strategy is described and is used to calculate the control input for the system. Finally, simulation results for the chaotic Duffing and Lorenz systems are provided in Section 6.

2 Adaptive Parameter Estimation

Consider the system described by:

$$\begin{cases} \dot{x}(t) = f(x(t), p(t)), \\ x(0): \text{ is given}, \end{cases} \tag{1}$$

where $t > 0$ is time, $x \in R^n$ is state vector of the plant, $p \in R^k$ is the vector of unknown parameters and $f\colon\ R^n \times R^k \to R$ is a vector function of state variables and parameters. Let the system estimator be described as follows:

$$\begin{cases} \dot{\hat{x}}(t) = f(\hat{x}(t), \hat{p}(t)), \\ \hat{x}(0): \text{ is given}, \end{cases} \tag{2}$$

where $\hat{x} \in R^n$ is the estimated state vector, $\hat{x} \in R^k$ is the vector of estimated parameters and $\hat{f}\colon\ R^n \times R^k \to R$ is a vector function of state variables and parameters. We make the assumption that the structure of the system is clear

$$f(\hat{x}(t), \hat{p}(t)) = \hat{f}(\hat{x}(t), \hat{p}(t)) = \left[\hat{f}_1(\hat{x}(t), \hat{p}(t)),\, \ldots,\, \hat{f}_n(\hat{x}(t), \hat{p}(t))\right]^{\mathrm{T}}, \tag{3}$$

where $\hat{f}_i\colon\ R^n \times R^k \to R$, $i = 1, 2, \dots, n$. The objective can be formulated as

$$\lim_{t\to\infty} |\hat{p}(t) - p(t)| = 0. \tag{4}$$

Define a positive scalar functional $J_1(x, \hat{x})$. We choose $J_1(x, \hat{x})$ in a way that when $J_1(x, \hat{x})$ is minimized, (4) is achieved. The total rate of change is given by the substantial derivatives of the $J_1(x, \hat{x})$

$$\frac{dJ_1}{dt} = \frac{\partial J_1}{\partial t} + \hat{f}(\hat{x}(t), \hat{p}(t))\nabla J_1, \tag{5}$$

where $\nabla = \left(\frac{\partial}{\partial \hat{x}_1}, \frac{\partial}{\partial \hat{x}_2}, \dots, \frac{\partial}{\partial \hat{x}_n}\right)^{\mathrm{T}}$ is the gradient operator in the estimated state space. Now, let

$$\frac{\partial \hat{p}}{\partial t} = -G\nabla_{\hat{p}} \frac{dJ_1}{dt}\,, \tag{6}$$

where $G > 0$ is the step length matrix. By defining,

$$J_1(x, \hat{x}) = \frac{w_1}{2}(\hat{x}_1 - x_1)^2 + \dots + \frac{w_n}{2}(\hat{x}_n - x_n)^2 = \sum_{i=1}^{n} \frac{w_i}{2}(e_i)^2, \tag{7}$$

where $e_i = \hat{x}_i - x_i$ are the state errors, we have

$$\frac{dJ_1}{dt} = \sum_{i=1}^{n} w_i e_i \left(\frac{de_i}{dt} + \hat{f}(\hat{x}(t), \hat{p}(t))\right). \tag{8}$$

As

$$\frac{de_i}{dt} = \frac{dx_i}{dt} - \frac{d\hat{x}_i}{dt} = \hat{f}(\hat{x}(t), \hat{p}(t)) - f(x(t), p(t)) \tag{9}$$

equation (8) reduces to

$$\frac{dJ_1}{dt} = \sum_{i=1}^{n} w_i e_i \left(2\hat{f}(\hat{x}(t), \hat{p}(t)) - f(x(t), p(t))\right). \tag{10}$$

Using equations (6) and (10) and because of $\nabla_{\hat{p}}\left\{f_i(x(t), p(t))\right\}$, we get

$$\frac{\partial \hat{p}}{dt} = -G\nabla_{\hat{p}} \frac{dJ_1}{dt} = -2G\nabla_{\hat{p}} \left\{\sum_{i=1}^{n} w_i e_i \hat{f}_i(\hat{x}(t), \hat{p}(t))\right\}. \tag{11}$$

This provides the updating law for estimated parameters in the identified system.

3 Improvement of the SG Method

In this part we adaptively select step length matrix, G, in a way to minimize a new local objective functional J_2. For this purpose we use descent gradient method

$$\frac{dg_{ij}}{dt} = -\alpha \frac{dJ_2}{dg_{ij}}\,, \tag{12}$$

where $G = |g_{ij}|,\ i,j = 1,2,\ldots,k$ and $\alpha > 0$. Consider the following objective functional candidate

$$J_2(x,\hat{x}) = \frac{v_1}{2}(\hat{x}_1 - x_1)^2 + \cdots + \frac{v_n}{2}(\hat{x}_n - x_n)^2 = \sum_{i=1}^{n} \frac{v_i}{2}(e_i)^2, \tag{13}$$

where $e_i = \hat{x}_i - x_i$ are the state errors, we will have

$$\frac{dJ_2}{dg_{ij}} = \frac{\partial J_2}{\partial \hat{x}} \frac{\partial \hat{x}}{\partial \hat{p}} \frac{\partial \hat{p}}{dg_{ij}}. \tag{14}$$

By using (13) we have

$$\frac{\partial J_2}{\partial \hat{x}} = [v_1 e_1,\ v_2 e_2,\ \ldots,\ v_n e_n]_{n\times 1}. \tag{15}$$

For calculation of $\frac{\partial \hat{x}}{\partial \hat{p}}$ we use (2)

$$\frac{\partial \dot{\hat{x}}}{\partial \hat{p}} = \frac{\partial}{\partial \hat{p}} \frac{d\hat{x}}{dt} = \frac{d}{dt} \frac{\partial \hat{x}}{\partial \hat{p}} = \frac{\partial \hat{f}}{\partial \hat{x}} \frac{\partial \hat{x}}{\partial \hat{p}} + \frac{\partial \hat{f}}{\partial \hat{p}}, \tag{16}$$

where $\hat{x} = [\hat{x}_1, \hat{x}_2, \ldots, \hat{x}_n]$ and it is assumed that

$$\frac{\partial}{\partial \hat{p}} \frac{d\hat{x}}{dt} = \frac{d}{dt} \frac{\partial \hat{x}}{\partial \hat{p}} \tag{17}$$

and the sufficient conditions for the validity of this equality are given in [23], page 279.

We have that $\hat{x}(t) = f(t,\hat{p})$ is continuous. $\frac{\partial \hat{x}}{\partial t}$, $\frac{\partial \hat{x}}{\partial \hat{p}}$ and $\frac{\partial}{\partial \hat{p}} \frac{\partial \hat{x}}{\partial t}$ exist and they are piece-wise continuous. Hence, equation (17) is valid. By using (3), (16) we get

$$\begin{aligned} \frac{d}{dt}\left(\frac{\partial \hat{x}}{\partial \hat{p}}\right)_{n\times k} &= \frac{d}{dt} \begin{bmatrix} \frac{\partial \hat{x}_1}{\partial \hat{p}_1} & \cdots & \frac{\partial \hat{x}_1}{\partial \hat{p}_k} \\ \vdots & \ddots & \vdots \\ \frac{\partial \hat{x}_n}{\partial \hat{p}_1} & \cdots & \frac{\partial \hat{x}_n}{\partial \hat{p}_k} \end{bmatrix} \\ &= \begin{bmatrix} \sum_{i=1}^{n} \left(\frac{\partial \hat{f}_1}{\partial \hat{x}_i} \frac{\partial \hat{x}_i}{\partial \hat{p}_1} \right) + \frac{\partial \hat{f}_1}{\partial \hat{p}_1} & \cdots & \sum_{i=1}^{n} \left(\frac{\partial \hat{f}_1}{\partial \hat{x}_i} \frac{\partial \hat{x}_i}{\partial \hat{p}_k} \right) + \frac{\partial \hat{f}_1}{\partial \hat{p}_k} \\ \vdots & \ddots & \vdots \\ \sum_{i=1}^{n} \left(\frac{\partial \hat{f}_n}{\partial \hat{x}_i} \frac{\partial \hat{x}_i}{\partial \hat{p}_1} \right) + \frac{\partial \hat{f}_n}{\partial \hat{p}_1} & \cdots & \sum_{i=1}^{n} \left(\frac{\partial \hat{f}_n}{\partial \hat{x}_i} \frac{\partial \hat{x}_i}{\partial \hat{p}_k} \right) + \frac{\partial \hat{f}_n}{\partial \hat{p}_k} \end{bmatrix}, \end{aligned} \tag{18}$$

where $\hat{x} \in R^n$ is the estimated state vector, $\hat{p}(t) \in R^k$ is the vector of estimated parameters.

For calculation of $\frac{\partial \hat{p}}{\partial g_{ij}}$ we use (6)

$$\frac{\partial \hat{p}}{dt} = -G\nabla_{\hat{p}} \frac{dJ_1}{dt} = -G f_{\hat{p}}(\hat{x}(t), \hat{p}(t), g_{ij}, t), \tag{19}$$

where $f_{\hat{p}}(\hat{x}(t),\hat{p}(t),g_{ij},t)=\left[f_{\hat{p}}^{1}(\hat{x}(t),\hat{p}(t),g_{ij},t),\,\dots,\,f_{\hat{p}}^{k}(\hat{x}(t),\hat{p}(t),g_{ij},t)\right]^{T}$ and we have

$$\frac{\partial\dot{\hat{p}}}{\partial g_{ij}}=\frac{\partial}{\partial g_{ij}}\frac{d\hat{p}}{dt}=\frac{d}{dt}\frac{\partial\hat{p}}{\partial g_{ij}}=\frac{\partial f_{\hat{p}}}{\partial\hat{p}}\frac{\partial\hat{p}}{\partial g_{ij}}+\frac{\partial f_{\hat{p}}}{\partial g_{ij}}\,,\quad \hat{p}=[\hat{p}_1,\hat{p}_2,\dots,\hat{p}_k]\,. \tag{20}$$

Using (20) gives

$$\frac{d}{dt}\left(\frac{\partial\hat{p}}{\partial\hat{g}_{ij}}\right)_{k\times k^2}=\frac{d}{dt}\begin{bmatrix}\frac{\partial\hat{p}_1}{\partial\hat{g}_{11}} & \frac{\partial\hat{p}_1}{\partial\hat{g}_{12}} & \cdots & \frac{\partial\hat{p}_1}{\partial\hat{g}_{kk}}\\ \frac{\partial\hat{p}_2}{\partial\hat{g}_{11}} & \ddots & & \vdots\\ \vdots & & & \\ \frac{\partial\hat{p}_k}{\partial\hat{g}_{11}} & \cdots & & \frac{\partial\hat{p}_k}{\partial\hat{g}_{kk}}\end{bmatrix}$$

$$=\begin{bmatrix}\sum_{i=1}^{k}\left(\frac{\partial\hat{f}_{\hat{p}}^{1}}{\partial\hat{p}_i}\frac{\partial\hat{p}_i}{\partial\hat{g}_{11}}\right)+\frac{\partial\hat{f}_{\hat{p}}^{1}}{\partial\hat{g}_{11}} & \sum_{i=1}^{k}\left(\frac{\partial\hat{f}_{\hat{p}}^{1}}{\partial\hat{p}_i}\frac{\partial\hat{p}_i}{\partial\hat{g}_{12}}\right)+\frac{\partial\hat{f}_{\hat{p}}^{1}}{\partial\hat{g}_{12}} & \cdots & \sum_{i=1}^{k}\left(\frac{\partial\hat{f}_{\hat{p}}^{1}}{\partial\hat{p}_i}\frac{\partial\hat{p}_i}{\partial\hat{g}_{kk}}\right)+\frac{\partial\hat{f}_{\hat{p}}^{1}}{\partial\hat{g}_{kk}}\\ \sum_{i=1}^{k}\left(\frac{\partial\hat{f}_{\hat{p}}^{2}}{\partial\hat{p}_i}\frac{\partial\hat{p}_i}{\partial\hat{g}_{11}}\right)+\frac{\partial\hat{f}_{\hat{p}}^{2}}{\partial\hat{g}_{11}} & \ddots & & \vdots\\ \vdots & & & \\ \sum_{i=1}^{k}\left(\frac{\partial\hat{f}_{\hat{p}}^{k}}{\partial\hat{p}_i}\frac{\partial\hat{p}_i}{\partial\hat{g}_{11}}\right)+\frac{\partial\hat{f}_{\hat{p}}^{k}}{\partial\hat{g}_{11}} & \cdots & & \sum_{i=1}^{k}\left(\frac{\partial\hat{f}_{\hat{p}}^{k}}{\partial\hat{p}_i}\frac{\partial\hat{p}_i}{\partial\hat{g}_{kk}}\right)+\frac{\partial\hat{f}_{\hat{p}}^{k}}{\partial\hat{g}_{kk}}\end{bmatrix} \tag{21}$$

By using (15), (18), (21) in (14), using (12), and by using appreciate numerical methods we can adaptively calculate G in each iteration. With the calculated G and (6) we can estimate system parameters. For assigning the initial value of step length matrix, $G(0)$, we could use genetic algorithms. In (12) $\alpha>0$ is arbitrary. But we can use a suitable 1-dimensional nonlinear programming method [17, 20], in each iteration, to calculate α.

4 Adaptive Calculation of Lyapunov Exponents

A Jacobian approach is used to calculate the Lyapunov exponents. Let the discrete time system be described by

$$x(k)=f(x(k-1)),\quad k=0,1,\dots, \tag{22}$$

where $x(k)\in R^n$ is the state vector and $f(.)$ is a continuously differentiable smooth function. Linearization of the system gives

$$x_k=J(k-1)x(k-1),\quad J(k-1)=\left(\frac{\partial f}{\partial x}\right)\bigg|_{k-1}\in R^{n\times n}. \tag{23}$$

Lyapunov exponents are defined as follows [14].

Definition 4.1 Let $Y^k=J_{k-1}J_{k-2}\dots J_0$, then the following symmetric positive definite matrix

$$\wedge=\lim_{t\to\infty}\left((Y^k)^{\mathrm{T}}\cdot Y^k\right)^{\left(\frac{1}{2k}\right)} \tag{24}$$

exists and the logarithms of its eigenvalues are called Lyapunov exponents.

To compute the Lyapunov exponents a QR factorization is used to decompose the Jocobian matrix as $J = QR$, where Q is an orthonormal matrix and R is upper triangular with positive diagonal elements. Then, using (23) Lyapunov exponents become

$$\lambda_i = \lim_{t\to\infty} \frac{1}{k} \ln(R_k^i \dots R_0^i) = \lim_{t\to\infty} \frac{1}{k} \sum_{i=1}^{k} \ln(R_k^i), \tag{25}$$

where R_k^i is the i-th diagonal element of R in k-th step. We can rewrite equation (24) into following recursive form

$$\lambda_i = \frac{t_{n-1}}{t_n} \lambda_{k-1}^i + \frac{1}{t_n} Ln(R_k^i). \tag{26}$$

5 Controller Design Methodology

In this section, an adaptive controller based on Lyapunov exponents placement is proposed. Calculating the Lyapunov exponents of the open loop system (λ_{ol}), if there exists at least one positive Lyapunov exponent, then the system is chaotic. For suppressing chaotic behavior of system, we choose some suitable negative Lyapunov exponents for closed loop system (λ_{cl}). Then the control input (u_k) is applied to the open loop system, equation (22)

$$\begin{cases} x(k) = f(x(k-1)) + u_k, \\ x(0) \text{ is given,} \end{cases} \tag{27}$$

where u_k is calculated from an adaptive state feedback law [16]

$$u_k = B_k x_k. \tag{28}$$

Let λ_{ol} and λ_{cl} be the Jacobians of the open loop and closed loop systems, respectively. Then

$$J_{cl} = J_{ol} + B_k. \tag{29}$$

To assign the Lyapunov exponents of the closed loop system in the desired locations, feedback matrix B_k, is calculated from following equation

$$B_k = -J_{cl}(k) + \begin{bmatrix} e^{\lambda_{cl}^1} & \dots & 0 \\ \dots & \dots & \dots \\ 0 & \dots & e^{\lambda_{cl}^n} \end{bmatrix}. \tag{30}$$

The Lyapunov exponent of the closed loop system will be the desired ones and since they are negative the system will suppress chaos.

If the control action is large and we want a smaller control input for suppressing chaos, we can apply control action when we are in a neighborhood of the desired (equilibrium) point.

6 Simulation Results

In this section, simulation results are used to show the main points of the paper. The first example is the NLP chaotic Duffing system. The second example is the Lorenz chaotic system which is LP and the proposed method, with fixed step length matrix, is compared with the previous Lyapunov exponent identification strategy based on recursive least squares estimation. The third example compares proposed method with fixed step length matrix and adaptive step length matrix to show the effectiveness of the improved method.

Example 6.1 State equations of the forced Duffing's oscillator are

$$\begin{cases} \dot{x}_1 = x_2, \\ \dot{x}_2 = -p_1 x_1 - p_2 x_1^3 - p x_2 + q\cos(wt), \end{cases} \tag{31}$$

where p_1, p_2, p, q and w are the parameters of the NLP system. And x_1, x_2 are the states of the system. This equation arises in models of the forced vibration of buckled beams and in electrical circuits [17, 18, 19, 20]. For $p = 0.168$, $p_1 = -0.5$, $p_2 = 0.5$, $q = 0.21$, $w = 1$ system is chaotic. Figure 6.1 is the Lyapunov exponents of this uncontrolled system. One of the exponents is positive then the system is chaotic.

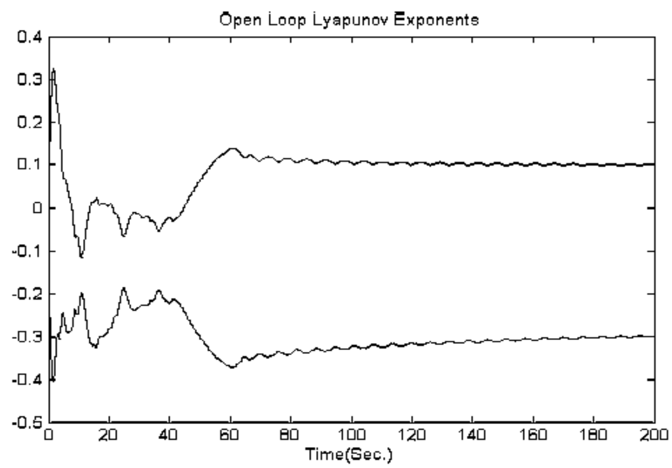

Figure 6.1: Lyapunov exponents of the open loop Duffing system.

Selected sampling period is 0.004 second and the desired closed loop Lyapunov exponents are $\lambda_{cl}^1 = -0.5$, $\lambda_{cl}^2 = -0.6$. Figure 6.2 shows the estimated parameters that converge to the real values. Figure 6.3 shows the states of the system where in the 30-th second, the control signal is applied to the system. Figure 6.3 shows the chaotic behavior of the open loop system. Chaotic System has aperiodic noise-like behavior.

Figure 6.4 shows the closed loop Lyapunov exponents that converge to the desired values. Prior to 30-th second Lyapunov exponents are for the open loop system and after that they converge to the desired values $(-0.5, -0.6)$. It is important to know that the control input implemented when system is chaotic. Figure 6.5 shows the control input. Figure 6.6 shows the states of the closed loop system that becomes a stable limit cycle.

Example 6.2 In this example, the proposed method is applied to the Lorenz system and the results are compared with the RLS method. State space equations of the system

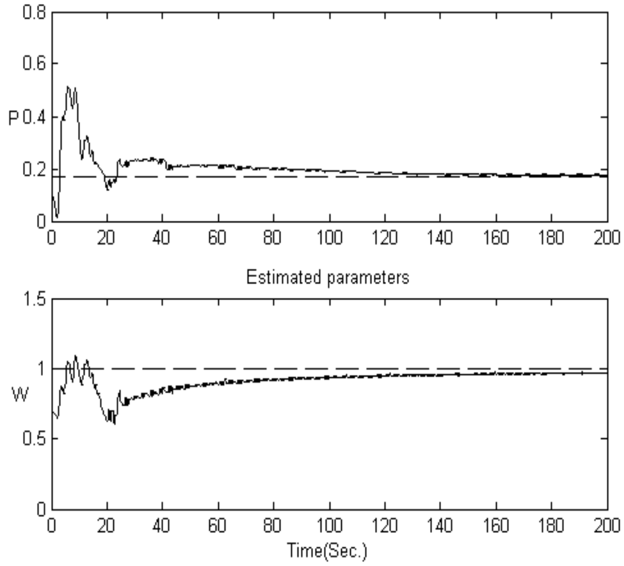

Figure 6.2: Estimated parameters.

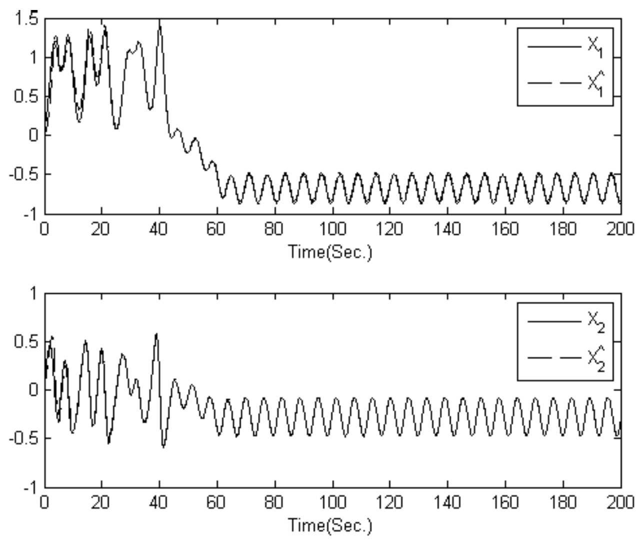

Figure 6.3: States of the Duffing system.

are

$$\begin{cases} \dot{x} = \sigma(y - x), \\ \dot{y} = rx - y - zx, \\ \dot{z} = yx - bz, \end{cases} \tag{32}$$

where parameters are $r = 27$, $\sigma = 10$ and $b = 8/3$. This equation arises in models of

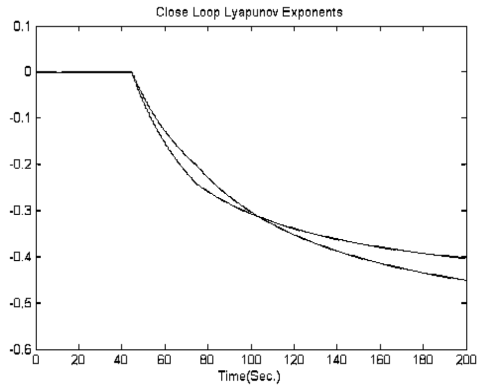

Figure 6.4: Closed loop system Lyapunov exponents.

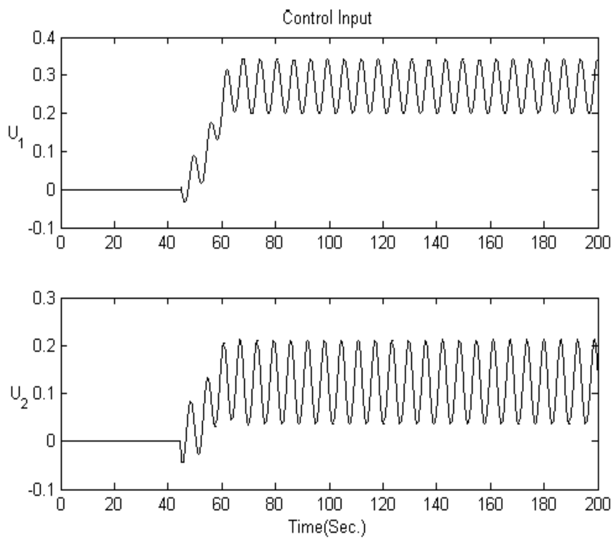

Figure 6.5: Control input.

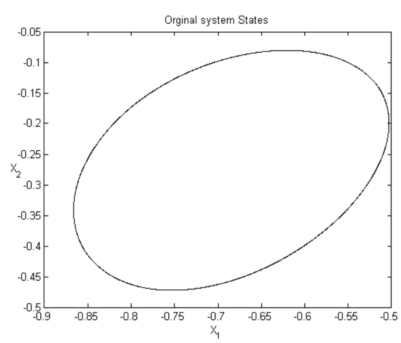

Figure 6.6: States of closed loop Duffing system.

the turbulent motion in convection systems [21, 22, 12]. The equilibrium points of this system are $(\pm\sqrt{b(r-1)},\ \pm\sqrt{b(r-1)},\ r-1)$ and $(0,0,0)$. Figure 6.7 shows estimated parameters with RLS method. And Figure 6.8 shows the estimated parameters with the proposed method.

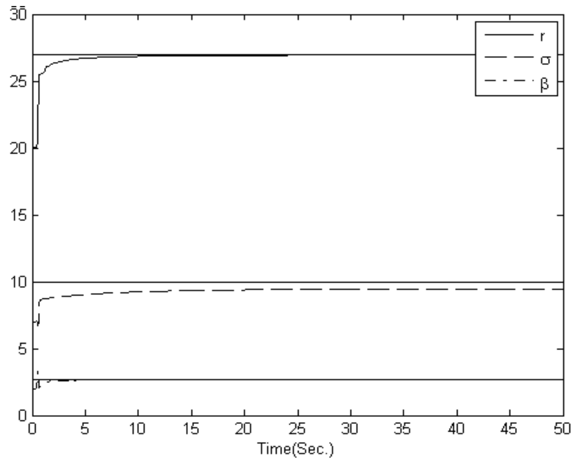

Figure 6.7: Estimated parameters of the system by RLS method.

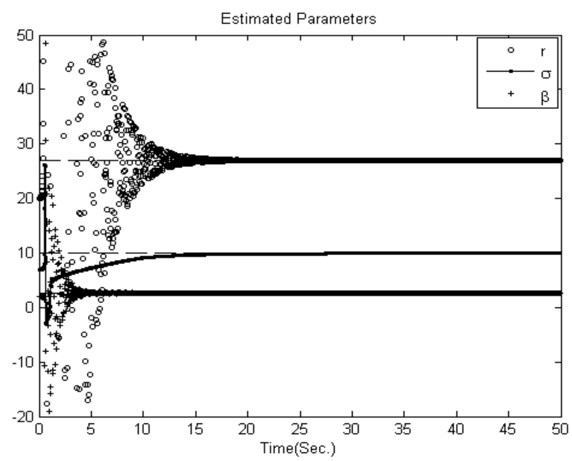

Figure 6.8: Estimated parameters of system by the proposed method.

It is obvious that the estimation performance of the proposed method is superior to the RLS based approach in faster convergence and unbiased estimates.

Example 6.3 In this example we want to show the effectiveness of the improved SG method. We have used the following $G(0)$, which is resulted from genetic algorithms. Figure 6.9 is resulted from the simulation of equation (6).

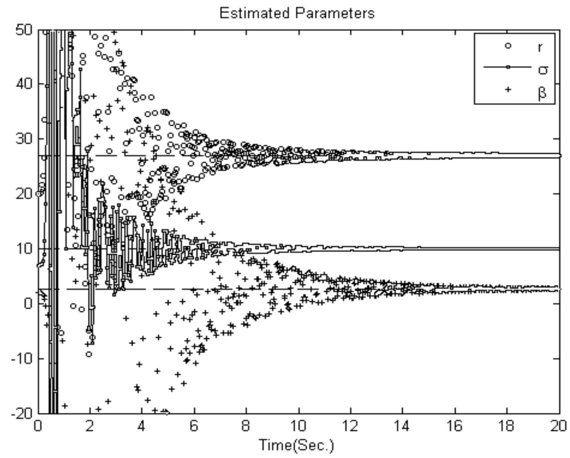

Figure 6.9: Estimated parameters of system by the proposed method.

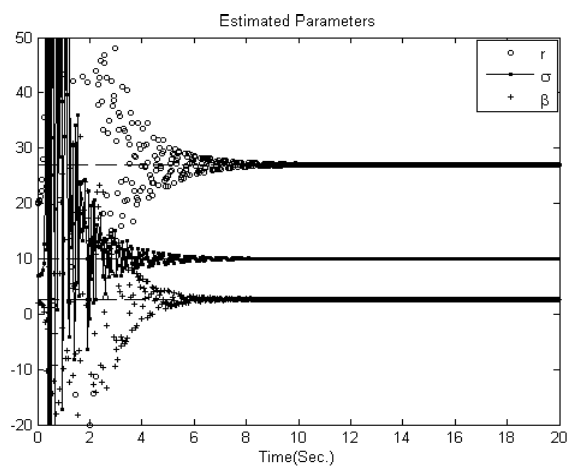

Figure 6.10: Estimated parameters of system by the Improved SG method.

Figure 6.10 is resulted from simulation of (6) and (12). Comparison of the figures intuitively clears that the Improved SG Method has faster convergence rate.

$$\begin{bmatrix} 48.5 & 0 & 5.5711 \\ 0 & 434.25 & 4815 \\ 1.2119 & 0.7902 & 48.1986 \end{bmatrix}.$$

7 Conclusions

This paper provides an estimation method for on-line identification of the Lyapunov exponents of nonlinear in parameters chaotic systems. This method is based on the minimization of two objective functionals. For faster convergence rate of the parameters, the new improved SG (ISG) method is developed. Also, the parameter estimation and Lyapunov exponent placement methods are combined for adaptive control of NLP chaotic systems. Simulation results are provided for adaptive control of Duffing's Oscillator. Also, a comparison with the RLS method in LP systems is given to show the superior performance of the proposed method. Finally, we showed the effectiveness of the improved SG Method in identification of the parameters of the Lorenz system.

References

[1] Boccaletti, S., Grebogi, C., Lai, Y.C., Mancici, H., and Maza, D. The Control of Chaos: Theory and Applications. *Physics Reports* **329** (2000) 107–193.

[2] Andrievskii, B.R. and Fradkov, A.L. Control of Chaos: Methods and Applications, II. Applications. *Automation and Remote Control* **65**(4) (2004) 505–533.

[3] Andrievskii, B.R. and Fradkov, A.L. Control of Chaos: Methods and Applications, I. Methods. *Automation and Remote Control* **64**(5) (2003) 673–713.

[4] Khaki-Sedigh, A. and Yazdanpanah-Goharrizi, A. Observer Based Design of Set-Point Tracking Adaptive Controller for Nonlinear Chaotic Systems. *Chaos – Solitons and Fractals* **23** (2006) 1063–1072.

[5] Tian, Yu-Ping and Yu, X. Adaptive Control of Chaotic Dynamical Systems Using Invariant Manifold Approach. *IEEE Trans. on Circuit and Systems–I* **47**(10) (2000) 1537–1542.

[6] Zhu, Y. Estimation of Nonlinear ARX Models. *IEEE Conference of Decision and Control.* **2** (2002) 2214–2219.

[7] Chau, K.T. and Chan, C.C. Nonlinear Identification of Power Electronic Systems. *IEEE Conference* **1** (1995) 329–334.

[8] Ljung, L. *System Identification Theory for Users.* Prentice Hall, Englewood Cliffs, 1999.

[9] Chong, E.K.P. and Zak, S.H. *An Introduction to Optimization.* John Wiley & Sons, New York, 2001.

[10] Rao, Singiresu S. *Engineering Optimization Theory and Practice.* New Age International, New Delhi, 2004.

[11] Crispin, Y. A Fluid Dynamical Approach to the Control, Synchronization and Parameter Identification of Chaotic Systems. *American Control Conference* (2002) 2245–2250.

[12] Hilborn, R.C. *Chaos and Nonlinear Dynamics an Introduction for Scientist and Engineers.* Oxford University Press, 2000. -

[13] Fradkov, A.L. and Pogromsky. A.Yu. *Introduction to Control of Oscillations and Chaos.* World Scientific, Singapore, 1998.

[14] Khaki-Sedigh, A., Ataei, M. Lohmann, B. and Lucas, C. Adaptive calculation of Lyapunov exponents from time series observations of chaotic time varying dynamical systems. *Nonlinear Dynamics and Systems Theory* **4**(2) (2004) 145–160.

[15] Lu, J., Yang, G., Oh, H. and Luo, A.C.J. Computing Lyapunov Exponents of Continuous Dynamical Systems: Method of Lyapunov Vectors. *Chaos – Solitons and Fractals* **23** (2005) 1879–1892

[16] Chen, G. and Lai, D. Making a Dynamical System Chaotic: Feedback Control of Lyapunov Exponents for Discrete-Time Dynamical Systems. *IEEE Trans. on Circuit and Systems–I* **44**(3) (1997) 250–253.

[17] Gao, X., Yu, J. Chaos in the Fractional Order Periodically Forced Complex Duffing's Oscillators. *Chaos, Solitons and Fractals* **24** (2005) 1097–1104.

[18] Mohamad, G.M., Mohamad, A.A. and Aly, S.A. Strange Attractors and Chaos Control in Periodically Forced Complex Duffing's Oscillators. *Physica A.* **292** (2001) 193–206.

[19] Tseng, W.Y. and Dugundji, J. Nonlinear Vibrations of a Buckled Beam under Harmonic Excitation. *J. of Appl. Mech.* **38** (1971) 467–476.

[20] Holmes, P. Averaging and Chaos in Forced Oscillations. *SIAM J. of Appl. Math.* **38** (1980) 65–80.

[21] Elwakil, A. S., Ozoguz, S. and Kennedy, M.P. Creation of a Complex Butterfly Attractor Using a Novel Lorenz-Type Syatem. *IEEE Trans. Circuit and Systems–I* **46**(4) (2002) 527–530.

[22] Osinga, Hinke M. and Kraus Kopf, B. Visualizing the Structure of Chaos in the Lorenz System. *Computer & Graphica.* **26** (2002) 815–823.

[23] Apostol, T.M. *Calculus. Vol. II: Multivariable Calculus and Linear Algebra, with Application to Differential Equations Probability.* Blaisdell Publishing Co., Waltham, 1969.

Nonlinear Dynamics and Systems Theory, 8 (2) (2008) 137–150

Quasi-Optimal Control for Path Constrained Relative Spacecraft Maneuvers Based on Dynamic Programming

R. Bevilacqua [1] and M. Romano [2*]

[1] *US Naval Postgraduate School, Department of Mechanical and Astronautical Engineering, Code MAE/RB, 699 Dyer Rd., Monterey, California, 93943.*

[2] *US Naval Postgraduate School, Department of Mechanical and Astronautical Engineering, Code MAE/MR, 700 Dyer Rd., Monterey, California, 93943.*

Received: February 13, 2007; Revised: June 11, 2007

Abstract: Autonomous close flight and docking of a chaser spacecraft to a target are still challenging problems. In this paper the Hill–Clohessy–Wiltshire equations are taken as dynamic model and inverted, after a variable change, in order to be used by a control algorithm to drive the chaser spacecraft along a specified path. The path parameterization is performed by using cubic B-splines and by having the curvilinear abscissa as parameter. The proposed optimization algorithm uses dynamic programming to find quasi-optimal controls. The number of optimization parameters is drastically reduced by working only on the acceleration component along the vehicle trajectory. The shape of the path can be chosen according to the specific maneuver requirements. In particular, the optimization algorithm is split into a trajectory planner which generates the best tangential acceleration sequence through backward exploration of a tree of possible policies, and a control generator which inverts the parameterized dynamics in order to get the thrusters commands sequence. The optimization algorithm has been coded in Simulink as a library of embedded functions and has been experimentally proved to run in real time.

Keywords: *Satellites rendezvous; dynamic programming; dynamic inversion; cubic B-splines.*

Mathematics Subject Classification (2000): 49K15, 70M20.

* Corresponding author: mromano@nps.edu.

Nomenclature

$\vec{a},\ a$ = Generic vector and its magnitude
$\mathbf{B}$ = Universal transformation matrix for cubic B-splines
ds = Path section length
$\frac{d^2(.)}{dt^2}$ = Time derivatives with respect to the inertial frame
$\frac{\delta(.)}{\delta s}$ = Partial derivative with respect to s
$\vec{\gamma}$ = Cubic B-splines parameter
J = Cost functional
$\mathbf{K}$ = Matrix containing the vector positions of the cubic B-splines control points
$LVLH$ = Local vertical local horizontal coordinate system
μ = Earth gravitational constant
N_L = Number of levels in dynamic programming tree
N_C = Number of values for control discretization
$\hat{n}$ = Path normal unit vector
$\vec{\omega}_{LVLH}$ = Angular velocity in LVLH
$\vec{r}$ = Position vector
$\underline{\underline{r}}$ = Dyadic of position vector $\vec{r}$
$\vec{r}_c$ = Chaser position vector in the inertial frame
$\vec{r}_t$ = Target position vector in the inertial frame
$\vec{r}_{rel}$ = Chaser-target relative position vector
$\vec{r}^* = [r_x, r_y, 0]^T$
ρ = Local curvature of path
s = Curvilinear abscissa
t = Time
$\hat{\tau}$ = Path tangent unit vector
$\vec{u}$ = Acceleration control vector
x, y, z = Components of $\vec{r}_{rel}$ in LVLH
$\underline{\underline{1}}$ = Unitarian dyadic
$(.)_0,\ (.)_f$ = Value at initial and final time
$\dot{(.)},\ \ddot{(.)}$ = Time derivatives in LVLH
$(.)_x\,(.)_y\,(.)_z$ = Components along $x,\ y,\ z$ axis of LVLH

1 Introduction

Many researches have been performed on modeling [1]–[8] and optimizing [9] the maneuvers for Spacecraft Rendezvous and Docking, but real-time implementation of the optimal control is still a difficult task. In [10] and [11] the maneuvers for passing from an initially stable relative motion to a final stable state are optimized. In these works there is no possibility of considering generic initial conditions for the relative position and velocity of the chaser vehicle with respect to the target. In [9] the optimization is performed in two stages: the first part of the trajectory is optimized without any restriction on the chaser vehicle position, the last phase of docking is along a fixed direction.

All of the above references prove the effectiveness of their respective approaches by using numerical simulations. None of them perform hardware experimentation on real-time computing. Furthermore, the current docking missions, such as the Space

Shuttle-International Space Station (ISS) mating, and the planned Automated Transfer Vehicle-ISS supply service, do not include any closed-loop optimization for the rendezvous trajectories.

The objective of our research is threefold: first, we want to be able to impose a certain path in order to guarantee a priori the safety of the maneuver, second, we want to track the set path with minimum propellant consumption, third, we want our solution to be suitable for real time implementation.

The proposed strategy is a direct optimization method similar to the one used in [12] and [13] for the control of robotic manipulators and in [14] for the control of aircraft. The basic idea is to parameterize the trajectory in a way that allows for independent choice of path and velocity profile. In order to obtain such feature, we use here the curvilinear abscissa as in [12] and [13].

Dynamic Programming [15] is used as the optimization method. This approach has been proved to be suitable for real-time implementation, especially when a sub-optimal solution is searched through a step-by-step optimization of the trajectory [16, 17].

Our contribution is focused on real-time autonomous control during the very last phases of satellites docking procedure.

The paper is organized as follows: Section 2 formally states the problem. Subsection 2.1 describes the dynamic model and the inversion of the dynamics. Section 3 presents the path parameterization via cubic B-splines. Section 4 is dedicated to the developed optimization algorithm. Section 5 reports some significant results obtained via numerical simulations. Section 6 illustrates the real-time test which has been performed to prove the capability of running in real-time. Finally, Section 7 concludes the paper.

2 Problem Statement

The aim of the present work is to quickly design an optimal control sequence which drives the chaser vehicle towards the target on a specified path $\vec{r}_{rel} = \vec{r}(s)$. Without loss of generality, the boundary conditions are assumed to be $\vec{r}_{rel}(t_0) = \vec{r}_0$, $\vec{r}_{rel}(t_f) = \vec{0}$.

The following minimum-propellant cost function is considered for the optimal control problem:

$$J = \int_{t_0}^{t_f} |\vec{u}|^2 dt. \tag{1}$$

2.1 Dynamic model and dynamics inversion

We use the well known Hill-Clohessy-Wiltshire equations in order to model the system dynamics. We consider the x axis of the LVLH coordinate system centered on the target directed along the radial line, the y axis directed along the orbital velocity, and the z axis consequently directed to complete the right frame.

The HCW equations can be written in vector form as:

$$\ddot{\vec{r}}_{rel} + 2\vec{\omega}_{LVLH} \times \dot{\vec{r}}_{rel} - \omega_{LVLH}^2 \vec{r}^{\,*}_{rel} = \frac{\mu}{r_t^5}\left(3\underline{\underline{r_t}} - r_t^2 \underline{\underline{1}}\right) \cdot \vec{r}_{rel} + \vec{u}. \tag{2}$$

As stated above, the proposed optimization approach is based on the search for a suboptimal policy to drive the chaser vehicle along a specified path. The specified path is parameterized in terms of the curvilinear abscissa as follows [13]:

$$\vec{r}_{rel} = \vec{r}\,(s) = [x\,(s)\,,\, y\,(s)\,,\, z\,(s)]. \tag{3}$$

Differentiation with respect to time and substitution of this relation into (2) gives:

$$\frac{\delta^2\vec{r}}{\delta s^2}\dot{s}^2 + \frac{\delta\vec{r}}{\delta s}\ddot{s} + 2\vec{\omega}_{LVLH} \times \frac{\delta\vec{r}}{\delta s}\dot{s} - \omega_{LVLH}^2\vec{r}^{*} = \frac{\mu}{r_t^5}\left(3\underline{\underline{r_t}} - r_t^2\underline{\underline{1}}\right)\cdot\vec{r} + \vec{u}. \tag{4}$$

The tangential acceleration profile $\ddot{s}$ to be tracked by the chaser spacecraft is considered as the free parameter for the optimization. Once the tangential acceleration profile is obtained, the actual controls (accelerations along the three axis) are then determined by inverting the dynamics equation. In particular, by starting from (4), it results:

$$\vec{u} = -\frac{\mu}{r_t^5}\left(3\underline{\underline{r_t}} - r_t^2\underline{\underline{1}}\right)\cdot\vec{r} + \frac{\delta^2\vec{r}}{\delta s^2}\dot{s}^2 + \frac{\delta\vec{r}}{\delta s}\ddot{s} + 2\vec{\omega}_{LVLH} \times \frac{\delta\vec{r}}{\delta s}\dot{s} - \omega_{LVLH}^2\vec{r}^{*}. \tag{5}$$

Since we work in terms of acceleration along the path, it is not practical to impose directly constraints on the controls by using (5).

3 Geometric Representation of the Path

We use cubic B-spline curves to represent the trajectory $\vec{r}_{rel} = \vec{r}(s)$. B-splines have the advantage of narrowly propagating the local changes [18]. Given n control points, a first and second order continuous curve which fits them is univocally determined by a composition of $n-1$ B-splines. As the positions of the control points change, the curve shape changes consequently. Each spline is defined by four control points and has the parametric representation:

$$\vec{r}(\vec{\gamma}) = \vec{\gamma}\mathbf{BK}, \tag{6}$$

where $\vec{r}(\vec{\gamma})$ is the position vector of a generic point of the spline, $\vec{\gamma}$ is the parameter vector, defined as:

$$\vec{\gamma} = \begin{bmatrix} \gamma^3 & \gamma^2 & \gamma & 1 \end{bmatrix}, \ 0 \le \gamma \le 1, \tag{7}$$

K contains the vector positions of the control points:

$$\mathbf{K} = \begin{bmatrix} \vec{r}_0 & \vec{r}_1 & \vec{r}_2 & \vec{r}_3 \end{bmatrix}^{\mathbf{T}} \tag{8}$$

and B is the universal transformation matrix, obtained by imposing continuity, which contains the same numerical values for every B-spline ([18]):

$$\mathbf{B} = \mathbf{\frac{1}{6}}\begin{bmatrix} -1 & 3 & -3 & 1 \\ 3 & 6 & 3 & 0 \\ -3 & 0 & 3 & 0 \\ 1 & 4 & 1 & 0 \end{bmatrix}. \tag{9}$$

Accordingly, the partial derivatives of the path with respect to the arc length, needed in Eq. (4) and Eq. (5), are given by:

$$\frac{\delta\vec{r}}{\delta s} = \frac{\frac{\delta\vec{r}}{\delta\gamma}}{\left|\frac{\delta\vec{r}}{\delta\gamma}\right|}, \ \ \frac{\delta^2\vec{r}}{\delta s^2} = \frac{\frac{\delta^2\vec{r}}{\delta\gamma^2}}{\left|\frac{\delta\vec{r}}{\delta\gamma}\right|^2} - \frac{\delta\vec{r}}{\delta\gamma}\frac{\frac{\delta\vec{r}}{\delta\gamma}\cdot\frac{\delta^2\vec{r}}{\delta\gamma^2}}{\left|\frac{\delta\vec{r}}{\delta\gamma}\right|^4}, \tag{10}$$

where

$$\frac{\delta\vec{r}}{\delta\gamma} = \begin{bmatrix} 3\gamma^2 & 2\gamma & 1 & 0 \end{bmatrix}\mathbf{BK}, \ \ \frac{\boldsymbol{\delta^2\tilde{r}}}{\boldsymbol{\delta\gamma^2}} = \begin{bmatrix} 6\gamma & 2 & 0 & 0 \end{bmatrix}\mathbf{BK}. \tag{11}$$

Since the B splines, by definition, do not pass through the end points, two additional artificial control points are added at the extremes of the curve.

In order to convert the value of the global arc length along the path s to the corresponding value of the parameter along the local spline γ it is sufficient to numerically find the zero of the following function:

$$h(\gamma) = s - \left(s_{0_{\text{current spline}}} + \int_0^{\gamma} \frac{ds}{d\gamma} d\gamma \right), \tag{12}$$

where

$$\frac{ds}{d\gamma} = \sqrt{\left(\frac{dx(\gamma)}{d\gamma}\right)^2 + \left(\frac{dy(\gamma)}{d\gamma}\right)^2 + \left(\frac{dz(\gamma)}{d\gamma}\right)^2}. \tag{13}$$

4 Optimization Approach by Dynamic Programming

Dynamic programming [15] is very useful in problems where one needs to take subsequent decisions. The word "dynamic" states that the decisions are sequentially taken. Sequenced problems can be solved according to the Bellman's principle of optimality:

Definition 4.1 An optimal strategy has the property that, no matter the initial state and decision, the future decision's set has to constitute an optimal strategy with respect to the state reached according to the decisions taken until that moment.

Dynamic programming takes the decisions one by one. At every step the optimal policy for the future is found, independently of the past decisions. The cost function is divided in the sum of elementary costs, one for each segment of the trajectory. In the present work we adopt a similar approach to the one of [16].

The curvilinear acceleration on the specified curve is taken as the parameter for the optimization. By limiting to one the number of variables the algorithm has to work with, the issue of "curse of dimensionality" [16] is greatly mitigated. Once the optimal $\ddot{s}$ profile is determined, the controls are calculated according to (5). On a certain segment of the entire path, where the acceleration $\ddot{s}$ is kept constant, we know that the section length ds needs a time interval t to be run:

$$\begin{gathered} t = -\frac{\dot{s}_0}{\ddot{s}} \pm \sqrt{\left(\frac{\dot{s}_0}{\ddot{s}}\right)^2 + \frac{2ds}{\ddot{s}}} \\ \left(s(t) = s_0 + \dot{s}_0 t + \ddot{s}\frac{t^2}{2} ds = \dot{s}_0 t + \ddot{s}\frac{t^2}{2} \rightarrow t^2 + \frac{2\dot{s}_0}{\ddot{s}} t - \frac{2ds}{\ddot{s}} = 0 \right). \end{gathered} \tag{14}$$

The complete path is divided into segments of length ds, the controls and time requested to run each segment are calculated and finally the integral 1 is evaluated. In particular, the algorithm tests different possibilities, in terms of possible sequence of levels of $\ddot{s}$, by using the tree approach described below. Feasibility of the sequences is tested by imposing the satisfaction of the following constraints:

$$\begin{cases} s(t_f) = s_f = trajectory\ length, \\ \dot{s}(t_f) = 0 = final\ velocity. \end{cases} \tag{15}$$

The tree of possible policies is a graph structure, with no cycles, in which every node generates different branches, every one connected to a subsequent node, called son-node. A son can generate other sons. Every node, but the root, has only one entering branch which belongs to the parental node. The root does not have any father. Starting from the initial condition, the tree of possible trajectories is built in an incremental way, by exploring the reachable states in order to find the optimal path. Every step adds new branches (so new nodes) to the tree, only if they are acceptable: in particular, only positive velocities are admitted. Therefore, nodes with zero velocity and zero acceleration are not taken into account. Moreover, the cases when equation (14) does not have real solutions are discarded, since this implies that the current section cannot be run with the current value of $\ddot{s}$. A cost value is associated to every node. The cost is calculated through a trapezoidal integration formula of the control magnitude. The algorithm goes on till the stopping condition is reached. At this point it is necessary to run the tree backwards in order to find the optimal policy, i.e. the one which brings to the final node at minimum cost.

The algorithm outline follows (see also Figure 4.1):

1. Start from the initial condition s_0, $\dot{s}_0$ (ROOT).
2. Apply one of the N_C possible value of $\ddot{s}$ until the trajectory segment ds is completed.
3. Repeat step 2 for each possible value of acceleration: one generation is then obtained.
4. Calculate the cost function for each node of the present generation.
5. Starting from every son, repeat step 2 and 3 and obtain the second generation.
6. Iterate step 2, 3 and 4 until the final desired condition s_f, $\dot{s}_f$ is reached.
7. Recognize the minimum cost node of the last generation. In Figure 4.1 the numbers at the top report, as an example, the total cost associated with every node.
8. Individuate the optimal policy, by starting from the optimal son of the last generation and run the tree backward.

From the software point of view each son-node is represented by a 7 elements array:

1. Value of the curvilinear abscissa s (this value is the same for every node of the same generation).
2. Value of the velocity along the path $\dot{s}$.
3. Value of the acceleration along the path $\ddot{s}$ ("control").
4. Time to reach the node from the previous one.
5. Cost associated to the last branch.
6. Total time (from beginning of the path) to run until that point.
7. Index (identifier of the father).

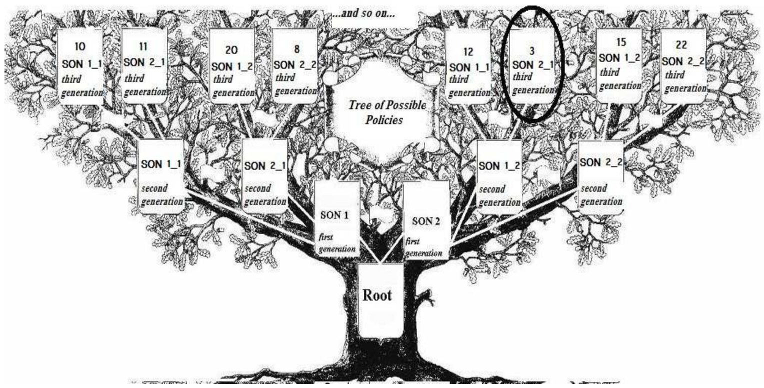

Figure 4.1: Tree of possible policies.

By keeping memory of the father for every node it is possible to quickly run the tree backwards once the final condition is reached in order to find the best $\ddot{s}$ profile. The number of generations N_L (that is, the number of segments in which the path is divided) and the number N_C of admissible acceleration values $\ddot{s}$ can be selected by the user.

The required memory and computation time increase very quickly with the number of levels, as the maximum number of nodes to be evaluated is $N_C^{N_L}$.

The tree exploration is the most time consuming portion of the algorithm. A pruning approach is implemented in order to increase the computation efficiency. The new nodes of a generation are analyzed while building the tree and pruned if the remaining length of trajectory to be run is not sufficient to brake down with the minimum available acceleration in order to reach the final point with zero velocity.

5 Simulation Results

Two sample simulation cases are here presented in order to show the main features of the proposed approach.

5.1 Simulation test case 1

The first simulation shows the behavior of the proposed algorithm in the computation of a quasi-optimal docking maneuver as a function of the number of path segments (number of generations or levels, of the dynamic programming algorithm). The parameters of the maneuver are reported in Table 5.1. A cubic path $(y = ({y_0}/{x_0^3})x)$ is taken as reference.

The same constrained path has been correctly obtained for any number of levels, as the nature of the algorithm implies. This result is reported in Figure 5.1.

Parameter	Units	Value
Height above the Earth surface	km	480
Maximum (minimum) tangential acceleration $\ddot{s}_{\max}$ $(-\ddot{s}_{\min})$	$\frac{m}{s^2}$	$5 \cdot 10^{-4}$
Initial velocity $\dot{s}_0$	$\frac{m}{s}$	0.2
Initial position $(x_0,\, y_0,\, z_0)$	m	(300, 400, 0)
Number of path segments N_L	-	5
Number of possible tangential acceleration values N_C	-	3

Table 5.1: Numerical values for cubic manoeuvre.

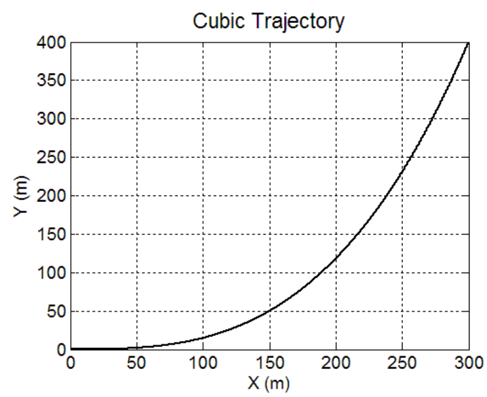

Figure 5.1: Cubic path tracked by the chaser.

Figure 5.2 shows the fuel consumption and time required for the manoeuvre, Figure 5.3 shows the CPU time (on a Pentium IV machine). The independent variable is the number of levels.

It is apparent in Figure 5.2 that increasing the number of levels means a larger tree to build and explore, i.e. higher CPU resources. Figure 5.3 is worth some comment on the goal of the proposed technique. The proposed approach gives a sub-optimal solution. In particular, by dividing the trajectory in a finite number of segments, and imposing a limited set of values for the command acceleration, we are clearly introducing considerable discretization into the problem. Therefore the solution is heavily dependent on the number of levels. For the presented simulation case and for several other tests we have run, it results that the algorithm gives the best result for a number of levels between 4 and 6, as indicated in Figure 5.2 (a). The CPU time is also reasonable within that range. Figure 5.4 reports the controls profile for three different numbers of levels.

5.2 Simulation test case 2

The second simulation (see Table 5.2) considers the final straight line maneuver (along the y direction) bringing a chaser spacecraft to dock with its target, as previously studied in [9]. We show here how the tree strategy is able to generate similar results to [9], but in a quicker way. Furthermore, initial and final conditions are exactly satisfied. The initial conditions here adopted are the intermediate conditions (breakpoint between two stages) reported in [9]:

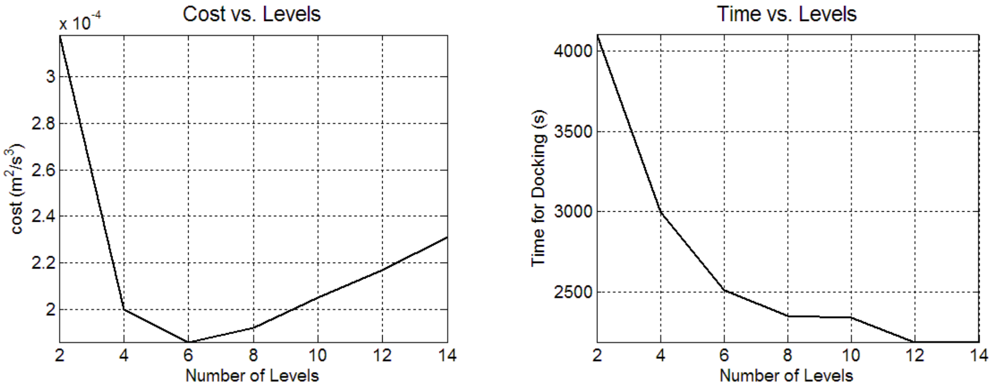

Figure 5.2: a) Fuel vs. levels; b) Time for manoeuvre vs. levels.

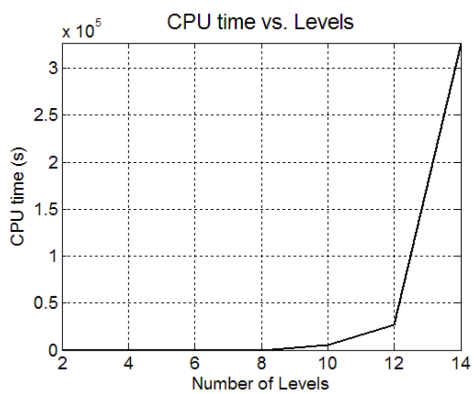

Figure 5.3: CPU time vs. n. of levels.

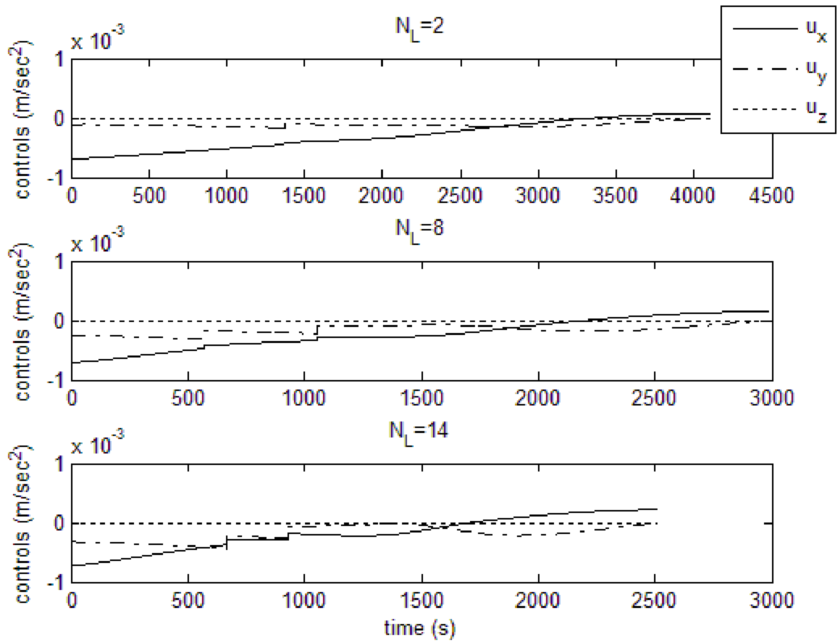

Figure 5.4: Controls vs. Time, increasing N_L

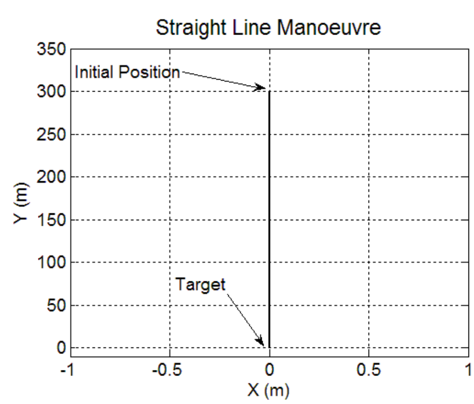

Figure 5.5: Straight line trajectory.

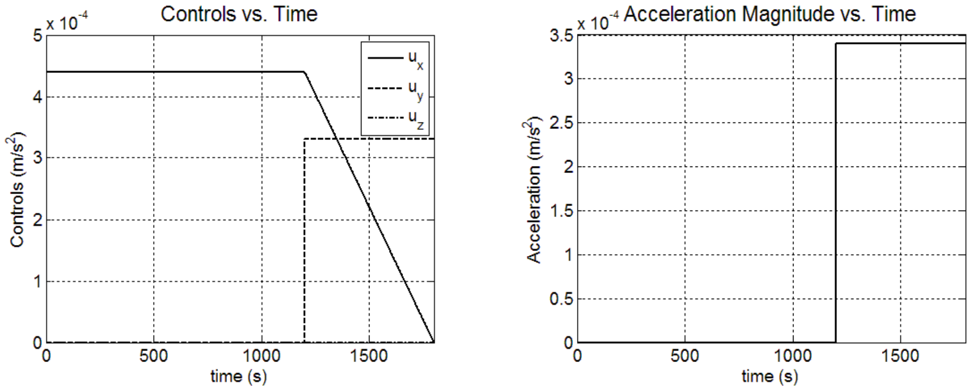

Figure 5.6: a) Controls vs. time; b) Acceleration vs. time.

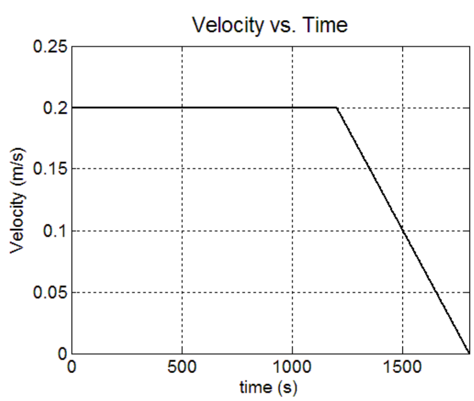

Figure 5.7: Velocity vs. time.

Parameter	Units	Value
Height above the Earth surface	km	480
Maximum (minimum) acceleration $\ddot{s}_{\max}$ $(-\ddot{s}_{\min})$	$\frac{m}{s^2}$	$5 \cdot 10^{-4}$
Initial velocity $\dot{s}_0$	$\frac{m}{s}$	0.2
Initial position $(x_0,\, y_0,\, z_0)$	m	(0, 300, 0)
Number of levels N_L	-	5
Number of possible tangential acceleration values N_C	-	3

Table 5.2: Numerical values for straight line maneuver.

Figure 5.5 shows that the trajectory is perfectly tracked. The controls, acceleration and velocity profile are reported on Figure 5.6 and Figure 5.7. The time required to complete the docking is $1800\,s$, with a total cost of $1.566 \cdot 10^{-4}\,\dfrac{m^2}{s^3}$, while in [9] the corresponding values are: $1885\,s$, $1.538 \cdot 10^{-4}\,\dfrac{m^2}{s^3}$. Discrepancies in cost and time are due to the fact that in [9] the final boundary conditions, are not exactly matched, whereas we are here maneuvering between two specified and accurately achieved positions and velocities.

6 Real-Time Validation

For the above reported simulations, the optimization algorithm was coded in Matlab-Simulink.

Furthermore, validation of the capability of our proposed approach to run in real time has been experimentally obtained. In particular, a desktop computer, running the Mathworks-XPC target operative system, has been used as target hardware by downloading the compiled version of the optimization software.

Figure 6.1 shows the Simulink model. It is composed by two main Embedded Functions. The Planner generates a sequence of nodes following the near-optimal $\ddot{s}$ profile. This sequence is feed forwarded to the dynamic inversion function (called "control generation"). On a Pentium II $800\,Mhz$ machine, the algorithm run in real time at a sample frequency of $5\,Hz$.

7 Conclusion

The present work uses a direct approach for real time sub-optimal control of spacecraft rendezvous and docking along a constrained path. The Hill–Clohessy–Wiltshire equations are used as basis for a dynamic inversion computation and the path is parameterized through cubic B-splines having the curvilinear abscissa as parameter. Dynamic programming operating on the curvilinear acceleration is proposed as optimization method in order to find the fuel optimal policy to drive the chaser spacecraft to the target spacecraft. The reliability of the algorithm has been assessed for different number of levels in the dynamic programming tree, and the results have been compared to an example reported in recent literature. Real time implementation of the optimization algorithm has been tested on a Pentium II machine with a sample time up to 0.2 seconds.

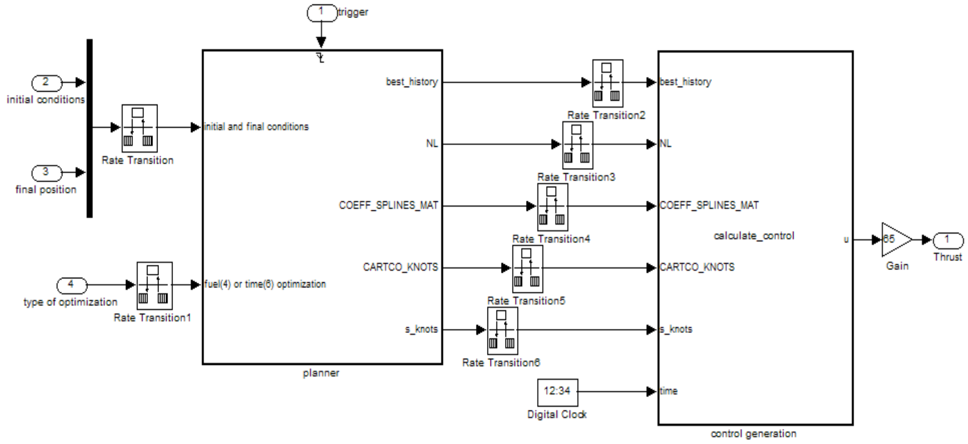

Figure 6.1: Simulink model for real time testing.

Further developments include modifying the path by moving the splines control points in order to optimize it, and adding control bounds. Further experiments are going to be performed on an hardware-in-the-loop laboratory test-bed [19].

References

[1] Clohessy, W. H. and Wiltshire, R. S. Terminal Guidance System for Satellite Rendezvous. *Journal of the Aerospace Sciences* **27**(9) (1960) 653–658.

[2] Tschauner, J. Elliptic orbit rendezvous. *AIAA journal* **5**(6) (1967) 1110–1113.

[3] Inalhan, G., Tillerson, M. and How, J.P. Relative dynamics and control of spacecraft formations in eccentric orbits. *Journal of Guidance, Control and Dynamics* **25** (1) (2002) 48–59.

[4] Izzo, D. Formation flying linear modelling. In: *Proceedings of the* 5^{th} *International Conference on Dynamics and Control of Systems and Structures in Space* Cambridge, UK (14-18 July 2002) 283–289.

[5] Izzo, D., Sabatini, M. and Valente, C. A new linear model describing formation flying dynamics under J_2 effects. *AIDAA, XVII Congresso Nazionale*. Roma, 15–19 September, 2003.

[6] Schaub, H. and Alfriend, K.T. J_2 invariant relative orbits for spacecraft formations. In: *Goddard Flight Mechanics Symposium* (May 18–20 1999), paper 11.

[7] Vadali, S.R. An analytical solution for relative motion of satellites. In: *Proceedings of the* 5^{th} *International Conference on Dynamics and Control of Structures and Systems in Space*, 2002.

[8] Sabatini M., Bevilacqua R., Pantaleoni, M. and Izzo D. Numerical Search of Bounded Relative Satellite Motion. *Nonlinear Dynamics and Systems Theory* **6**(4) (2006) 411–419.

[9] Guelman, M., Aleshin, M. Optimal Bounded Low-Thrust Rendezvous with Fixed Terminal-Approach Direction. *Journal of Guidance, Control and Dynamics* **24**(2) (2001) 378–385.

[10] Campbell, M.E. Planning Algorithm for Multiple Satellite Clusters. *AIAA Journal of Guidance, Control and Dynamics* **26**(5) (2003) 770–780.

[11] Vadali, S.R., Vaddi, S.S. and Alfriend, K.T. An Intelligent Control Concept for Formation Flying Satellite Constellations. *International Journal of Nonlinear and Robust Control, dedicated to Formation Flying* **12** (2002) 97–115.

[12] Shiller, Z. and Dubowsky, S. Robot Path Planning with Obstacles, Actuator, Gripper and Payload Constraints *The International Journal of Robotics Research* **8**(6) (1989) 3–18.

[13] Bernelli-Zazzera, F. and Romano, M. Time-Optimal Motion for Robotic Manipulators with Obstacles Avoidance. In: *Proceedings of* 4^{th} *International Conference on Dynamics and Control of Structure in Space*. Cranfield University, Cranfield, UK (May 1999).

[14] Yakimenko, O.A. Direct Method for Rapid Prototyping of Near-Optimal Aircraft Trajectories. *Journal of Guidance, Control, and Dynamics* **23**(5) (2000) 865–875.

[15] Bellman, R. *Dynamic Programming*. Princeton University Press, Princeton, New Jersey, 1957.

[16] Cruciani, I., De Divitiis, N., De Matteis, G., Filippone, E. Autonomous Guidance for a Sub-Orbital Re-Entry Vehicle. *Paper IAC-03-A.7.06,* 54*th International Astronautical Congress*. Bremen, Germany, September 2003.

[17] Miles, D.W. *Real Time Dynamic Trajectory Optimization with Application to Free-Flying Space Robots*. Stanford University Ph. D. Thesis, 1997.

[18] Mortensons, M.E. *Geometric Modeling*. John Wiley & Sons: New York, 1985.

[19] Romano, M., Friedman, D.A. and Shay, T.J. Laboratory Experimentation of Autonomous Spacecraft Approach and Docking to a Collaborative Target. *AIAA Journal of Spacecraft and Rockets* **44**(1) (2007) 164–173.

Nonlinear Dynamics and Systems Theory, 8 (2) (2008) 151–167

On Nonlinear Control and Synchronization Design for Autonomous Chaotic Systems

A. Boukabou*

Department of Electronics, Faculty of Engineer Sciences, Jijel University, BP 98 Ouled Assa, 18000, Jijel, Algeria

Received: February 26, 2007; Revised: May 29, 2007

Abstract: In this paper, a chaos control and synchronization technique is presented. The proposed technique is applied to achieve both control and synchronization for some autonomous chaotic dynamical systems. Numerical simulations are used to show the effectiveness of the proposed technique.

Keywords: *Chaos; autonomous systems; control; synchronization.*

Mathematics Subject Classification (2000): 34C15, 34C28, 49J15, 93B52.

1 Introduction

Control and synchronization of chaotic dynamical systems have received a great deal of interest among scientists from various fields [5, 13]. These two ideas were first proposed in 1990 [22, 24]. The idea of controlling chaos consists on stabilizing one of the unstable periodic orbits within the strange attractor of the chaotic dynamics, and the task was fulfilled by perturbing an accessible parameter around its nominal value. The idea of synchronizing chaotic systems refers to a process wherein two or many chaotic systems starting from different initial conditions adjust a given property of their motion to a common behaviour. Since then, many possible applications of chaos control and synchronization methods have been discussed by computer simulation and realized in laboratory condition [3, 8, 12, 14, 17, 19, 20, 21, 26, 28].

The Ott–Grebogi–Yorke method, known as OGY method, is a feedback control method, which uses the chaos in system to stabilize an unstable periodic orbit. The main idea of the method is to adjust the parameter perturbations for relatively small time in order to stabilize the desired unstable periodic orbit (UPO) and obtain an attracting time-periodic motion. This control technique is practical from an experimental standpoint because it requires no analytical model of the system. It just requires determining the fixed point and the stable and unstable directions. However, the success of

* Corresponding author: aboukabou@gmail.com

the original OGY theory is limited by the fact that, it applies only to systems where the manifolds are constructed directly by using the Jacobian eigenvalues and eigenvectors. In most of dynamical systems, the dynamics is not confined to a lower-dimensional attractor. Chaos control in higher dimensional systems is technically difficult because it may be impossible to construct the stable and unstable directions.

The aim of this letter is to apply both control and synchronization to some chaotic dynamical systems. This is done by extending the OGY chaos control method. As a potential application of the proposed control strategy, we used it to study the synchronization of some high order chaotic systems.

The principles of control and synchronization of autonomous chaotic systems are given in Section 2. In Section 3 we apply control and synchronization to Lorenz dynamical system and numerical simulations are used to show this process. In Section 4 synchronization and control are applied to Chen chaotic system. Section 5 is devoted to the control and synchronization of Chua system. We conclude in Section 6.

2 Control and Synchronization Principles

Consider the two nonlinear systems

$$\dot{X}_1 = f(X_1, p), \tag{1}$$
$$\dot{X}_2 = g(X_1, X_2), \tag{2}$$

where $f : R^N \times R \to R^N$, $g : R^N \times R^N \to R^N$ are continuous, $X_1, X_2 \in R^N$ are the state variables and $p \in R$ is a parameter control.

The system given by equation (1) will be called the drive system and the system given by equation (2) will be called the response system.

2.1 Chaos control principle

The chaos control algorithm that we introduce in the following uses, in a large sense, the Poincaré section properties. Since chaos is the superposition of a number of periodic motions, it is represented in the Poincaré section by a number of fixed points, called the system chaotic attractor. The chaos control algorithm developed here relies on the knowledge of the chaotic attractor and its response to small perturbations of the system. It is based on the analysis of the Poincaré section to determine how the system approaches the desired orbit or fixed point. The analysis is carried out in three steps:

1. Among the unstable periodic orbits (UPO) of the attractor, choose the one that represents the desired performances.

2. Determine the influence of control parameter on the chosen UPO. For this, we vary the control parameter around the value for which we want to control the system and each time to generate the associated Poincaré section.

3. Determine the variation that should be applied to the control parameter in order to force the system to rejoin the desired UPO or fixed point.

After information about this Poincaré section has been gathered, the system is kept to remain on the desired orbit by perturbing the appropriate parameter. Similar to the original OGY control method, we wish to make only small controlling perturbations to the system. We do not envision creating new orbits with different properties from the already existing orbits.

The basic idea of our control algorithm is as follows. Given a periodic orbit represented by a fixed points at the Poincaré section, we wait for the system trajectory to come close to the control region (which will be defined later) of the desired UPO to bring the system trajectory near the control region. When the system state is in the control region, we will try to use a small parametric perturbation to control the unstable directions of the chaotic state variables x. In other words, we attempt to bring the deviation $\delta x = x - x_f$ to lie on the linearized stable direction. where x_f represents the unstable fixed point obtained by the Poincaré section.

The control law (3) below is directly derived from the Poincaré section and will be applied to the drive system as follows:

$$\delta p = \frac{\partial p}{\partial x_f}(x - x_f), \tag{3}$$

where $\frac{\partial p}{\partial x_f}$ determines the influence of small parametric variation on fixed points variation.

This perturbation control law acts instantaneously on the system. However, in real cases, the future system state of a chaotic system depends on the current parametric variation as well as the previous parametric variations, so the system must take sometime to react to the correction. It seems more sensitive, from a practical point of view, to introduce some delay between the computation of the control law and the effective modification of the control parameter. This is realized by adding to the computed law a term depending on the previous value of the control parameter weighted with a parameter γ, which is determined by trial and error.

Thus, equation (3) becomes:

$$\delta p_{new} = \frac{\partial p}{\partial x_f}(x - x_f) + \gamma \delta p_{old}. \tag{4}$$

However, in terms of the quality of control performance, once the control is activated, the controlled system must be maintained at its new trajectory along its evolution. This stability criterion is assured by a good choice of γ for each chaotic system to be controlled.

We expect that, under forward applications of the control law (4), points in the local neighbourhood of the fixed point will eventually fall into the local neighbourhood and then be controlled.

2.2 Chaos synchronization principle

Let $X_1(t, X_1(0))$ and $X_2(t, X_2(0))$ be solutions to the drive system (1) and to the response system (2) respectively.

In this framework, complete synchronization is defined as the identity between the trajectories of the response system X_2 and of one replica X_2' of it $\dot{X}_2' = g(X_1, X_2')$ for the same chaotic driving system X_1.

If the solutions $X_1(t, X_1(0))$ and $X_2(t, X_2(0))$ satisfy

$$\lim_{t\to\infty} \|X_1(t, X_1(0)) - X_2(t, X_2(0))\| = 0. \tag{5}$$

Then, the drive system and the response system are said *synchronized*. In other words, the response system *forgets* its initial conditions, though evolving on a chaotic attractor.

In [24, 25], authors established that this kind of synchronization can be achieved and provide that all the Lyapunov exponents of the response system under the action of the driver (the conditional Lyapunov exponents) are negative. This implies that the response system is asymptotically stable.

3 Control and Synchronization of Lorenz System

The Lorenz system is a differential system with a chaotic behaviour for some values of parameters, described by:

$$\begin{cases} \dot{x} = \sigma(y - x), \\ \dot{y} = (r - z)x - y, \\ \dot{z} = xy - bz. \end{cases} \tag{6}$$

The parameters setting for the Lorenz system to display chaos are: $\sigma = 10, b = 8/3$ and $r = 28$.

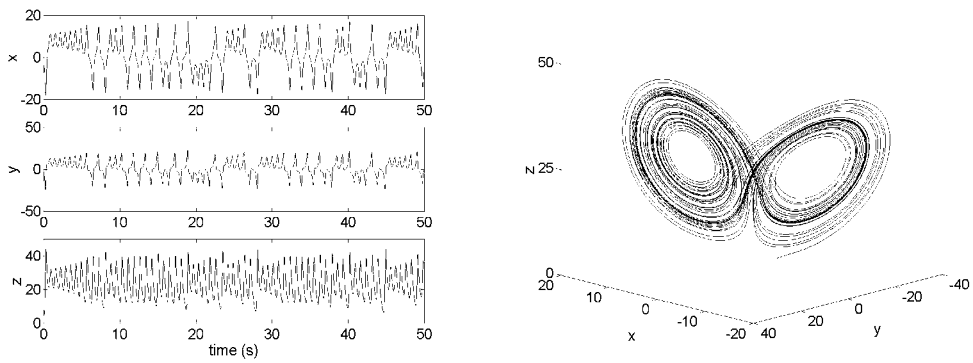

(a) (b)

Figure 3.1: Lorenz chaotic attractor. (a) Time response. (b) Phase plane.

The drive system is given by:

$$\begin{cases} \dot{x}_1 = \sigma(y_1 - x_1), \\ \dot{y}_1 = ((r + \delta r) - z_1)x_1 - y_1, \\ \dot{z}_1 = x_1 y_1 - b z_1. \end{cases} \tag{7}$$

Here r is used as the control parameter with δr is the perturbing parameter control.

To apply the chaos control algorithm to the drive system, we have to determine the Poincaré section. This section is described by one dimensional map and corresponds to the set of points where attractor is at its maximum. That is $z = \max(z_1)$.

Figure 3.2 shows the plots given the maxima of $z(n+1)$ against those of $z(n)$. The fixed points are then obtained at the intersection of these plots with the straight line $z(n+1) = z(n)$.

The value of the third state variable of the fixed point is determined as $z_f = 39.82$.

To determine parametric influence of the small parametric variation on fixed-points variation, we generate a Poincaré section at $r = 28.2$ as shown in Figure 3.3.

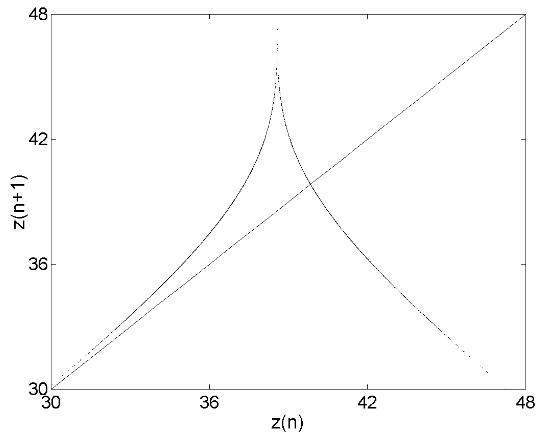

Figure 3.2: Successive maxima map of state variable z_1.

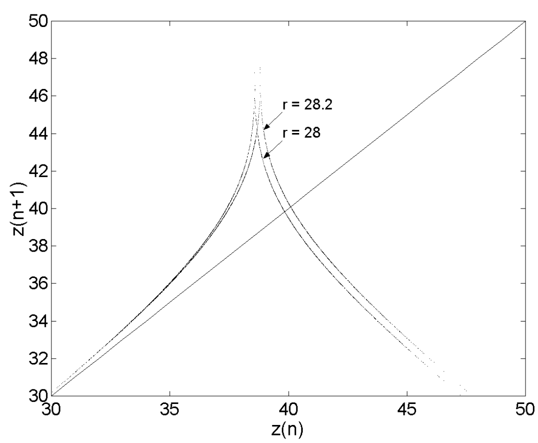

Figure 3.3: Superposition of two successive maxima map of state variable z_1.

In this case, we find $z'_f = 40.09$.

The drive system is under chaos control law (3) of the form:

$$\begin{aligned} \delta r_{new} &= \frac{\partial r}{\partial z_f}(z_1 - z_f) + \gamma \delta r_{old} \\ &= \frac{28.2 - 28}{40.09 - 39.82}(z_1 - z_f) + \gamma \delta r_{old}. \end{aligned} \tag{8}$$

Our control method needs to determine the stabilizer parameter γ in the feedback control. This parameter must be small, so it is chosen from the interval [0.01, 0.5].

The drive system is under control of the form:

$$\delta r_{new} = 0.74(z_1 - 39.82) + 0.2\delta r_{old}. \tag{9}$$

This control law is activated only when the state variables x and z are located in the neighbourhood of the appropriates fixed points x_f and z_f respectively. The condition is defined by:

$$(x_1 - x_f)^2 + (z_1 - z_f)^2 < 1 \tag{10}$$

with $x_f = 14.89$.

The result of the control of the drive system is depicted in Figure 3.4.

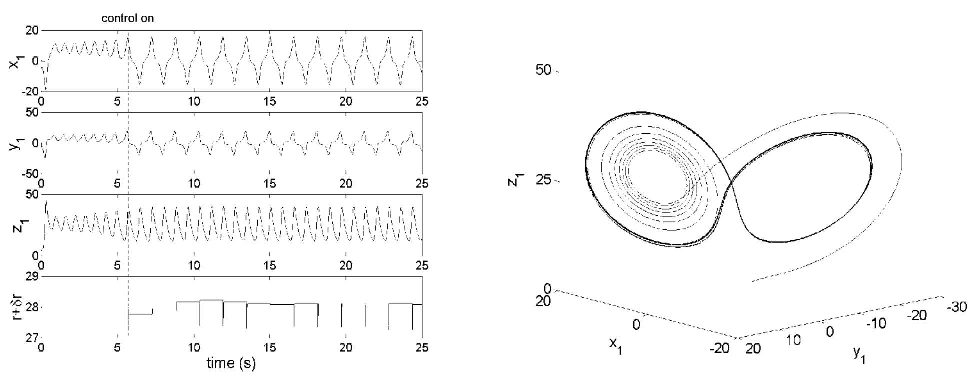

(*a*) (*b*)

Figure 3.4: Control of the Lorenz chaotic driver. (a) Time response. (b) Phase plane.

To stabilize the chaos on its real unstable periodic orbit, one can see that control generate a pulse train, each pulse is activated automatically so that, at a sufficient amplitude, determined by the Poincaré section at each travelling from the fixed point, eventually the system orbit converges to the desired unstable periodic orbit. We also tested our chaos control strategy with different initial conditions and it was found to be robust.

Once controlled drive system is obtained, we construct a response system which exhibits a generalized kind of synchronization motion with the driver based on the Pecora and Caroll concept, by making a simple nonlinear transformation among the response variable x_2.

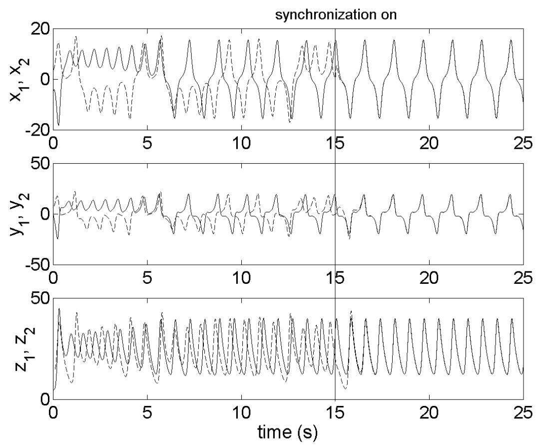

Figure 3.5: Synchronization of the Lorenz drive-response systems.

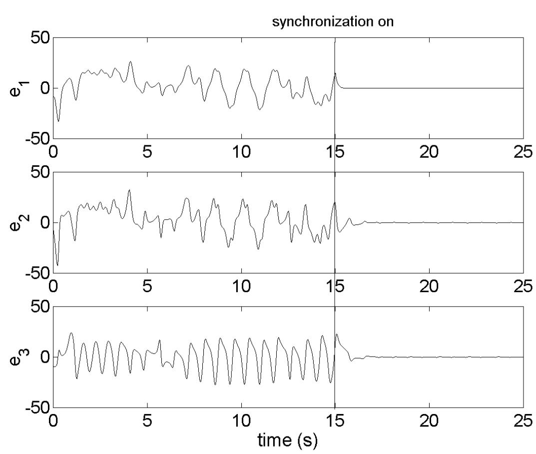

Figure 3.6: Time response of the error variables.

Thus, the response system will be given by:

$$\begin{cases} \dot{x}_2 = \sigma(y_1 - x_2), \\ \dot{y}_2 = (r - z_2)x_2 - y_2, \\ \dot{z}_2 = x_2 y_2 - b z_2. \end{cases} \tag{11}$$

Notice that (11) consists of a copy of (7) without control ($\delta r = 0$) and in the synchronization Pecora and Carroll concept, y_1 is the drive signal.

Introducing the error variables $e_1 = x_1 - x_2$, $e_2 = y_1 - y_2$ and $e_3 = z_1 - z_2$, we obtain the error dynamics

$$\begin{cases} \dot{e}_1 = -\sigma e_1, \\ \dot{e}_2 = r e_1 - e_2 - z_1 x_1 + z_2 x_2 + \delta r x_1, \\ \dot{e}_3 = -b e_3 + x_1 y_1 - x_2 y_2. \end{cases} \tag{12}$$

From (12), we should choose the synchronization subsystem such that an equilibrium state can be achieved. To find the equilibrium state, we set the three equations equals to zero, that is:

$$\begin{cases} \dot{e}_1 = -\sigma e_1 = 0, \\ \dot{e}_2 = -e_2 + r e_1 - z_1 x_1 + z_2 x_2 + \delta r x_1 = 0, \\ \dot{e}_3 = -b e_3 + x_1 y_1 - x_2 y_2 = 0, \end{cases}$$

$$\Rightarrow \begin{cases} -\sigma e_1 = 0, \\ -e_2 + r e_1 - z_1 x_1 + z_2 x_2 + x_1 z_2 - x_1 z_2 + \delta r x_1 = 0, \\ -b e_3 + x_1 y_1 + x_1 y_2 - x_1 y_2 - x_2 y_2 = 0, \end{cases}$$

$$\Rightarrow \begin{cases} -\sigma e_1 = 0, \\ -e_2 + r e_1 - x_1 e_3 - z_2 e_1 + \delta r x_1 = 0, \\ -b e_3 - x_1 e_2 - y_2 e_1 = 0, \end{cases}$$

$$\Rightarrow \begin{cases} -\sigma e_1 = 0, \\ -e_2 + (r - z_2) e_1 + (\delta r - e_3) x_1 = 0, \\ -b e_3 - x_1 e_2 - y_2 e_1 = 0. \end{cases} \tag{13}$$

Because the parameters σ, b, r and the state variables x_1, y_2, z_2 are different from zero and $\delta r \to 0$, it follows that the error states (e_1, e_2, e_3) asymptotically converges to $(0, 0, 0)$. In other words, the response system (11) asymptotically synchronizes with the drive system (7) no matter how they are initialized.

The initial values of the drive system are $(x_1(0), y_1(0), z_1(0)) = (-5, 0, 5)$ and the initial values of the response system are $(x_2(0), y_2(0), z_2(0)) = (3, 6, 15)$.

Synchronization law is applied for $t > 15$ and the drive-response systems are in a perfect synchronized state. The results of the simulation are shown in Figures 3.5 and 3.6.

4 Control and Synchronization of Chen System

Recently, Chen found another chaotic attractor, also in a simple three-dimensional autonomous system, which nevertheless is not topologically equivalent to the Lorenz's [6]:

$$\begin{cases} \dot{x} = a(y - x), \\ \dot{y} = (c - a - z)x + cy, \\ \dot{z} = xy - bz. \end{cases} \tag{14}$$

System (14) has chaotic behaviour at the parameters values $c = 35, a = 28$ and $b = 3$. This system has the same complexity as the Lorenz equation – they are both three-dimensional autonomous with only two quadratic terms. The chaotic behaviour of the system is shown in Figure 4.1.

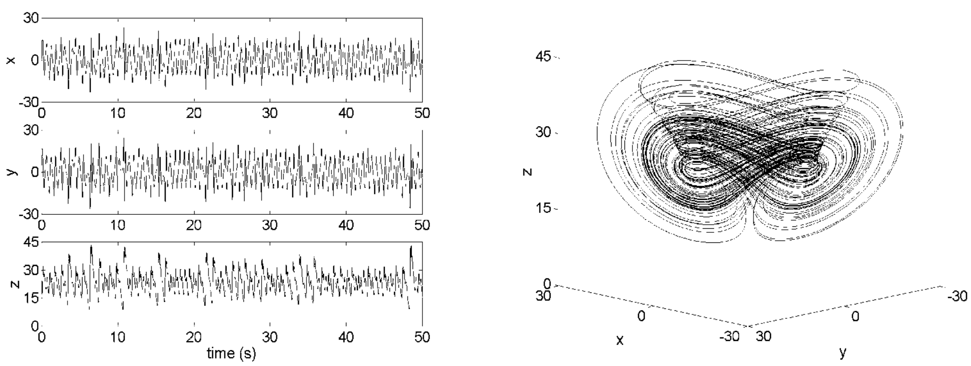

(a) (b)

Figure 4.1: Chen chaotic attractor. (a) Time response. (b) Phase plane.

For Chen chaotic attractor, the drive system is defined as follows:

$$\begin{cases} \dot{x}_1 = a(y_1 - x_1), \\ \dot{y}_1 = ((c + \delta c) - a - z_1)x_1 + cy_1, \\ \dot{z}_1 = x_1 y_1 - bz_1. \end{cases} \tag{15}$$

Here c is used as the control parameter.

Figure 4.2 shows the Poincaré section realized on the third state variable for different values of parameter c.

At $c = 28$, the value of the third state variable of the fixed point is determined as $z_f = 27.29$ and at $c = 28.2$, $z'_f = 27.75$.

The control law is defined by

$$\begin{aligned} \delta c_{new} &= \frac{\partial c}{\partial z_f}(z_1 - z_f) + \gamma \delta c_{old} \\ &= \frac{28.2 - 28}{27.75 - 27.29}(z_1 - z_f) + \gamma \delta c_{old}. \end{aligned} \tag{16}$$

Then we obtain

$$\delta c_{new} = 0.43(z_1 - 27.29) + 0.1\delta c_{old}. \tag{17}$$

This control law is activated only when:

$$(x_1 - x_f)^2 + (z_1 - z_f)^2 < 1 \tag{18}$$

with $x_f = 14.89$.

The result of the control is shown in Figure 4.3. Figure 4.3(b) depicts the orbit of the controlled Chen's chaotic system in the phase space. From Figure 3(a), one can see

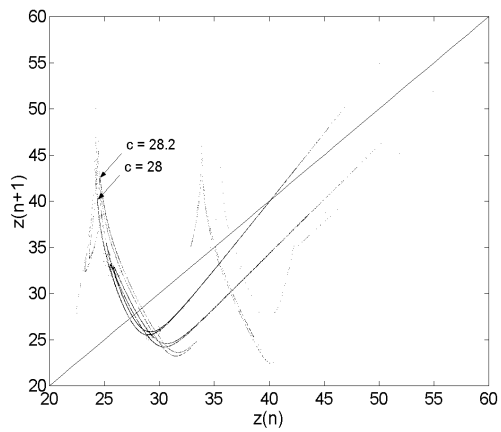

Figure 4.2: Return map of state variable z_1.

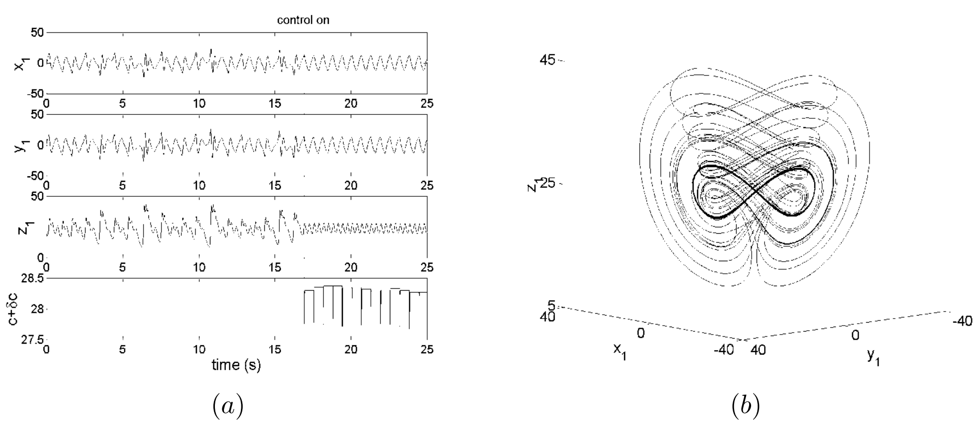

Figure 4.3: Control of the Chen chaotic driver. (a) Time response. (b) Phase plane.

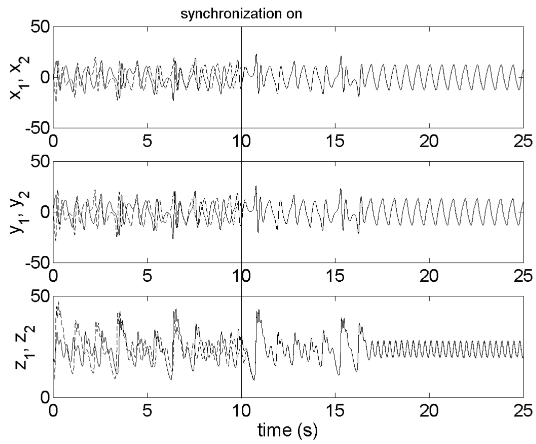

Figure 4.4: Synchronization of the Chen drive-response systems.

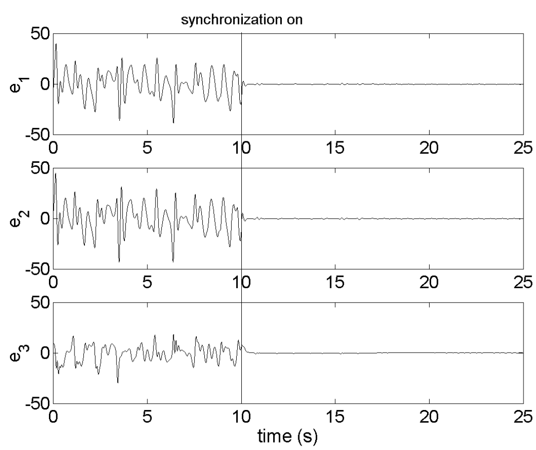

Figure 4.5: Time response of the error variables.

that, to stabilize chaos, the method works by applying instantaneous periodic kicks to the system variables and eventually the system orbits converge to the desired UPO.

We construct a Pecora-Caroll drive–response configuration with a drive signal y_1 introduced in the y_2 dynamics of the response system given by:

$$\begin{cases} \dot{x}_2 = a(y_2 - x_2), \\ \dot{y}_2 = (c - a - z_2)x_2 + cy_1, \\ \dot{z}_2 = x_2 y_2 - bz_2. \end{cases} \tag{19}$$

The dynamic of the error variables will be given by:

$$\begin{cases} \dot{e}_1 = -a(e_1 - e_2), \\ \dot{e}_2 = (c - a)e_1 - z_1 x_1 + z_2 x_2 + \delta c x_1, \\ \dot{e}_3 = -be_3 + x_1 y_1 - x_2 y_2. \end{cases} \tag{20}$$

Demanding that all of the equations of system (20) are zero, we get the following:

$$\begin{aligned} &\begin{cases} \dot{e}_1 = -a(e_1 - e_2) = 0, \\ \dot{e}_2 = (c - a)e_1 - z_1 x_1 + z_2 x_2 + \delta c x_1 = 0, \\ \dot{e}_3 = -be_3 + x_1 y_1 - x_2 y_2 = 0, \end{cases} \\ \Rightarrow &\begin{cases} e_1 = e_2, \\ (c - a - z_2)e_1 + (\delta c - e_3)x_1 = 0, \\ -be_3 - x_1 e_2 - y_2 e_1 = 0, \end{cases} \\ \Rightarrow &\begin{cases} e_1 = 0, \\ e_2 = 0, \\ e_3 = 0. \end{cases} \end{aligned} \tag{21}$$

The initial values of the drive system are $(x_1(0), y_1(0), z_1(0)) = (-3, 2, 20)$ and the initial values of the response system are $(x_2(0), y_2(0), z_2(0)) = (5, -2, 10)$. In this case, synchronization was applied before applying the control law and simulation results are given in Figures 4.4 and 4.5.

5 Control and Synchronization of Chua System

The Chua circuit is a nonlinear circuit with chaotic behaviour for some values of parameters. The normalized equations representing the circuit are:

$$\begin{cases} \dot{x} = \alpha(y - x - h(x)), \\ \dot{y} = x - y + z, \\ \dot{z} = -\beta y, \end{cases} \tag{22}$$

where

$$h(x) = m_1 x + \frac{m_0 - m_1}{2}\left(|x + 1| - |x - 1|\right) \tag{23}$$

represents the nonlinear element of the circuit.

When $\alpha = 10, \beta = 14.87, m_0 = -1.27, m_1 = -0.68$, Chua attractor is chaotic and has a plot as shown in Figure 5.1.

The drive system is given by:

$$\begin{cases} \dot{x}_1 = (\alpha + \delta\alpha)(y_1 - x_1 - h(x_1)), \\ \dot{y}_1 = x_1 - y_1 + z_1, \\ \dot{z}_1 = -\beta y_1. \end{cases} \tag{24}$$

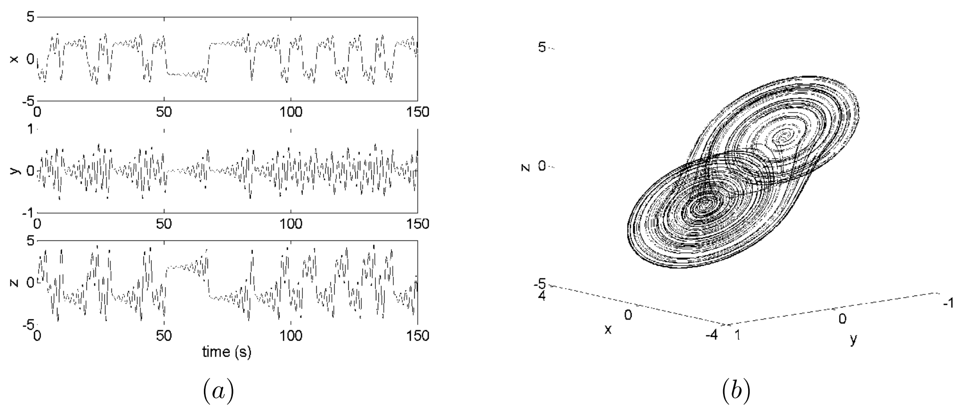

Figure 5.1: Chua's circuit. (a) Time response. (b) Phase plane.

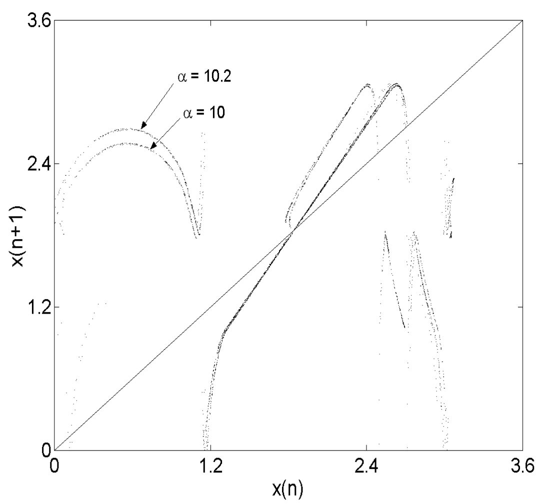

Figure 5.2: Return map of state variable x_1.

In Chua's circuit, we chose the Poincaré section by plotting the current maxima $x(n+1)$ against the previous maxima $x(n)$.

The first state of the fixed point is determined by $x_f = 2.70$. At $\alpha = 10.2$, in this case, $x'_f = 3.31$.

The deduced control law is

$$\begin{aligned} \delta\alpha_{new} &= \frac{\partial\alpha}{\partial x_f}(x_1 - x_f) + \gamma\delta\alpha_{old} \\ &= \frac{10.2 - 10}{3.31 - 2.70}(x_n - x_f) + \gamma\delta\alpha_{old}. \end{aligned} \tag{25}$$

Then we obtain

$$\delta\alpha_{new} = 0.32(x_n - x_f) + 0.1\delta\alpha_{old}. \tag{26}$$

The activation region of the control is defined by:

$$(x_n - x_f)^2 + (y_n - y_f)^2 < 1, \tag{27}$$

where $y_f = 0.27$. In the Chua system, the response system is chosen as follows:

$$\begin{cases} \dot{x}_2 = \alpha(y_2 - x_2 - h(x_2)), \\ \dot{y}_2 = x_1 - y_2 + z_2, \\ \dot{z}_2 = -\beta y_2. \end{cases} \tag{28}$$

Consequently, the error variables will be defined by:

$$\begin{cases} \dot{e}_1 = \alpha(e_1 - e_2 - h(x_1) + h(x_2)) + \delta\alpha(y_1 - x_1 - h(x_1)), \\ \dot{e}_2 = -e_2 + e_3, \\ \dot{e}_3 = -\beta e_{2.} \end{cases} \tag{29}$$

To find the equilibrium state of (29), we rewrite as follows:

$$\begin{cases} \alpha(e_1 - e_2 - h(x_1) + h(x_2)) + \delta\alpha(y_1 - x_1 - h(x_1)) = 0, \\ -e_2 + e_3 = 0, \\ -\beta e_2 = 0, \end{cases}$$
$$\Rightarrow \begin{cases} e_1 = 0, \\ e_2 = 0, \\ e_3 = 0. \end{cases} \tag{30}$$

Starting from the initial values $(x_1(0), y_1(0), z_1(0)) = (-0.1, -0.1, -0.1)$ of the drive system and from $(x_2(0), y_2(0), z_2(0)) = (0.1, 0.1, 0.1)$ of the response system, controlled drive system (24), synchronization of the response system (28) with the controlled drive system and time response of the error variables (29) are shown together in Figure 5.3(a), (b) and (c) respectively.

6 Conclusion

This letter demonstrates that control and synchronization can be achieved in autonomous chaotic systems by different ways. The response system is synchronized with the drive system even if synchronization is activated before, after or simultaneously with the control law.

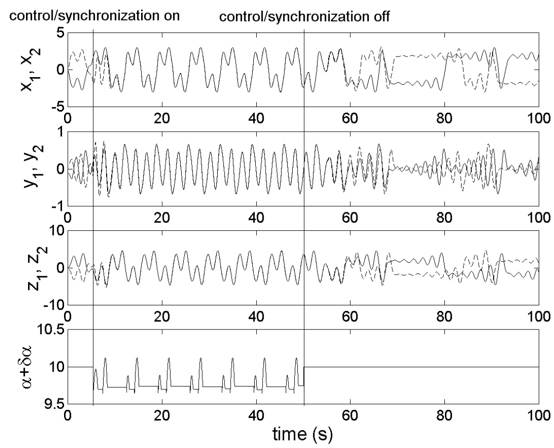

(*a*)

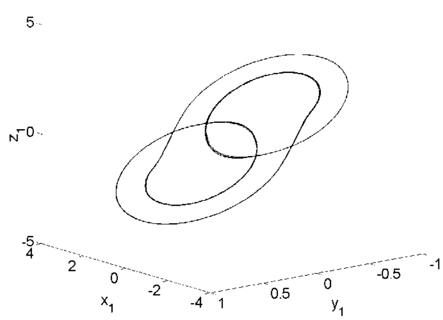

(*b*)

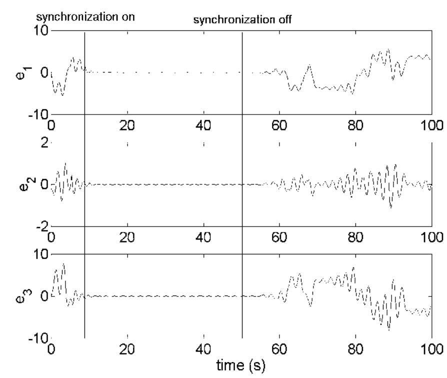

(*c*)

Figure 5.3: Control and synchronization of the Chua system. (a) Time response of the drive and response systems. (b) Phase plane of the controlled trajectory. (c) Time response of the error variables.

References

[1] Agiza, H.N. and Yassen, M.T. Synchronization of Rossler and Chen chaotic dynamical systems using active control. *Phys. Lett. A* **278** (2001) 191–197.

[2] Bai, E.-W., Lonngren, K. E. and Sprott, J. C. On the synchronization of a class of electronic circuits that exibit chaos. *Chaos Solit. & Fract.* **13** (2002) 1515–1521.

[3] Boccaletti, S., Kurths, J., Osipov, G., Valladares, D.L. and Zhou, C.S. The synchronization of chaotic systems. *Phys. Rep.* **366** (2002) 1–101.

[4] Boukabou, A. and Mansouri, N. Controlling chaos in higher-order dynamical systems. *Int. J. Bifurcation & Chaos* **14**(12)(2004) 4019–4025.

[5] Chen, G. and Dong, X. *From Chaos to Order: Methodologies, Perspectives and Applications.* World Scientific, Singapore, 1998.

[6] Chen, G. and Lü, J. A new chaotic attractor coined. *Int. J. Bifurcation & Chaos* **12**(3) (2002) 659–661.

[7] Chen, M.-Y., Han, Z.-Z. and Shang, Y. General synchronization of Genesio-Tesi systems. *Int. J. Bifurcation & Chaos* **14**(1) (2004) 347–354.

[8] Cruz, C. and Nijmeijer, H. Synchronization through filtering. *Int. J. Bifurcation & Chaos* **10**(4) (2000) 763–775.

[9] Cruz-Hernández, C., López-Mancilla, D., García, V., Serrano, H. and Núñez, R. Experimental realization of binary signal transmission using chaos. *J. Circ. Syst. Computers* **14**(3) (2005) 453–468.

[10] Cuomo, K.M., Oppenheim, A.V. and Strogratz, S.H. Synchronization of Lorenz-based chaotic circuits with applications to communications. *IEEE Trans. Circuits & Syst. II* **40**(10) (1993) 626–633.

[11] Dedieu, H., Kennedy, M.P., Hasler, M. Chaotic shift keying: Modulation and demodulation of a chaotic carrier using self-synchronizing Chua's circuits. *IEEE Trans. Circuits & Syst. II* **40**(10) (1993) 634–642.

[12] Ding, M., Yang, W., In, V., Ditto, W.L., Spano, M.L. and Gluckman, B. Controlling chaos in high dimensions: Theory and experiment. *Phys. Rev. E* **53** (1996) 4334–4344.

[13] Fradkov, A.L. and Pogromsky, Yu., A. *Introduction to control of oscillations and chaos*. World Scientific, Singapore, 1998.

[14] Feldmann, U., Hasler, M. and Schwarz, W. Communication by chaotic signals: the inverse system approach. *Int. J. Circuits Theory & Applications* **24** (1996) 551–579.

[15] Hegazi, A., Agiza, H.N. and El-Dessoky, M.M. Controlling chaotic behaviour for spin generator and Rossler dynamical systems with feedback control. *Chaos Solit. & Fract.* **12**(4) (2001) 631–658.

[16] Lai, Y.C. and Grebogi, C. Synchronization of chaotic trajectories using control. *Phys. Rev. E* **47** (1993) 2357–2360.

[17] López-Mancilla, D. and Cruz-Hernández, C. Output synchronization of chaotic systems: Model-matching approach with application to secure communication. *Nonlinear Dynamics & Systems Theory* **5**(2) (2005) 141–156.

[18] Matias, M.A. and Güémez, J. Chaos suppression in flows using proportional pulses in the system variables. *Phys. Rev. E* **54** (1996) 189–209.

[19] Nijmeijer, H. and Mareels, I.M.Y. An observer looks at synchronization. *IEEE Trans. Circuits & Syst.-I* **44**(10) (1997) 882–890.

[20] Nijmeijer, H. A dynamical control view on synchronization. *Physica D* **154** (2001) 219–228.

[21] Ogorzalek, M.J. Taming chaos – Part I: Synchronization; Part II: Control. *IEEE Trans. Circuits & Syst.-I* **40** (1993) 693–706.

[22] Ott, E., Grebogi, C. and Yorke, J.A. Controlling chaos. *Phys. Rev. Lett.* **64** (1990) 1196–1199.

[23] Parlitz, U., Chua, L.O., Kocarev, L.J., Halle, K.S. and Shang, A. Transmission of digital signals by chaotic synchronization. *Int. J. Bifurcation & Chaos* **2**(4) (1992) 973–977.

[24] Pecora, L.M., Carroll, T.L. Synchronization in chaotic systems. *Phys. Rev. Lett.* **64** (1990) 821–824.

[25] Pecora, L.M., Carroll, T.L., Johnson, G.A. and Mar, D.J. Fundamentals of synchronization in chaotic systems, concepts, and applications. *Chaos* **7** (1997) 520–543.

[26] Pyragas, K. Continuous control of chaos by self-controlling feedback. *Phys. Lett. A* **170** (1992) 421–428.

[27] Sarasola, C., Torrealdea, F. J., D'anjou, A., Moujahid, A. and Grana, M. Feedback synchronization of chaotic systems. *Int. J. Bifurcation & Chaos* **13**(1) (2003) 177–191.

[28] Sira-Ramírez, H. and Cruz, C. Synchronization of Chaotic Systems: A Generalized Hamiltonian Systems Approach. *Int. J. Bifurcation & Chaos* **11**(5) (2001) 1381-1395. And in Procs. of American Control Conference (ACC'2000), Chicago, USA, 769–773.

[29] Yang, T. and Chua, L.O. Secure communication via chaotic parameter modulation. *IEEE Trans. Circuits & Syst. I* **43**(9) (1996) 817–819.

[30] Yang, T. and Chua, L.O. Impulsive control and synchronization of nonlinear dynamical systems and application to secure communication. *Int. J. Bifurcation & Chaos* **7**(3) (1997) 645–664.

[31] Yang, X. S. A framework for synchronization theory. *Chaos Solit. & Fract.* **11** (2000) 1365–1368.

[32] Zhou, T., Lü, J., Chen, G. and Tang, Y. Synchronization stability of three chaotic systems with linear coupling. *Phys. Lett. A* **301** (2002) 231–240.

Nonlinear Dynamics and Systems Theory, 8 (2) (2008) 169–194

Chaotic Dynamics in Hybrid Systems

P. Collins *

Centrum voor Wiskunde en Informatica, Postbus 94079
1090 GB Amsterdam, The Netherlands

Received: March 20, 2007;   Revised: February 25, 2008

Abstract: In this paper we give an overview of some aspects of chaotic dynamics in hybrid systems, which comprise different types of behaviour. Hybrid systems may exhibit discontinuous dependence on initial conditions leading to new dynamical phenomena. We indicate how methods from topological dynamics and ergodic theory may be used to study hybrid systems, and review existing bifurcation theory for one-dimensional non-smooth maps, including the spontaneous formation of robust chaotic attractors. We present case studies of chaotic dynamics in a switched arrival system and in a system with periodic forcing.

Keywords: *Chaotic dynamics; hybrid systems; symbolic dynamics; nonsmooth bifurcations.*

Mathematics Subject Classification (2000): 34A37, 37B10, 37A40, 34A36, 37G35.

1 Introduction

A hybrid system is a dynamic system which comprises different types of behaviour. Classic examples of hybrid dynamical systems in the literature are impacting mechanical systems, for which the behaviour consists of continuous evolution interspersed by instantaneous jumps in the velocity, and dc-dc power converters, in which the behaviour depends on the state of a diode and a switch. Hybrid control systems occur when a continuous system is controlled using discrete sensors and actuators, such as thermostats and switched heating/cooling devices. Hybrid dynamics may also occur due to saturation effects on components of a system, and in idealized models of hysteresis. Finally, we mention that hybrid systems can be derived as singular limits of systems operating in multiple time-scales; indeed we may consider almost all hybrid systems to arise in this way.

From a mathematical point of view, hybrid systems typically exhibit non-smoothness or discontinuities in the dynamics, and these properties induce new dynamical phenomena

* Corresponding author: pieter.collins@cwi.nl

which are not present in non-hybrid (i.e. smooth) systems. Most notably, hybrid systems can exhibit robust chaotic attractors, which have been conjectured not to exist for smooth systems.

This article is designed to give an introduction to hybrid systems for a specialist in dynamical systems theory, and an introduction to chaotic dynamics for an expert in hybrid systems. We cover modelling formalisms and solution concepts for hybrid systems, and discuss three of the main branches of chaotic dynamical systems theory, namely symbolic dynamics, ergodic theory and bifurcation theory. We assume that the reader is familiar with basic concepts of dynamical systems theory, including topological dynamics, ergodic theory and elementary smooth bifurcation theory. This material can be found in many of the excellent and accessible textbooks on dynamical systems, such as [24, 27, 42, 21]. The field of hybrid systems is not as mature, and many of the fundamental theoretical concepts have not yet been developed. The only introductory general textbook on hybrid systems currently available is [47], and the book [32] contains qualitative analysis of some classes of hybrid system.

The article is organised as follows. In Section 2, we give an overview of chaotic hybrid systems and introduce some representative examples. In Section 3, we give a brief introduction to hybrid systems theory. In Section 4 we discuss statistical and symbolic techniques for studying hybrid systems. In Section 5, we discuss bifurcation theory for hybrid systems. In Section 6 we present some case studies showcasing chaotic dynamics. Finally, we give some concluding remarks in Section 7.

2 Overview

We now give an informal overview of hybrid systems and chaotic dynamics, and give some motivational examples from the literature.

2.1 Hybrid systems

What exactly do we mean by a *hybrid system*? For our purposes, the following informal definition is appropriate:

a hybrid system is a dynamic system for which the evolution has a different form or structure in different parts of the state space.

Examples of hybrid system include piecewise-affine maps, differential equations with discontinuous right-hand sides, and systems in which the evolution jumps between multiple modes. The meaning of "different form or structure" is deliberately vague, and may depend on the tools we use to study the system. For example, a continuous piecewise-affine map may be considered "hybrid" when studying bifurcations, since bifurcation theory deals with the differential category, but from the point of view of topological or statistical properties it is just a single continuous function.

Within the class of all hybrid systems, we may identify *discrete-time*, *continuous-time* and *hybrid-time* systems.

Discrete-time hybrid systems are typically the easiest to study, and in applications usually arise as simplifications of continuous- or hybrid-time systems, such as the stroboscopic map of a periodically-forced oscillator or the hitting map of an impact system. Important classes of discrete-time systems in the literature include *piecewise-affine maps*, in which the dynamics is affine, $x_{n+1} = A_i x_n + b_i$ on each element P_i of a polyhedral partition of the state space. These systems can be studied by their *symbolic dynamics* in terms of the state-space partition, or by looking at *border collision bifurcations* which occur when periodic points cross the partition element boundaries, and may result in spontaneous transitions to chaos.

A continuous-time hybrid system is described by a differential equation or differential inclusion in which the right-hand side is non-smooth or discontinuous. If the right-hand side is continuous and piecewise-smooth, then it is locally Lipschitz, so local existence and uniqueness of solutions are immediate. The hybrid nature comes up when attempting to find efficient numerical methods to integrate such systems, since crossings of the switching boundary must be detected, and when considering bifurcations, since *corner-collisions* in the dynamics may lead to border collision bifurcations in time-discretisations. If the right-hand side is discontinuous, then the system can be reformulated as a differential inclusion using the Filippov solution concept [18]. Uniqueness of solutions is not guaranteed, and we shall see that this may result in *discontinuous* dependence on initial conditions due to *corner-collisions* and *grazing* phenomena, though as we shall see later, a grazing impact in a mechanical system does not induce discontinuous spacial dependence.

A *hybrid-time* system has both discrete-time and continuous-time dynamics. Hybrid-time systems naturally occur when continuous systems are controlled by actuators with a finite number of states, such as an electronic switch or a three-level induction motor, or using sensors which can only detect a finite number of states, such as a thermostat. Instantaneous transitions in the state occur when a *discrete event* is activated, causing a change in the *mode* of the system. Between discrete events the system evolves continuously. Although a discrete event causes a discontinuity in the system state, if an orbit crosses a guard set transversely, then nearby orbits undergo the same discrete event at nearly the same time, and no lasting discontinuities in the spacial dependence occur. However, a tangency of the system evolution with the activation set of a discrete event does introduce discontinuous spacial dependence, as does a situation when two discrete transitions are simultaneously activated.

The non-smooth or discontinuous dependence on initial conditions which can occur in hybrid systems is the main phenomenological difference between hybrid and non-hybrid systems. This often causes difficulties—invariant measures need not exist, topological methods either fail outright or need to be modified, and new bifurcations are seen to occur. However, these features also allow the possibility of *robust chaos*, by which we mean the presence of a chaotic attractor over an open set in parameter space; behaviour which is not seen in non-hybrid systems. Since non-smooth and discontinuous dependence on initial conditions are the key of hybrid systems, we shall pay considerable attention to determining the discontinuities and singularities of the evolution.

Discontinuous dependence on initial conditions can cause fundamental difficulties in applying existing techniques of dynamical systems theory, which were originally developed for systems without discontinuities. However, many methods can be modified to apply to either *upper-semicontinuous* or *lower-semicontinuous* systems. Hence a *regularisation* step is required to bring the system into a form which is amenable to analysis. As part of this regularisation, either existence or uniqueness of solutions is typically lost.

2.2 Chaos in hybrid systems

There are many definitions of "chaos" in the literature. We shall adopt the terminology that a system is chaotic if it has positive topological entropy. Chaotic behaviour may be *transient*, which means that the positive entropy is supported on a repelling set, or *attracting*, which means that the positive entropy is supported on a *minimal* attractor, i.e. an attractor with a dense orbit and hence no proper sub-attractors. From an applications point of view, transient chaotic behaviour is often unimportant; it is the dynamics on the attractors which is important. However, in practice it is impossible to distinguish between a very-high period limit cycle and a chaotic attractor.

It is often fairly easy to prove the existence of chaotic dynamics using techniques based on topological index theories, either the Lefschetz-Nielsen theory [6] for periodic points and the Conley index theory [34] for more general invariant sets. For interval maps, the ordering of points of a periodic orbit can be used to prove the existence of chaos, and for two-dimensional homeomorphisms, there is a rich theory based around periodic and homoclinic orbits. These tools are relevant for hybrid systems since they require only (local) continuity of the system evolution, and can be used directly for non-smooth hybrid systems, and with some modifications to piecewise-continuous systems. However, the main disadvantage of these methods is that they cannot distinguish between chaotic transients and a chaotic attractor.

The most important quantitative measure of chaos in a dynamical system is the *topological entropy*. It is known [51] that the topological entropy is upper-semicontinuous for the class of C^∞-smooth systems. It is also know that topological entropy is lower-semicontinuous for C^0 maps in one dimension, but not for C^∞ maps in $d \geq 2$ dimensions [35]. This means that for non-hybrid (i.e. smooth) systems, chaos cannot be spontaneously created, and for low-dimensional systems, chaos cannot be spontaneously destroyed.

In differentiable systems, it is extremely difficult to rigorously prove the existence of a minimal attractor with "high" topological entropy; the unimodal map [3] and the Lorenz system [46] are notable exceptions. Let us consider the simplest smooth chaotic family, namely the *unimodal family* $x_{n+1} = f_a(x_n) := 1 - ax_n^2$. It is well-known that if f_a has a periodic orbit of period m which is not a power of two, then f has a chaotic set with positive topological entropy. In [3] it was shown that for a positive measure set of parameters, there exists a minimal chaotic attractor. For other parameter values, almost all points lie in the basin of a stable periodic orbit, though this orbit may have a very high period, and numerically appear to be "chaotic". However, the proof of this result is highly delicate, and it has been conjectured that there does not exist an open and dense set of smooth C^2 maps of the interval with a minimal chaotic attractor.

The situation for hybrid systems is quite different. For the non-smooth equivalent of the unimodal family, namely the family of *tent maps* $x_{n+1} := \epsilon - a|x_n|$, it is possible to spontaneously create chaos, in the form of chaotic attractors with non-vanishing topological entropy which are robust with respect to perturbation. From this point of view alone, hybrid systems are important for the study of chaotic dynamics.

The intuitive explanation for this difference between non-hybrid and hybrid systems is that to generate chaos, we need "stretching" and "folding" in the map. In one dimension, the existence of a critical point c is needed for the "folding" property, but since $f'(c) = 0$, this orbit is highly attracting, and it is difficult to get enough stretching away from the critical point to compensate.

2.3 Examples of chaotic hybrid systems

We now present some examples of hybrid systems which have been extensively studied in the literature.

Electronic circuits are one of the most well-studied experimental examples of chaotic systems. Perhaps the most well-studied example is Chua's circuit [11, 10], which contains a nonlinear resistor with piecewise-linear characteristic. Another interesting example is a circuit with a hysteresis element [36, 43]. The books [48, 45] contain an overview on chaotic dynamics in electronic circuits.

From a practical perspective, the most relevant examples are the boost and buck dc-dc power converters, as shown in Figure 2.1. The boost power converter is used to

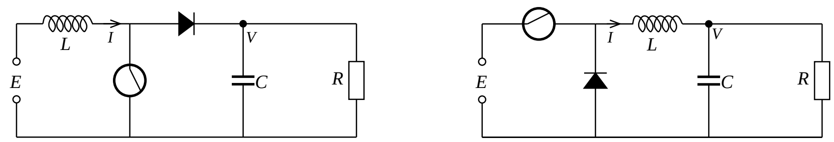

Figure 2.1: (a) Boost dc-dc power converter. (b) Buck dc-dc power converter

step-up a voltage E, and the buck power converter to step-down a voltage. The equations of motion for the boost converter are

$$\begin{aligned} S\ \textsc{Open},\ I \geq 0 \text{ or } V \leq E: &\quad \frac{dV}{dt} = \frac{I}{C} - \frac{V}{RC}, \quad L\frac{dI}{dt} = E - V; \\ S\ \textsc{Open},\ I = 0 \text{ and } V < E: &\quad \frac{dV}{dt} = -\frac{V}{RC}; \\ S\ \textsc{Closed}: &\quad \frac{dV}{dt} = -\frac{V}{RC}, \quad L\frac{dI}{dt} = E. \end{aligned} \tag{1}$$

When the switch is closed, the diode isolated the inductor from the capacitor. The capacitor supplies energy to the load resistance, while the power supply supplies energy to the inductor. When the switch is open, the energy in the inductor is transferred to the capacitor. However, the diode prevents the current through the inductor falling below zero; if the current reaches zero, then no energy is supplied to the circuit until the voltage at the capacitor drops below that of the power supply. The system is controlled by opening and closing the switch in response to the voltage V. Some possible switching strategies are

Duty cycle: $S = \textsc{Closed}$ for $t/T \bmod 1 \leq \alpha$.

Ramp switching: $S = \textsc{Closed}$ for $V \geq V_R$, where $V_R = V_L + (V_U - V_L)(t/T \bmod 1)$.

Hysteresis: $S \to \textsc{Open}$ if $V \leq V_L$; $S \to \textsc{Closed}$ if $V \geq V_U$.

Chaotic behaviour in power converters has been extensively discussed in the literature [2, 17, 25].

Another important source of examples of chaotic hybrid systems arise in mechanics, especially the mechanics of impacting systems or systems with stick-slip behaviour caused by friction. The book [30] contains an overview of the dynamics of non-smooth mechanical systems.

A simple impact oscillator with chaotic dynamics [7] is given by the equations

$$\ddot{x} + \zeta\dot{x} + x = \cos(\omega t), \quad x < d;$$
$$\dot{x} \mapsto -\lambda\dot{x}, \quad x = d.$$

We let the phase ϕ be given by $\phi = t \bmod T$. Note that despite the discontinuity in the velocity at an impact, the time evolution has continuous dependence on initial conditions since the velocity reset is the identity for $\dot{x} = 0$.

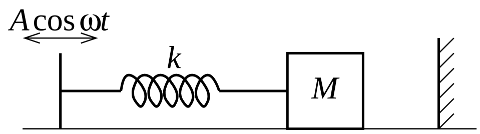

Figure 2.2: A simple mechanical impact oscillator.

A *grazing bifurcation* occurs at a parameter value for which a periodic motion of the body oscillator has an impact with zero relative velocity. The grazing bifurcation was independently discovered by Peterka [41], Whiston [50, 49] and Nordmark [37]. There have been many subsequent analyzes, including [9, 19, 28, 52, 16].

One way of studying grazing phenomena is to consider the *impact map*. If (v, ϕ) are the velocity and phase of an impact, then (v', ϕ') are the velocity and phase of the next impact. The advantage of the impact map are that it is fairly easy to compute, and is derived naturally from the system. However, the impact map has the disadvantage of being discontinuous at the preimage of the grazing surface, whereas the time evolution of the system is continuous. For this reason, it may be preferable to study the stroboscopic (time T) map. A normal-form analysis shows that the grazing impact gives rise to a square-root singularity in the return map, which gives rise to many bifurcation scenarios, including period-adding and spontaneous transitions to chaos.

3 Basic Hybrid Systems Theory

In this section, we give a brief introduction to hybrid-time systems, including appropriate solution spaces, frameworks for system modelling and definition, and semantics of solution. Frequently, the appropriate definitions depend on the class of system being studied, or the properties of interest; here we give definitions which are appropriate for the study of chaotic dynamics.

3.1 Solution spaces for hybrid-time evolution

The evolution of a hybrid-time system consists of both continuous-time evolution and discrete transitions. Hence the state $x(t)$ of the system is a discontinuous function of time. We adopt the convention of taking *cadlag (continue à droit, limit à gauche)* functions, as shown in Figure 3.1, and let t_n be the time of the n^{th} discrete transition.

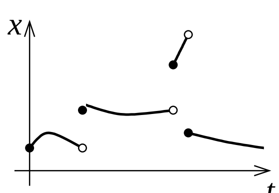

Figure 3.1: A cadlag solution of a hybrid-time system.

The cadlag representation of solutions is sufficient for hybrid-time systems with at most one discrete-event at any time instance. For hybrid-time systems which admit the possibility of two or more events at any time instant, the cadlag representation is not appropriate as the intermediate points are lost. Instead, we represent solutions on a *hybrid time domain* [1, 23, 12], which also records the number of discrete events which have occurred.

For continuous-time systems, an appropriate topology on solution spaces is the *compact-open* topology, with basic open sets

$$U_{(\xi,K,\epsilon)} = \{x : \mathbb{R} \to X \mid \forall t \in K,\ d(x(t), \xi(t)) < \epsilon\}. \tag{2}$$

In other words, solutions are close if they are uniformly close on compact sets.

Taking the uniform distance between solutions leads for trajectories which are close, but have slightly different event times, being considered far apart. For if

$$x_1(t) = \begin{cases} 0 & \text{if } t < t_1, \\ 1 & \text{if } t \geq t_1; \end{cases} \qquad x_2(t) = \begin{cases} \delta & \text{if } t < t_2, \\ 1+\delta & \text{if } t \geq t_2; \end{cases} \tag{3}$$

with $t_1 < t_2 < t_1 + \epsilon$, then the uniform distance between the solutions at time t with $t_1 < t < t_2$ is equal to $1 + \delta$, so $d(x_1, x_2) = 1$. This is usually inappropriate, since the distance between solutions is large even if the initial conditions are close and there are no irregularities in the behaviour.

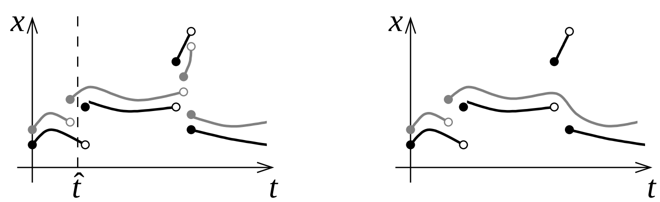

Figure 3.2: (a) Two solutions which are close in the hybrid Skorohod topology despite being far apart at time $\hat{t}$. (b) Two solutions which are far apart in the hybrid Skorohod topology despite the interval on which they are not close being small.

A better topology on solutions is the *compact-open Skorohod topology* [5], originally developed for stochastic processes. The Skorohod topology allows small reparameterisations of the time domain. An equivalent topology is the *graph* topology, which is simply the Fell topology on the solution graphs. The basic open sets are:

$$U_{(\xi,K,\delta,\epsilon)} = \{x : \mathbb{R}^+ \to X \mid \forall \tau \in K,\ \exists t \in (\tau - \delta, \tau + \delta)\ d(x(t), \xi(\tau)) < \epsilon\}. \tag{4}$$

An equivalent metric description of the topology can also be formulated.

A solution $x(t)$ of a hybrid system is *Zeno* if infinitely many discrete events occur in finite time T. This means that $\lim_{n\to\infty} t_n < \infty$, where t_n is the time of the n^{th} discrete transition. Zeno behaviour in a hybrid-time model is often exhibited as chattering in the real-life system.

3.2 Modelling frameworks for hybrid systems

A commonly used framework for describing hybrid-time systems is the *hybrid automaton* framework. Informally, a hybrid automaton is based on an underlying *discrete-event system*, with *discrete modes* connected by *discrete events*. Within each discrete mode, the *continuous state* evolves under a flow until the *guard set* corresponding to a discrete event is reached. A *discrete transition* the occurs, and the discrete mode and continuous state are instantaneously updated according to a *reset* map.

The hybrid automaton framework is usually very convenient for modelling, but contains details which are superfluous for describing the dynamics. A simpler modelling framework is that of *impulse differential inclusions*, introduced in [1].

Definition 3.1 An impulse differential inclusion is a tuple $H = (X, D, F, G, R)$ where

- The *state space* X is a differential manifold;
- $D \subset X$ is the *domain* or *invariant*;
- $\dot{x} \in F(x)$ is a differential inclusion defining the *flow* or *dynamic* $\Phi : X \times \mathbb{R} \rightrightarrows X$;
- $G \subset X$ is the *guard set* or *activation*;
- $R : X \rightrightarrows X$ is the *reset* relation.

Here, we use the notation $X \rightrightarrows Y$ to denote a multiple-valued map from X to Y.

A solution of an impulse differential inclusion is a cadlag function $x : \mathbb{R}^+ \to X$ with finitely or infinitely many discontinuities which occur at times $t_1, t_2, \ldots$ such that

1. between event times, we have $x(t) \in D$ and $x(t)$ is absolutely continuous with $\dot{x}(t) \in F(x(t))$ almost everywhere.
2. at event times times, we have $x^-(t_i) \in G$ and $x(t_i) \in R(x^-(t_i))$.

where $x^-(t_i) := \lim_{t \nearrow t_i} x(t)$.

Notice that if $x(t) \in D^\circ \cap G$, then both continuous evolution and a discrete transition are possible, hence the evolution is multivalued or indeterminate. As we shall see in the next section, the solutions of an arbitrary impulse differential inclusion may have irregularities which need to be tamed, giving rise to different solution concepts.

Henceforth we make the following simplifying assumptions on our hybrid systems with respect to the general framework of Definition 3.1:

- The guard set G is a subset of the boundary of the domain D.
- The continuous dynamics is given by a locally Lipschitz differential equation $\dot{x} = f(x)$.
- The guard set G is partitioned into subsets G_i such that the reset map $r_i := r|_{G_i}$ is single-valued and continuous.

In the hybrid automaton framework, the sets G_i correspond to activation sets for different discrete events.

Given a hybrid time system, we can define the *return map* which takes an initial point to the point We alternatively define the *hitting map* as the set of points which can be reached by a discrete transition followed by continuous evolution into a guard set.

3.3 Solution concepts

Many techniques of dynamical systems rely on the solutions having continuous or smooth dependence on initial conditions. As previously mentioned, the evolution of a hybrid system may not have continuous dependence on initial conditions. Further, this property is lost in hybrid systems in the following situations, which are depicted in Figure 3.3

- A solution of the differential equation $\dot{x} = f(x)$ crosses ∂D at a point not in G. At this time, no further evolution is possible and the system is said to be *blocking*.
- A solution of the differential equation touches ∂D at a point of G but does not leave D. At this time, both a discrete transition and further continuous evolution may be allowed.
- A solution of the differential equation reaches a point at which the reset map r is discontinuous. At this point, continuous dependence on initial conditions is lost.

However, it is often sufficient to have *semicontinuous* dependence on initial conditions, giving rise to two different *semantics of evolution*.

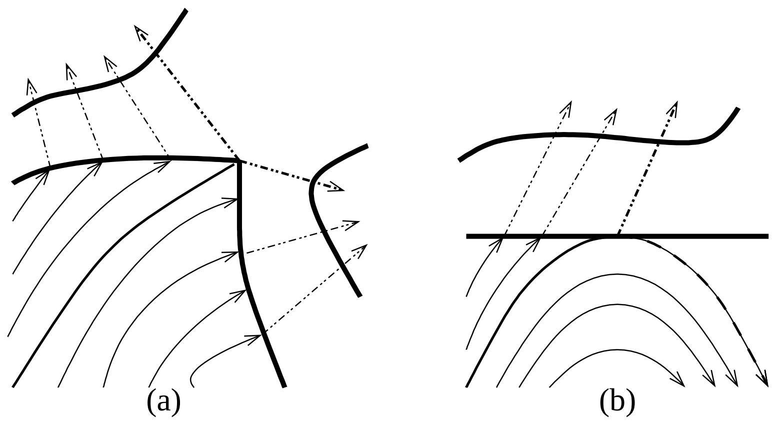

Figure 3.3: (a) Discontinuity of solutions due to multiply-enabled transitions (corner collision). (b) Discontinuity of solutions due to tangency with the guard set.

For *upper semantics*, we assume that at a tangency with the guard set, then both a discrete transition and continuous evolution are possible. Further, if the continuous evolution reaches a point in $\overline{G}_i \cap \overline{G}_j$, then both resets r_i and r_j are possible. Hence the system evolution is multivalued or nondeterministic, but under these semantics, the limit of a sequence of solutions is also a solution, and the solution set varies upper-semicontinuously with the system parameters [22]. Further, it is possible to effectively compute over-approximations to the set of points which can be reached from a given initial set [13, 20].

For *lower semantics*, we assume that at a tangency with the guard set, at a discontinuity point of the reset map, then no further evolution is possible. Hence solutions which exist for all time only exist on the set of initial conditions from which further evolution does not reach a discontinuity point. Under fairly mild conditions on the reset map, finite-time evolution is defined on an open set of initial conditions, and solutions vary continuously on this set. This property is useful for topological techniques based on index theory. Under the same conditions, infinite-time evolution is defined on a G_δ set of initial conditions, which is dense by the Baire category theorem.

3.4 Dependence on initial conditions in continuous time

We have seen that for hybrid-time systems, discontinuous dependence on initial conditions occurs at tangencies with the guard set and on the boundary of activation sets for different discrete events. However, discontinuities in the evolution may also occur in continuous-time hybrid systems.

Given a differential equation $\dot{x} = f(x)$ with discontinuous right-hand side, or a differential inclusion $\dot{x} \in F(x)$, the *Filippov regularisation* of F is the function

$$\hat{F}(x) = \bigcap_{\epsilon \to 0} \overline{\text{conv}} F(N_\epsilon(x)). \tag{5}$$

The Filippov regularisation of F is an upper-semicontinuous multivalued function with closed, convex values.

Theorem 3.1 *If $F : \mathbb{R}^n \to \mathbb{R}^n$ is an upper-semicontinuous multivalued function with compact, convex values, then for every $x_0 \in \mathbb{R}^n$ there exists an absolutely continuous function $x : [0, T) \to X$ such that $x(0) = x_0$ and $\dot{x}(t) \in F(x(t))$ a.e.*

Additionally, the set of solutions is a closed set in the compact-open topology, and the set of points reachable from a given x_0 at time $t > 0$ is closed.

Hence Filippov solution concept gives existence of solutions for arbitrary differential equations, possibly at the expense of introducing nondeterminism.

Filippov solutions are useful when a discontinuity set of the right-hand side is attracting from both sides, since one obtains *sliding* orbits. Using an explicit hybrid model, one would obtain Zeno or chattering behaviour, as the solution would constantly switch from one mode to the other.

In some circumstances, the set of Filippov solutions may be larger than one would obtain using a hybrid-time model with explicit mode switching. Consider the generic

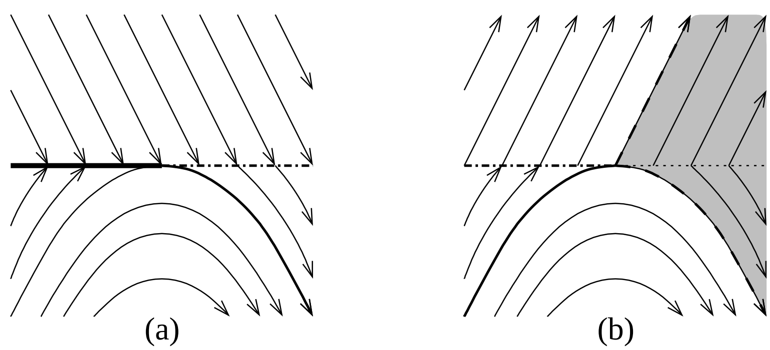

Figure 3.4: (a) Grazing at a sliding mode causes instability. (b) Discontinuity on a sliding mode.

situations shown in Figure 3.4. In (a), orbits which reach the sliding surface have the same future behaviour, and leave the sliding surface by the indicated trajectory. In (b) orbits which reach the sliding surface from below cross it immediately, *except* for the indicated orbit. Using the classical Filippov solution concept, the grazing orbit may slide along the discontinuity surface, even though this is unstable, and leave the switching hypersurface at any time. The evolution is nondeterministic, and any point and continues nondeterministically into the shaded region. Using a mode-switching solution concept, the grazing orbit either switches immediately into the upper region, or continues in the lower region. Which solution is more appropriate depends on the system being modelled.

In a system in which the discontinuity of the right-hand side is an approximation to a fast-varying function, then the Fillipov solution concept is appropriate, since it captures approximations to the solution of the original system. If the discontinuity of the right-hand side is due to a state-dependent switching, then a mode-switching solution concept is more appropriate, since the system is either in one mode or the other.

Whichever solution concept is used in (b), the solution varies discontinuously with initial condition. In contrast, the solution in (a) varies continuously with initial conditions. This is because one side of the switching hypersurface is attracting.

Theorem 3.2 *Let $\dot{x} = f(x)$ be a system with discontinuous right-hand side, and let M be a codimension-1 switching boundary. Suppose that at every point of M, at least one side is strictly attracting. Then the evolution across M is continuous, and for every initial point there exists a unique Filippov solution.*

A special case of grazing behaviour occurs in impact oscillators.

Definition 3.2 An *impact oscillator* is a dynamical system such that that is $\dot{x} = f(x)$ for $g(x) \geq 0$, and $x' = r(x)$ if $g(x) = 0$ and $f(x) \cdot \nabla g(x) < 0$. where $g : M^- \to M^+$ is such that $g(x) \to x$ as $x \to M^0$, where $M_0 = \{x \in X \mid g(x) = 0 \text{ and } f(x) \cdot \nabla g(x) = 0\}$, $M^- = \{x \in X \mid g(x) = 0 \text{ and } f(x) \cdot \nabla g(x) < 0\}$ and $M^+ = \{x \in X \mid g(x) = 0 \text{ and } f(x) \cdot \nabla g(x) > 0\}$.

Theorem 3.3 *Let (f, g, r) define an impact oscillator. Then under the identification $x \sim r(x)$ on $M^- \times M^+$, the evolution is continuous.*

A similar situation to that shown in Figure 3.4 occurs at corner collisions, as shown in Figure 3.5.

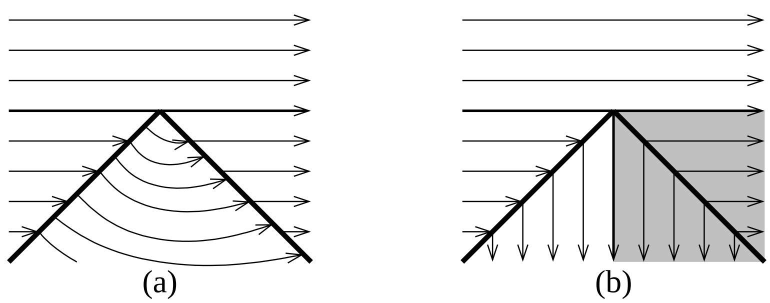

Figure 3.5: (a) A corner collision causing non-smoothness. (b) A corner collision causing discontinuity in the evolution.

We may obtain continuous (but non-smooth) evolution, or may obtain discontinuities in the evolution, the exact nature of which depends on whether we use Filippov semantics or switching semantics. The following result gives conditions under which a corner collision does not induce discontinuities in the system evolution.

Theorem 3.4 *Let $\dot{x} = f(x)$ be a system with discontinuous right-hand side, let $g : X \to \mathbb{R}^2$ be such that $\nabla g_i(x) \neq 0$ if $g_i(x) = 0$. Let $X^- = \{x \mid g(x) < 0\}$ and $X^+ = \{g_1(x) > 0 \vee g_2(x) > 0\}$. Let $M^C = \{g(x) = 0\}$ Suppose that $f(x) \cdot \nabla g_1(x) > 0$ and $f(x) \cdot \nabla g_2(x) < 0$ for all $x \in X^C$. Then evolution is continuous in a neighbourhood of X^C.*

Proof In a neighbourhood of X^C, the time spent in X^0 is continuous, and tends to 0 as $x \to X^C$. Hence $\Phi_t(x) = \Phi^+_{t_3} \circ \Phi^-_{t_2} \circ \Phi^+_{t_1}(x)$ with t_1, t_2, t_3 continuous functions of x and $t_2 \to 0$ as $x \to X_C$.

4 Symbolic Dynamics and Invariant Measures

Symbolic dynamics is potentially a powerful tool to study hybrid systems, since these have a naturally-defined partition of the state space into the discrete modes. Since symbolic dynamics is most naturally defined for discrete-time systems, in this section, we assume that we are considering a discrete-time hybrid system, possibly originating as a time-discretisation of a continuous- or hybrid-time system.

Given a finite collection of sets $\{R_s \subset X : s \in S\}$, which need not be disjoint or cover X, we say that a sequence $(s_0, s_1, s_2, \ldots)$ is an *itinerary* for an orbit $(x_0, x_1, x_2, \ldots)$ of a discrete-time system f if $x_k \in R_{s_k}$ for all k. The closure of the set of allowed itineraries of a system f is called the *shift space* of f, denoted Σ_f. The shift space of f is invariant under the *shift map* $\sigma : S^{\mathbb{N}} \to S^{\mathbb{N}}$ defined by $\sigma(s_0, s_1, s_2, \ldots) = (s_1, s_2, \ldots)$. The main aim of symbolic dynamics is to compute the set of itineraries and/or the shift space.

If the R_s are mutually disjoint compact sets, then every point has at most one itinerary, and if f is continuous, then the set of itineraries itself is closed. Further, if we define $R_{s_0,s_1,\ldots,s_k} = \{x \in X \mid f^i(x) \in R_i \, \forall i = 0, \ldots, k\}$, then $(s_0, s_1, s_2, \ldots)$ is an itinerary for f if, and only if, every $R_{s_j,\ldots,s_k}$ is nonempty. Hence it is possible to compute over-approximations to Σ_f by starting with the entire space $S^{\mathbb{N}}$ and removing all sequences which contain a *forbidden* word, that is, a word $(s_j, \ldots, s_k)$ with $R_{s_j,\ldots,s_k} = \emptyset$.

In many applications, the sets R_s are not disjoint, but form a *topological partition* of X, which means that $X = \bigcup_{s\in S} \overline{R_s^\circ}$ and $R_{s_1}^\circ \cap R_{s_2}^\circ = \emptyset$ if $s_1 \neq s_2$. In this case, we obtain different shift spaces depending on whether the sets R_s to be open or closed. However, if the sets R_s are closed, we often obtain too many itineraries, since for example, a fixed point $p \in \partial R_s \cap \partial R_{s'}$ would have any sequence with $s_i \in \{s, s'\}$ as an itinerary, so it is usually preferable to consider itineraries with respect to R_s° and take the closure in $S^{\mathbb{N}}$ to obtain the shift space. If $\vec{x}$ is an orbit, then we say $\vec{s}$ is a *limit itinerary* for $\vec{x}$ if there exist orbits $\vec{x}_i$ with itineraries $\vec{s}_i$ such that $\vec{x}_i \to \vec{x}$ and $\vec{s}_i \to \vec{s}$

If f has the property that the preimage of an open and dense set is dense, then $\bigcap_{i=0}^{\infty} f^{-i}(R^\circ)$, where $R^\circ = \bigcup\{R_s^\circ \mid s \in S\}$ is a G_δ set, and hence is dense by the Baire Category Theorem. Therefore, for a dense set of points, the itinerary exists and is unique.

Computing under-approximations to the shift space is usually much more difficult than computing over-approximations. This is because although we can deduce that $s^{\mathbb{N}}$ is not an itinerary of f if $R_s \cap f^{-1}(R_s) = \emptyset$, we cannot deduce that $s^{\mathbb{N}}$ *is* an itinerary of f even if $R_{s,s} \neq \emptyset$, since we may have $R_{s,s,s} = \emptyset$. The most important methods for proving that an itinerary exists are based Lefschetz and Nielsen fixed-point theory, and the Conley index theory, all of which can be used to prove the existence of periodic itineraries $s_{n+i} = s_i$.

In one dimension, it is easier to compute infinitely many periodic orbits using covering relations. If I, J are intervals, we say that I f-covers J if $f(I) \supset J$. Using the intermediate value theorem, we can show that if $I_0, I_1, I_2, \ldots$ is a sequence of intervals and I_k covers I_{k+1} for all k, then there exists a point x such that $f^k(x) \in I_k$ for all k. Further, if $I_{n+k} = I_k$ for all k, then x can be chosen such that $f^n(x) = x$.

4.1 Piecewise-continuous systems

Let $f : X \to X$ a single-valued, piecewise-continuous function. Let $\mathcal{P} = \{P_s \mid s \in S\}$ be a locally-finite topological partition of X such that f is continuous when restricted to each P_s°, and that $f|_{P_s^\circ}$ extends over each P_s to a continuous function f_s. Let $\partial\mathcal{P} = \bigcup\{\partial P \mid P \in \mathcal{P}\}$ and $\mathcal{P}^\circ = \bigcup\{P^\circ \mid P \in \mathcal{P}\}$ Define $\bar{f} : X \rightrightarrows X$ by $\bar{f}(x) = \bigcup\{f_s(x) \mid x \in P_s\}$, and assume that $\bar{f}(x) \supset f(x)$ (notice that $\bar{f}(x) = f(x)$ unless f is discontinuous at x. We may also define f° by $f^\circ := f|_{\bigcup\{P_s^\circ \mid s \in S\}}$.

The function $\bar{f}$ is a finite-valued upper-semicontinuous over-approximation to f obtained by taking all accumulation points of the graph of f. By *upper-semicontinuous*, we mean $\bar{f}^{-1}(A)$ is closed whenever A is closed. Consequently, the set of itineraries of $\bar{f}$ is an over-approximation to the set of itineraries of f.

The function f° is a single-valued partially-defined lower-semicontinuous under-approximation to f obtained by discarding all values of f at discontinuity points. By *lower-semicontinuous*, we mean that $(f^\circ)^{-1}(U)$ is open whenever U is open. taking all accumulation points of the graph of f. By *upper-semicontinuous*, we mean $\bar{f}^{-1}(A)$ is closed whenever A is closed.

4.2 Computing over-approximations to the shift space

If f is not continuous, computing over-approximations of the set of itineraries is more complicated. For if $f(R_s) \cap R_{s'} = \emptyset$ but $\overline{f(R_s)} \cap R_{s'} \neq \emptyset$, it may be extremely difficult to show that the word (s, s') is forbidden. However, if we take the upper-semicontinuous over-approximation of f, then we can compute itineraries in a similar way to the continuous case, though a little care is needed over the definitions.

We define

$$R_{s_0,s_1,\ldots,s_k} = \{x \in X \mid \exists x_0, x_1, \ldots, x_k \text{ such that } x = x_0, x_i \in P_i \text{ and } x_i \in f(x_{i-1})\}. \quad (6)$$

We can compute the sets $R_{s_0,s_1,\ldots,s_k}$ by the recurrence relation

$$R_{s_0,s_1,\ldots,s_k} = R_{s_0} \cap f^{-1}(R_{s_1,\ldots,s_k}). \quad (7)$$

We can then define a finite-type shift on S by taking disallowed words

$$\{s_0, s_1, \ldots, s_k \mid R_{s_0,\ldots,s_k} = \emptyset\}. \quad (8)$$

By disallowing successively more words, we can construct a sequence of finite type shifts converging to Σ_f.

Theorem 4.1 $(s_0, s_1, \ldots) \in \Sigma_f \iff \forall k,\ X_{s_0,s_1,\ldots,s_k} \neq \emptyset$.

For many hybrid systems, the state space X is disconnected, with the components $\{X_q \mid q \in Q\}$ corresponding to the discrete modes of the system. In this case, by taking the upper-semicontinuous over-approximation $\bar{f}$ to f, we can compute over-approximations to the set of allowed sequences of discrete events. An example is given in Section 6.

4.3 Computing under-approximations to the shift map

We can compute lower approximations to the shift space by attempting to compute periodic orbits. We recall the *Lefschetz fixed point index*, which for each triple (f, X, U)

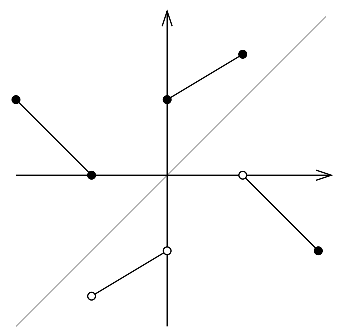

Figure 4.1: A piecewise-continuous interval map.

where $f : X \to X$ is a continuous map and $U \subset X$ is an open set such that $\operatorname{fix} f \cap \partial U = \emptyset$, assigns an index $\operatorname{ind}(f, X, U) \in \mathbb{Z}$ such that if $\operatorname{ind}(f, X, U) \neq \emptyset$, then f has a fixed point in U. Further, the index is local, which means that it depends only on the values of f on $\overline{U}$.

If we define $P^{\circ}_{s_0,s_1,\ldots,s_{k-1}}$ analogously to in Section 4.2, then f^k is continuous on $P^{\circ}_{s_0,s_1,\ldots,s_{k-1}}$ and indeed extends to a continuous function $f_{s_0,s_1,\ldots,s_{k-1}} := f_{s_{k-1}} \circ \cdots \circ f_{s_1} \circ f_{s_0}$ on $P_{s_0,s_1,\ldots,s_{k-1}}$. Hence for any open set U in X such that $U \subset P_{s_0,s_1,\ldots,s_{k-1}}$, we can define the fixed-point index of $f_{s_0,s_1,\ldots,s_{k-1}}$ over U. Then if $\operatorname{ind}(f_{s_0,s_1,\ldots,s_{k-1}}, P_0, U) \neq \emptyset$, then f has a periodic orbit with itinerary $s_0, s_1, \ldots, s_{k-1}, s_0, s_1, \ldots$.

Just as for continuous functions, the methods presented here can only be used to deduce the existence of finitely many periodic orbits. However, since the functions $f_{s_0,s_1,\ldots,s_{k-1}}$ are continuous on $P_{s_0,s_1,\ldots,s_{k-1}}$, we can in principal use advanced topological methods to approximate the dynamics. Again, the one-dimensional case is much easier. Using the regularisation of f, we can show that if $f_{s_i}(P_{s_i}) \supset P_{s_{i+1}}$ for all i, then there exists an orbit $(x_0, x_1, x_2, \ldots)$ with $x_i \in P_{s_i}$ for all i.

4.4 Ergodic theory and statistical behaviour

We now try to give a probabilistic description of a hybrid system by finding an invariant probability measure for its return map. If $f : X \to X$ is a single-valued map, a measure μ on X is *invariant* under f if $\mu(f^{-1}(A)) = \mu(A)$ for all measurable sets A. Any continuous map on a compact metric space has an invariant probability measure.

It is known that for piecewise-expanding maps of the interval, there exists an absolutely-continuous invariant measure [29]. A major generalization of this result is that certain piecewise monotone-convex mappings also have an absolutely continuous invariant measure [4]. In higher dimensions the situation is considerably more complicated, though for a generic class of piecewise-expanding maps, there do exist absolutely-continuous invariant measures [14, 15].

The following example shows that discontinuous maps of the interval need not have an invariant probability measure.

Example 4.1 Let

$$f(x) = \begin{cases} -1 - x \text{ if } -2 \le x \le -1; \\ x/2 - 1 \text{ if } -1 < x < 0; \\ x/2 + 1 \text{ if } 0 \le x \le 1; \\ 1 - x \text{ if } 1 < x \le 2, \end{cases}$$

as shown in Figure 4.1. Then every orbit starting in $[-2, 2]$ converges to the sequence $(0^+, 1^+, 0^-, -1^-, 0^+, \ldots)$ but the sequence $(0, 1, 0, -1, 0, \ldots)$ cannot be an orbit of and single-valued map.

The difficulty in the above example is that the the natural "invariant" measure would assign nonzero weight to the discontinuity point. In cases where an absolutely-continuous invariant measure exists, the discontinuity points have measure zero and therefore cause no difficulties.

To obtain an invariant measure for general piecewise-continuous maps, we can lift the map to the product of the state space and the symbol space.

Let f be piecewise-continuous, with $f_s := f|_{P_s}$ continuous on each element P_s of a topological partition $\mathcal{P}$, and such that f_s extends continuously over $\overline{P}_s$. Let Σ_f be the shift space of f with respect to the partition elements P_s°.

For each itinerary $\vec{s}$, let $X_{\vec{s}}$ be the set of points with itinerary or limit itinerary $\vec{s}$, and define $\widehat{X} := \bigcup_{\vec{s} \in \Sigma_f} \{X_{\vec{s}} \times \vec{s}\}$ with the inherited product topology. Then $\widehat{X}$ is compact if X is compact, and f lifts to a continuous function $\widehat{f} : \widehat{X} \to \widehat{X}$.

There must therefore always exist an invariant measure $\widehat{\mu}$ for $\widehat{f}$. Further, define $\mu(A) := \widehat{\mu}(\pi^{-1}(A))$, where $\pi(x, \vec{q}) = x$. We call μ a *shift-invariant measure* for f. If $\widehat{\mu}(\partial\mathcal{P}) = 0$, then μ is an invariant measure for f.

We therefore have the following simple theorem.

Theorem 4.2 *If f is piecewise-continuous, then f has a shift-invariant measure.*

5 Bifurcation Theory for Non-smooth Maps

In this section we describe the most important *border-collision bifurcations* for one-dimensional piecewise-smooth maps. The analysis of these bifurcations is considerably simpler than the analysis of bifurcations in three-dimensional flows, but provides insight into the higher-dimensional cases. In particular, the nonsingular border-collision bifurcations provide a model for corner-collision bifurcations in continuous- and hybrid-time systems, and the border-collision bifurcations with a square-root singularity provide a model for grazing bifurcations. and use these to study *corner-collision* and *grazing* bifurcations in continuous- and hybrid-time systems. In both cases, we consider the continuous and discontinuous cases separately.

For more detailed exposition of bifurcations in non-smooth systems, see the book [53].

5.1 Continuous border-collision bifurcations

The border-collision bifurcation can occur in systems with continuous evolution, such as piecewise-affine maps. Border-collision bifurcations were observed in [26, 44, 31, 39, 38]; here we follow the exposition in [40].

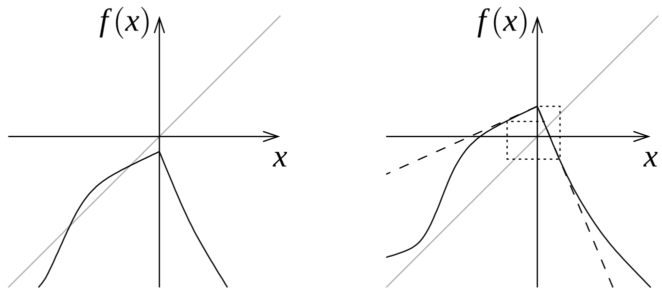

Figure 5.1: A border collision bifurcation for a non-smooth map.

Let $f_\epsilon : \mathbb{R} \to \mathbb{R}$ be a continuous piecewise smooth map with parameter ϵ whose derivative is discontinuous at 0, as shown in Figure 5.1. The simplest example of a *border-collision* bifurcation occurs when $f_\epsilon(0) = 0$. Assume further that f_ϵ is differentiable in ϵ and $c = df_\epsilon(0)/d\epsilon > 0$ at $\epsilon = 0$. We let $a = \lim_{x \nearrow 0} f_0'(x)$ and $b = -\lim_{x \searrow 0} f_0'(x)$, and assume $0 < a < 1 < b$.

Now for $\epsilon > 0$ small, we have $f_\epsilon(0) = c\epsilon + O(\epsilon^2) > 0$, and $f_\epsilon^2(0) = c(1-b)\epsilon - O(\epsilon)^2 < 0$. Further, if $x_\epsilon = \xi\epsilon + O(\epsilon^2)$ for $\xi \leq 0$, then $f_\epsilon(x) = (c + a\xi)\epsilon + O(\epsilon^2) > x$. Taking $I_\epsilon = [f_\epsilon^2(0), f_\epsilon(0)]$, we see that $f_\epsilon(I_\epsilon) \subset I_\epsilon$. Hence for $\epsilon > 0$ small, the dynamics is contained in an interval of size $O(\epsilon)$ about 0. The linearization of $f_\epsilon(x)$ about $x = 0$ is therefore a good approximation to f_ϵ in I_ϵ.

It can be rigorously shown that linearising at $x = 0$ yields a *normal form* of the bifurcation as an affine map

$$F_{a,b,\epsilon}(x) = \begin{cases} \epsilon + ax \text{ if } x \leq 0; \\ \epsilon - bx \text{ if } x \geq 0, \end{cases} \qquad \text{with} \quad 0 < a < 1 \text{ and } b > 0. \tag{9}$$

as shown in Figure 5.2. For simplicity, we henceforth only consider the map (9). linearized

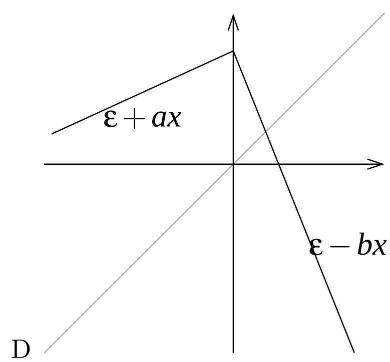

Figure 5.2: Near a border collision bifurcation and for a piecewise-affine map.

If $\epsilon < 0$, then $x_p := \epsilon/(1-a) \leq 0$ is a fixed point, and since $F_{a,b,\epsilon}(x) \leq \epsilon$ for all x, all orbits converge to x_p. If $\epsilon = 0$, then 0 is a fixed point, which is stable if $b < 1$ and one-sided unstable if $b > 1$. If $\epsilon > 0$ and $0 < b < 1$ then $x_0 = \epsilon/(1+b)$ is a stable fixed point.

Note that $f(0) = 1$ and $f(1) = 1 - b < 0$, and that if $x < 0$, then $x < f(x) < 1$. Hence all orbits eventually enter the interval $[0, 1]$.

The interesting case is $\epsilon > 0$ and $b > 1$.

Note that by the coordinate transformation $x \mapsto x/\epsilon$, we can scale ϵ to equal 1; we define $F_{a,b} := F_{a,b,\epsilon}$. Taking $c = 0$, the critical point, we see that $F_{a,b}(0) = 1$, $F^2_{a,b}(0) = 1 - b < 0$, and $F^3_{a,b}(0) = 1 + a - ab$. Let $I_0 = [1 - b, 0]$ and $I_1 = [0, 1]$. Clearly $F_{a,b}(I_1) = I_0 \cup I_1$. Then if $1 < b < 1 + 1/a$, we have $F_{a,b}(1 - b) = 1 + a - ab > 1 + a - (1 + a) = 0$, so $f(I_0) \subset I_1$. Then for all $x \in [1 - b, 1]$, we have $(f^2)'(x)$ is either $-ab$ or b^2, so if $b > 1/a$, then $|(f^2)'(x)| > 1$.

We have therefore shown that

1. $F_{a,b}([1 - b, 1]) \subset [1 - b, 1]$, and
2. $|(F^2_{a,b})'(x)| > 1$ for all $x \in [1 - b, 1]$.
3. $[1 - b, 1] = \bigcap_{n=0}^{\infty} F^n_{a,b}(U)$ for all bounded $U \supset [1 - b, 1]$.

Hence $[1 - b, 1]$ is a minimal chaotic attractor for $F_{a,b}$; in particular, $F_{a,b}$ has no stable periodic orbits and strictly positive topological entropy.

Since this situation occurs for any $\epsilon > 0$ regardless of the value of ϵ, we have a bifurcation to a robust chaotic attractor. Note that the entropy of the attractor is bounded away from zero, but the size of the attractor is ϵb.

Following [40] we see that the map $F_{a,b}$ has positive entropy and may have a chaotic attractor. Similar windows exist in which the system has a chaotic attractor with k pieces, separated by periodic orbits.

Note that for smooth interval maps, the entropy varies continuously with the parameters. Here, the entropy jumps *discontinuously* at the border-collision bifurcation. By considering the change in a and b, we can *rigorously* prove the existence of a chaotic attractor with high entropy in a generic two-parameter family of maps. Since f_ϵ is unimodal, the symbolic dynamics is determined by the kneading theory [33].

5.2 Singular border-collision bifurcation

In an impact oscillator, grazing the impact set causes a square root singularity in the evolution. If this occurs on a periodic orbit, we have a *grazing bifurcation.* A normal form for the grazing bifurcation is given by

$$f(x) = \begin{cases} \epsilon + ax \text{ if } x \le 0; \\ \epsilon - b\sqrt{x} \text{ if } x \ge 0, \end{cases} \tag{10}$$

as shown in Figure 5.3. Note that unlike the affine border collision, we cannot scale away the bifurcation parameter ϵ without affecting the form of the square root term:

$$F(y) = \begin{cases} 1 + ay \text{ if } y \le 0; \\ 1 - (b/\sqrt{\epsilon})\sqrt{y} \text{ if } y \ge 0, \end{cases} \tag{11}$$

where $y = x/\epsilon$. We therefore prefer to work with the original form (10).

We again look for conditions under which there exists a chaotic attractor. It is easy to see that the interval $[-b\sqrt{\epsilon} + \epsilon, \epsilon]$ is globally attracting. There is a single fixed point $p = (1 + 2\epsilon - \sqrt{1 + 4\epsilon})/2\epsilon$, so $p \sim \epsilon^2$ for small ϵ. We also have have $f'(\epsilon) = -1/2\sqrt{\epsilon}$.

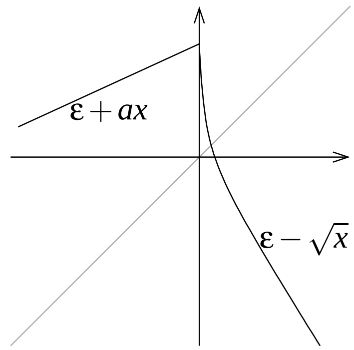

Figure 5.3: A border collision bifurcation for a map with a square-root singularity.

Now, if $-\sqrt{\epsilon} < x < 0$, then $f^n(x)$ is first greater than 0 for $n \sim \log(c-x)$, so if we let $n(x)$ be the minimum n such that $F^{n(x)}(x) > 0$, then $(f^{n(x)})'(x) \geq 1/(c+x)$ for some constant c depending only on a. Hence for ϵ sufficiently small, there must be a chaotic attractor of f for $x \in [-\sqrt{\epsilon}+\epsilon, \epsilon]$. This is a one-piece attractor if $0 < 1-a+a/\sqrt{\epsilon} < q \sim \epsilon$, which is impossible for small ϵ. Indeed, as $\epsilon \to 0$, the critical point spends increasingly long in $[\epsilon-\sqrt{\epsilon}, 0]$, and the kneading theory shows that the topological entropy approaches $\log 2$.

5.3 Discontinuous border-collision bifurcation

We now consider a discontinuous border-collision bifurcation of a stable fixed-point.

$$f(x) = \begin{cases} ax + \epsilon \text{ if } x \leq 0; \\ bx - c \text{ if } x \geq 0, \end{cases} \tag{12}$$

as shown in Figure 5.4.

Assume $a < 1$, and $a^N b > 1$ for some least integer $N \geq 0$. Assume further that $\epsilon < 1/b$. Then $f(0^-) = \epsilon$, $f(\epsilon) = b\epsilon - 1 < 0$, and $f(b\epsilon-1) > b\epsilon-1$. If $f^i(x) < 0$ for $0 \leq i < n$, then a closed form for $f^n(x)$ is $f^n(x) = a^n x + \epsilon(1-a^n)/(1-a)$. Since $x \geq b\epsilon - 1$, we have $f^n(x) \geq a^n b\epsilon - a^n + \epsilon(1-a^n)/(1-a)$, so $f^n(x) > 0 \iff \epsilon(a^n b(1-a) + 1 - a^n) > a^n(1-a)$.

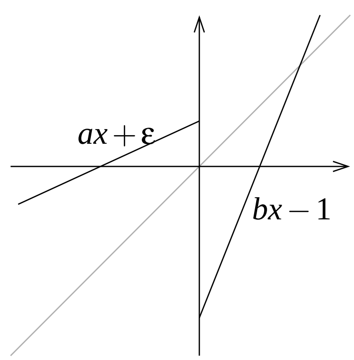

Figure 5.4: A border collision bifurcation for a discontinuous affine map.

We again look for conditions under which there exists a chaotic attractor. It is easy to see that the interval $[b\epsilon-1,\epsilon]$ is globally attracting. However, since expansion only occurs on the interval $[0,\epsilon]$, and this interval maps to $[-1,b\epsilon-1]$, for small ϵ, the contraction for $x<0$ outweighs the expansion for $x>0$. Hence, the the bifurcation, the fixed point first jumps to a periodic orbit, and this periodic orbit may then split up into a chaotic attractor as ϵ increases. Hence spontaneous chaos does not occur at this bifurcation.

5.4 Discontinuous singular border-collision bifurcation

We now consider a discontinuous border-collision bifurcation of a stable fixed-point with a square-root singularity.

$$f(x)=\begin{cases} ax+\epsilon \text{ if } x\le 0;\\ b\sqrt{x}-c \text{ if } x\ge 0,\end{cases} \tag{13}$$

as shown in Figure 5.5.

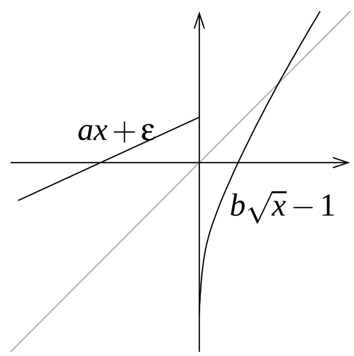

Figure 5.5: A border collision bifurcation for a map with a discontinuity.

Let $d=0$, the discontinuity point, and suppose $0<a,\epsilon<1$ Then $f(0^-)=\epsilon$, $f(\epsilon)=\sqrt{\epsilon}-1<0$, and $f'(x)>1/2\sqrt{\epsilon}$ for $x>0$. Similarly to the case studied in Section 5.3, a point $x<0$ becomes positive if

$$f^n(x)=a^n x+\epsilon(1-a^n)/(1-a) \tag{14}$$

which takes at most $n=\log(1-x(1-a)/\epsilon)/\log(1/a)$ steps. Since $x>-1$, we find $n\sim-\log\epsilon$ for fixed a. Hence the derivative of the return map is $(a^n)/2\sqrt{\epsilon}\sim\sqrt{\epsilon}$ for small ϵ, and so the singularity in the derivative is not sufficient to compensate for the discontinuity, and the bifurcation causes high-period periodic orbits which may later break-up to give a chaotic attractor.

6 Case Studies

6.1 Switched queueing/arrival systems

The following switched arrival system was first considered in [8], and later in the book [32].

Tanks T_i, $i=1,2,3$ containing volume x_i of fluid with constant outflows ρ_1, ρ_2 and ρ_3 can be filled by a single pipe with inflow $\rho_{\text{in}}=\rho_{\text{out}}:=\rho_1+\rho_2+\rho_3$. There are three

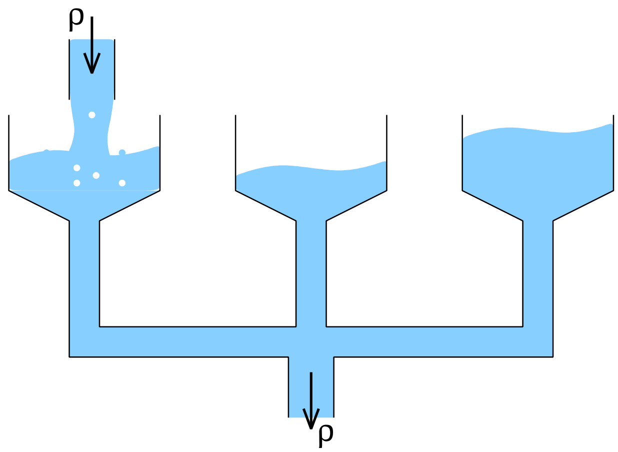

Figure 6.1: A switched arrival system.

modes q_i corresponding to filling tank T_i. Since the total volume is preserved, we have $x_1 + x_2 + x_3 = x_{\text{tot}}$.

A simple switching law is to switch to filling tank T_i whenever $x_i = 0$. The dynamics of the system is shown in Figure 6.2. If the system begins in mode q_i with $x_i = 0$, then the system switches to mode q_j over mode q_k if tank T_j empties first, which occurs if $x_j/\rho_j < x_k/\rho_k$. Hence the return map f is defined on the sets $I_i := \{(x, q_i) \mid x_i = 0\}$. Under the return map we have $f(I_1) \supset I_2 \cup I_3$, $f(I_2) \supset I_3 \cup I_1$ and $f(I_3) \supset I_1 \cup I_2$. Hence any sequence of mode switches is possible.

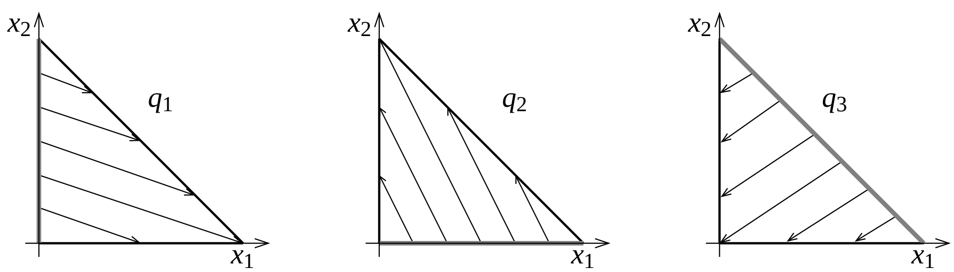

Figure 6.2: A simple switching law with Zeno behaviour.

Since the system on average spends time ρ_i/ρ filling tank i, an invariant measure for the flow is given by $2\rho_i\lambda/\rho$, where λ is Lesbesgue measure. An invariant measure for the return map f is given by a measure which is uniform on each I_i, with

$$\mu(I_i) = \frac{1}{2}\frac{\rho_i(\rho - \rho_i)}{\rho_1\rho_2 + \rho_2\rho_3 + \rho_3\rho_1}.$$

Using this, we can deduce that the average switching time is

$$T_{\text{av}} = \frac{1}{4}\frac{\rho_1 + \rho_2 + \rho_3}{\rho_1\rho_2 + \rho_2\rho_3 + \rho_3\rho_1} = \frac{1}{2}\frac{\rho}{\rho^2 - \rho_1^2 + \rho_2^2 + \rho_3^2}.$$

If all inflows are equal, this yields $3/4\rho$, and if one inflow is twice the other two, this yields $4/5\rho$. Compare this with a regular cyclic switching strategy with an average switching time of $1/3\rho$.

A major problem with this switching law is that if two tanks are both close to being empty, then we switch rapidly between them, and if two tanks become empty at exactly the same time, then the system deadlocks due to Zeno behaviour. We therefore seek a switching law with a lower average number of switches.

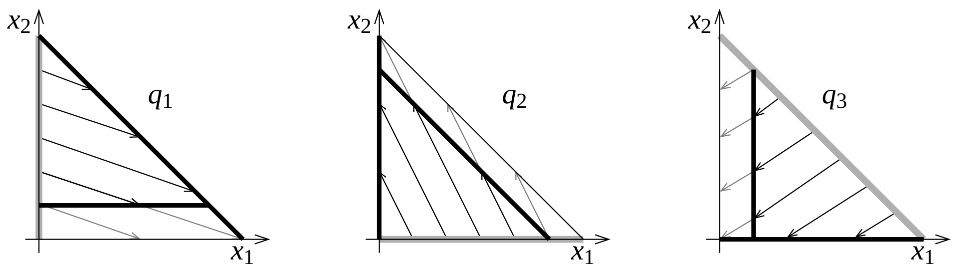

Figure 6.3: A switching law without Zeno behaviour.

A modified switching law is to switch preferentially from tank T_1 to tank T_2, from T_2 to T_3, and from T_3 to T_1. We accomplish this by switching from mode q_i to mode q_{i+1} if x_{i+1} drops below a non-zero threshold ξ_{i+1}. This succeeds in avoiding Zeno behaviour, since if x_1 and x_2 are both low in mode q_3, the system switches to mode q_1 before x_1 reaches 0, and then immediately to mode q_2 if x_2 is small. The system then remains away from mode q_3 until both x_1 and x_2 have recovered.

To obtain a return map f in the form of a self map on the sets I_i defined above, we take the state after switching to mode q_i and flow backwards until $x_i = 0$. The resulting map is shown in Figure 6.4. Notice that we do not now have $f(I_1) \supset I_3$, as it is not possible to switch from mode q_1 to mode q_2 with a value of x_1 greater than $x_{\rm tot} - \xi_2$. As a result, the symbolic dynamics will not include all transition sequences, but sequences with a large number of repetitions of two modes will be cut (see Figure 6.3).

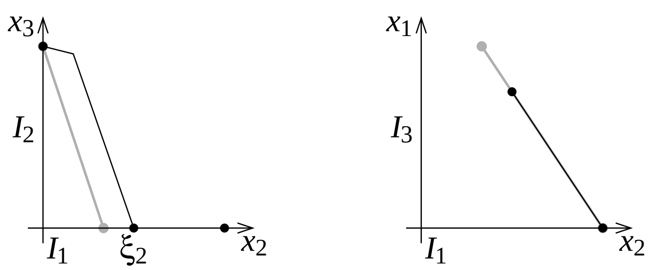

Figure 6.4: The return map from interval I_1 in mode q_1 for threshold-controlled preferred switching compared with switching when empty (light).

6.2 Control systems with periodic forcing

We finally consider a simple example of a control system with periodic forcing, where the control objective is to keep some value within a certain bound.

$$\dot{x} = k(a + b\sin\omega t - x) + u, \tag{15}$$

where u is some input. Taking period $T = 2\pi/\omega$ and $\phi = t \bmod T$, we obtain an autonomous system with two degrees of freedom.

We assume x is some quantity which we need to control below some safe threshold x_{MAX} by means of an safety system described by the input u, which can take values $u_{\text{OFF}} = 0$ and $u_{\text{ON}} < 0$. Without any control i.e. $u = 0$, there is a unique globally asymptotically stable periodic orbit,

$$x = a + \frac{b}{1+\omega^2/k^2}\sin(\omega t - \alpha) \text{ where } \alpha = \tan^{-1}(\omega/k). \tag{16}$$

We consider a number of switching strategies, which illustrate the various bifurcation scenarios mentioned in Section 5.

First, consider the switching law:

$$s \rightsquigarrow \text{ON if } x \geq x_{\text{MAX}} \text{ and } \phi < \phi_L; \quad s \rightsquigarrow \text{OFF if } \phi \geq \phi_U. \tag{17}$$

The control is turned on if x becomes too high, but the phase is less than a critical value; the rationale being that if the phase is above the critical value, then the maximum value of x will only be slightly higher than x_{MAX}. The system is turned off at a fixed time ϕ_U. As shown in Figure 6.5, this leads to a discontinuous corner collision if $\dot{x} > 0$ and $(x, \phi) = (x_{\text{MAX}}, \phi_L)$, and a discontinuous grazing if $\dot{x} = 0$ and $\phi < \phi_L$ when $x = x_{\text{MAX}}$. The bifurcations indicated in Section 5 occur if the corner collision or grazing occur on the periodic orbit.

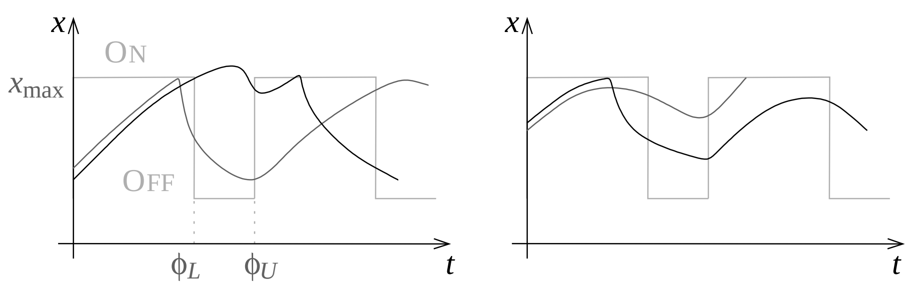

Figure 6.5: (a,b) Discontinuous corner collision and discontinuous grazing in a switched control system. (c) Continuous grazing. (d) Hysteresis switching.

An alternative control law is given by

$$s \rightsquigarrow \text{ON if } x \geq x_{\text{MAX}}; \quad s \rightsquigarrow \text{OFF if } x < a + b\sin\omega t. \tag{18}$$

The control is turned on when $x \geq x_{\text{MAX}}$, and is turned off when the external forcing $a + b\sin\omega t$ is sufficiently low that x would decrease without the input u. This leads to a continuous grazing bifurcation scenario, as depicted in Figure 6.5(c), since we always have $\dot{x} = 0$ immediately after the control is turned off.

Hysteresis switching is a commonly used technique to control a variable within bounds and avoid overly fast switching. The control law is given by

$$s \rightsquigarrow \text{ON if } x \geq x_{\text{MAX}}; \quad s \rightsquigarrow \text{OFF if } x < x_{\text{OFF}}. \tag{19}$$

Assuming $-u_{\mathrm{ON}}$ is sufficiently large, the system turns before the end of forcing period at time T. This gives rise to a discontinuous square-root singularity.

Another possible control law is a switching law with fixed hold,

$$s \rightsquigarrow \text{ON if } x \geq x_{\text{MAX}}; \quad s \rightsquigarrow \text{OFF after time } \tau. \tag{20}$$

This always gives rise to a stable periodic orbit, since the switching does not introduce stretching between nearby orbits.

7 Conclusions

In this article, we have considered chaotic dynamics in low-dimensional hybrid systems. We have seen that the key feature of such systems is discontinuous or non-differentiable spacial dependence, which allows for the formation of robust chaotic attractors. We have seen that discontinuous hybrid systems can be regularized to give shift-invariant measures, and that it is possible to effectively compute approximations to the symbolic dynamics. We have also considered bifurcations in non-smooth systems arising from corner collisions and grazing, and shown that these features can spontaneously generate chaos. Finally, we have illustrated these features using examples from hybrid control systems.

References

[1] Aubin, Jean-Pierre, Lygeros, J., Quincampoix, M., Sastry, S. and Seube, N. Impulse differential inclusions: a viability approach to hybrid systems. *IEEE Trans. Automat. Control* **47**(1) (2002) 2–20.

[2] Banerjee, S., Karthik, M.S., Guohui Yuan, and Yorke, J.A. Bifurcations in one-dimensional piecewise smooth maps — theory and applications in switching circuits. *IEEE Trans. Circuits Systems* **47**(3) (2000) 389–394.

[3] Benedicks, M. and Carleson, L. On iterations of $1 - ax^2$ on $(-1, 1)$. *Ann. of Math.* **122**(2) (1985) 1–25.

[4] Bose, C. Maume-Deschamps, V., Schmitt, B. and Sujin Shin. Invariant measures for piecewise convex transformations of an interval. *Studia Math.* **152**(3) (2002) 263–297.

[5] Broucke, M. and Arapostathis, A. Continuous selections of trajectories of hybrid systems. *Systems Control Lett.* **47**(2) (2002) 149–157.

[6] Brown, R. *The Lefschetz Fixed Point Theorem.* Scott, Foresman and Company, Glenview, Illinois, 1971.

[7] Budd, C. Non-smooth dynamical systems and the grazing bifurcation. In: *Nonlinear mathematics and its applications.* Cambridge University Press, Cambridge, 1996, 219–235.

[8] Chase, C., Serrano, J. and Ramadge, P.J. Periodicity and chaos from switched flow systems: Contrasting examples of discretely controlled continuous systems. *IEEE Trans. Automatic Control* **38** (1993) 70–83.

[9] Wai Chin, Ott, E., Nusse, H.E. and Grebogi, C. Grazing bifurcations in impact oscillators. *Phys. Rev. E (3)* **50**(6) (1994) 4427–4444.

[10] Leon O. Chua, Motomasa Komuro, and Takashi Matsumoto. The double scroll family. I. Rigorous analysis of bifurcation phenomena. *IEEE Trans. Circuits and Systems* **33**(11) (1986) 1097–1118.

[11] Leon O. Chua, Motomasa Komuro, and Takashi Matsumoto. The double scroll family. I. Rigorous proof of chaos. *IEEE Trans. Circuits and Systems* **33**(11) (1986) 1072–1097.

[12] Collin, P. Generalised hybrid trajectory spaces. In: *Proceedings of the 17th International Symposium on the Mathematical Theory of Networks and Systems, Kyoto, Japan, July 24-28, 2006*, P. 2101–2109, 2006.

[13] Collin, P. and Lygeros, J. Computability of finite-time reachable sets for hybrid systems. In *Proceedings of the 44th IEEE Conference on Decision and Control, and the European Control Conference 2005*. New York, IEEE Press, 2005, 4688–4693.

[14] Cowieson, W.J. Stochastic stability for piecewise expanding maps in $\mathbf{R}^d$. *Nonlinearity* **13**(5) (2000) 1745–1760.

[15] Cowieson, W.J. Absolutely continuous invariant measures for most piecewise smooth expanding maps. *Ergodic Theory Dynam. Systems* **22**(4) (2002) 1061–1078.

[16] Bernardo, M. di, Budd, C. J. and Champneys, A. R. Normal form maps for grazing bifurcations in n-dimensional piecewise-smooth dynamical systems. *Phys. D* **160**(3-4) (2001) 222–254.

[17] Bernardo, M. Di, Garofalo, F., Iannelli, L. and Vasca, F. Bifurcations in piecewise-smooth feedback systems. *Internat. J. Control* **75**(16-17) (2002) 1243–1259.

[18] Filippov, A.F. *Differential equations with discontinuous righthand sides*, volume 18 of *Mathematics and its Applications (Soviet Series)*. Kluwer Academic Publishers Group, Dordrecht, 1988. (Translated from the Russian)

[19] Fredriksson, M.H. and Nordmark, A.B. Bifurcations caused by grazing incidence in many degrees of freedom impact oscillators. *Proc. Roy. Soc. London Ser. A* **453**(1961) (1997) 1261–1276.

[20] Yan Gao, Lygeros, J. and Quincapoix, M. The reachability problem for uncertain hybrid systems revisited: a viability theory perspective. In: *Hybrid systems: computation and control*, vol. 3927 of *Lecture Notes in Comput. Sci.* Springer, Berlin, 2006, 242–256.

[21] Gilmore, R. and Lefranc, M. *The topology of chaos*. Wiley-Interscience [John Wiley & Sons], New York, 2002.

[22] Goebel, R. and Teel, A. R. Solutions to hybrid inclusions via set and graphical convergence with stability theory applications. *Automatica J. IFAC* **42**(4) (2006) 573–587.

[23] Goebel, R., Hespanha, J., Teel, A.R., Chaohong Cai, and Sanfelice, R. Hybrid systems: Generalized solutions and robust stability. In: *Proceedings of the Symposium on Nonlinear Control Systems*. Elsevier, 2004.

[24] Guckenheimer, J. and Holmes, P. *Nonlinear oscillations, dynamical systems, and bifurcations of vector fields*, vol. 42 of *Applied Mathematical Sciences*. Springer-Verlag, New York, 1990.

[25] Hamill, D., Deane, J. and Jeffries, D. Modelling of chaotic dc-dc converters by iterated nonlinear mappings. *IEEE Trans. Power Electron.* **7** (1992) 25–36.

[26] Shunji Ito, Shigeru Tanaka, and Hitoshi Nakada. On unimodal linear transformations and chaos. I, II. *Tokyo J. Math.* **2**(2) (1979) 221–239, 241–259.

[27] Katok, A. and Hasselblatt, B. *Introduction to the modern theory of dynamical systems*, vol. 54 of *Encyclopedia of Mathematics and its Applications*. Cambridge University Press, Cambridge, 1995.

[28] Kunze, M. and Küpper, T. Qualitative bifurcation analysis of a non-smooth friction-oscillator model. *Z. Angew. Math. Phys.* **48**(1) (1997) 87–101.

[29] Lasota, A. and Yorke, James A. On the existence of invariant measures for piecewise monotonic transformations. *Trans. Amer. Math. Soc.* **186** (1974) 481–488.

[30] Leine, R.I. and Nijmeijer, H. *Dynamics and bifurcations of non-smooth mechanical systems*, vol. 18 of *Lecture Notes in Applied and Computational Mechanics*. Springer-Verlag, Berlin, 2004.

[31] Maĭstrenko, Yu.L., Maĭstrenko, V.L. and Chua, L.O. Cycles of chaotic intervals in a time-delayed Chua's circuit. *Internat. J. Bifur. Chaos Appl. Sci. Engrg.* **3**(6) (1993) 1557–1572.

[32] Matveev, A.S. and Savkin, A.V. *Qualitative theory of hybrid dynamical systems*. Control Engineering. Birkhäuser, 2000.

[33] Milnor, J. and Thurston, W. On iterated maps of the interval. In: *Dynamical systems (College Park, MD, 1986–1987)*, vol. 1342 of *Lecture Notes in Math.* Springer, Berlin, 1988, 465–563.

[34] Mischaikow, K. and Mrozek, M. Conley index. In: *Handbook of dynamical systems*, vol. 2. North-Holland, Amsterdam, 2002, 393–460.

[35] Misiurewicz, M. On non-continuity of topological entropy. *Bull. Acad. Polon. Sci. Sér. Sci. Math. Astronom. Phys.*, **19** (1971) 319–320.

[36] Newcomb, R.W. and El-Leithy, N. Chaos generation using binary hysteresis. *Circuits Systems Signal Process.* **5**(3) (1986) 321–341.

[37] Nordmark, A.B. Non-periodic motions caused by grazing incidence in an impact oscillator. *J. Sound Vib.* **145** (1991) 279–297.

[38] Nusse, H.E., Ott, E. and Yorke, J.A. Border-collision bifurcations: An explanation for observed bifurcation phenomena. *Phys. Rev. E* **49**(2) (1994) 1073–1076.

[39] Nusse, H.E. and Yorke, J.A. Border-collision bifurcations including "period two to period three" for piecewise smooth systems. *Phys. D* **57**(1-2) (1992) 39–57.

[40] Nusse, H.E. and Yorke, J.A. Border-collision bifurcations for piecewise smooth one-dimensional maps. *Internat. J. Bifur. Chaos Appl. Sci. Engrg.* **5**(1) (1995) 189–207.

[41] Peterka, F. and Vacík, J. Transition to chaotic motion in mechanical systems with impacts. *J. Sound Vibration* **154**(1) (1992) 95–115.

[42] Robinson, C. *Dynamical systems*. Studies in Advanced Mathematics. CRC Press, Boca Raton, FL, second edition, 1999.

[43] Toshimichi Saito and Shinji Nakagawa. Chaos from a hysteresis and switched circuit. *Phil. Trans. R. Soc. Lond. A* **353** (1995) 47–57.

[44] Takens, F. Transitions from periodic to strange attractors in constrained equations. In: *Dynamical systems and bifurcation theory (Rio de Janeiro, 1985)*, vol. 160 of *Pitman Res. Notes Math. Ser.* Longman Sci. Tech. Harlow, 1987, 399–421.

[45] Chi Kong Tse. *Chomplex behaviour of switching power converters*. Power Electronics and Applications. CRC Press, Boca Raton, 2004.

[46] Tucker, W. The Lorenz attractor exists. *C. R. Acad. Sci. Paris Sér. I Math.* **328**(12) (1999) 1197–1202.

[47] Arjan van der Schaft and Schumacher, H. *An introduction to hybrid dynamical systems*. Number 251 in Lecture notes in control and information sciences. Springer, London, 2000.

[48] M. A. van Wyk and Steeb, W.H. *Chaos in electronics*, vol. 2 of *Mathematical Modelling: Theory and Applications*. Kluwer Academic Publishers, Dordrecht, 1997.

[49] Whiston, G.S. Global dynamics of a vibro-impacting linear oscillator. *J. Sound Vibration* **118**(3) (1987) 395–424.

[50] Whiston, G.S. The vibro-impact response of a harmonically excited and preloaded one-dimensional linear oscillator. *J. Sound Vibration* **115**(2) (1987) 303–319.

[51] Yomdin, Y. Volume growth and entropy. *Israel J. Math.* **57**(3) (1987) 285–300.

[52] Guohui Yuan, Banerjee, S., Ott, E. and Yorke, J.A. Border-collision bifurcations in the buck converter. *IEEE Trans. Circuits Systems I Fund. Theory Appl.* **45**(7) (1998) 707–716.

[53] Zhusubaliyev, Z.T. and Mosekilde, E. *Bifurcations and chaos in piecewise-smooth dynamical systems*, vol. 44 of *World Scientific Series on Nonlinear Science. Series A: Monographs and Treatises.* World Scientific Publishing Co. Inc., River Edge, NJ, 2003.

Nonlinear Dynamics and Systems Theory, 8 (2) (2008) 195–204

Output Feedback Passive Control of Neutral Systems with Time-Varying Delays in State and Control Input

X.Y. Lou [1,2] and B.T. Cui [1*]

[1] *College of Communication and Control Engineering, Jiangnan University 1800 Lihu Road, Wuxi, Jiangsu 214122, China*

[2] *CSIRO Division of Mathematical and Information Sciences Waite Road, Urrbrae, South Australia 5064*

Received: October 5, 2007; Revised: March 18, 2008

Abstract: This paper is concerned with the passive control problem of neutral systems with time-varying delays. Time-varying delays are assumed to appear in both the state and the control input. A state feedback passive controller and an output feedback passive controller for neutral systems with time-varying delays in state and control input are presented. Through modifying algebraic Riccati equation, we can construct controllers which depend on the maximum value of the time derivative of time-varying delays. A numerical example is also given to illustrate the effectiveness of the proposed design method.

Keywords: *Neutral system; output feedback passive control; time-varying delays; Riccati equation.*

Mathematics Subject Classification (2000): 34K40, 93C23.

1 Introduction

The theory of neutral delay-differential systems, which contain delays both in its state and in the derivatives of its states, is of both theoretical and practical interest. For example, functional differential equations of neutral type are the natural models of fluctuations of voltage and current in problems arising in transmission lines [1]. Also, the neutral systems often appear in the study of automatic control, population dynamics, and vibrating masses attached to an elastic bar. Recently, considerable attention has first been focused on the stability analysis of various neutral differential systems [2-10]. And there are

* Corresponding author: louxuyang28945@163.com

authors pay attention to the oscillation of parabolic equations of neutral type [11-13] and H_∞ control of neutral type [14].

The passivity theory intimately related to the circuit analysis methods [15,16] has received a lot of attention from the control community since the 70s (see [17-23], to cite only a few). On the other hand, many efforts have been devoted to the study of output feedback control of uncertain systems [24-26]. However, to the best of our knowledge, few authors pay attentions to study the output feedback passive control of neutral systems with time-varying delays.

In this paper, we shall discuss the passive control problem of neutral systems with time-varying delays. A state feedback passive controller and an output feedback passive controller which render the closed-loop system to be quadratic stable and passive for neutral systems with time-varying delays in state and control input are presented.

The layout of this paper is as follows. In Section 2, the problem to be studied is stated and some preliminaries are presented. The asymptotical stability and passivity of neutral system condition is derived in Section 3. A state feedback passive controller and an output feedback passive controller for neutral systems with time-varying delays in state and control input are proposed in Section 4 and Section 5, respectively. In Section 6, a numerical example is given to demonstrate the effectiveness of the theoretical results. And finally, conclusions are drawn in Section 7.

Notation and fact. In the sequel, we denote A^T and A^{-1} the transpose and the inverse of any square matrix A. We use $A > 0$ ($A < 0$) to denote a positive- (negative-) definite matrix A; and I is used to denote the $n \times n$ identity matrix. $\mathbf{L}_2[0, \infty]$ is the space of integrable function vector over $[0, \infty]$. $\mathbf{R}^n$ denotes the n-dimensional Euclidean space. The symbol "$\star$" within a matrix represents the symmetric term of the matrix.

Fact 1 (Schur complement). Given constant matrices $\Omega_1, \Omega_2, \Omega_3$, where $\Omega_1 = \Omega_1^T$ and $0 < \Omega_2 = \Omega_2^T$, then $\Omega_1 + \Omega_3^T \Omega_2^{-1} \Omega_3 < 0$ if and only if

$$\begin{pmatrix} \Omega_1 & \Omega_3^T \\ \Omega_3 & -\Omega_2 \end{pmatrix} < 0 \quad \text{or} \quad \begin{pmatrix} -\Omega_2 & \Omega_3 \\ \Omega_3^T & \Omega_1 \end{pmatrix} < 0.$$

2 System Description and Preliminaries

In this paper, we consider a class of neutral functional differential equation (NFDE) described as follows:

$$\begin{cases} \dot{x}(t) = A_0 x(t) + A_1 x(t-\tau_1(t)) + A_2 \dot{x}(t-\tau_2(t)) + B_1 w(t) + B_2 u(t-\tau_3(t)), \\ z(t) = C_1 x(t) + D_1 u(t) + D_{11} w(t), \\ y(t) = C_2 x(t) + D_2 w(t), \\ x(t) = \phi(t), t \geq 0. \end{cases} \tag{1}$$

where $x(t) \in R^n$ is the state; $u(t) \in R^m$ is the control input with $u(t) = 0$ for $t < 0$; $y(t) \in R^q$ is the output measurement; $w(t) \in R^p$ is the square-integrable disturbance input; $z(t) \in R^p$ is the controlled output; $\phi(t)$ are continuous functions defined on $(-\infty, 0]$. A_0, A_1, A_2, B_1, B_2, C_1, C_2, D_1, D_2, D_{11} are given constant matrices with appropriate dimensions and $\tau_1(t)$, $\tau_2(t)$ and $\tau_3(t)$ are arbitrary differentiable function satisfying

$$\begin{cases} 0 \leq \tau_1(t) < \infty,\ 0 \leq \tau_2(t) < \infty,\ 0 \leq \tau_3(t) < \infty, \\ \dot{\tau_1}(t) \leq \sigma_1 < 1,\ \dot{\tau_2}(t) \leq \sigma_2 < 1,\ \dot{\tau_3}(t) \leq \sigma_3 < 1. \end{cases} \tag{2}$$

Our problem is to establish the passive control for the system (1) to determine the conditions. First, we introduce the following definition of passivity.

Definition 2.1 The dynamical system (1) is called passive if

$$\int_0^\infty w^T(t)z(t)dt > \beta, \ \ \forall w \in L_2[0,\infty), \tag{3}$$

where β is some constant which depends on the initial condition of the system. In addition, the system is said to be strictly passive (SP) if it is passive and $D_{11} + D_{11}^T > 0$.

3 Asymptotical Stability and Passivity of Neutral System

Now, we consider a class of neutral system with time-varying delays described by:

$$\begin{cases} \dot{x}(t) = A_0x(t) + A_1x(t-\tau_1(t)) + A_2\dot{x}(t-\tau_2(t)) + A_3x(t-\tau_3(t)) + B_1w(t), \\ z(t) = C_1x(t) + D_{11}w(t), \\ y(t) = C_2x(t) + D_2w(t), \\ x(t) = \phi(t), \ \ t \geq 0. \end{cases} \tag{4}$$

Our first result establishes the passive control of the time-varying delay system (4).

Theorem 3.1 *Consider a state-delay neutral system (4), if there exist positive definite matrices P and Q which satisfy the following algebraic Riccati inequality (ARI):*

$$\begin{gathered} A_0^TP + PA_0 + 2Q + (1-\sigma_1)^{-1}PA_1Q^{-1}A_1^TP + (1-\sigma_2)^{-1}PA_2Q^{-1}A_2^TP \\ +(1-\sigma_3)^{-1}PA_3Q^{-1}A_3^TP + (PB_1 - C_1^T)(D_{11}+D_{11}^T)^{-1}(B_1^TP - C_1) + M < 0, \end{gathered} \tag{5}$$

where

$$\begin{aligned} M \ = \ & A_0^TQA_0 + A_0^TQA_1 + A_0^TQA_2 + A_0^TQA_3 + A_0^TQB_1 \\ & +A_1^TQA_0 + A_1^TQA_1 + A_1^TQA_2 + A_1^TQA_3 + A_1^TQB_1 \\ & +A_2^TQA_0 + A_2^TQA_1 + A_2^TQA_2 + A_2^TQA_3 + A_2^TQB_1 \\ & +A_3^TQA_0 + A_3^TQA_1 + A_3^TQA_2 + A_3^TQA_3 + A_3^TQB_1 \\ & +B_1^TQA_0 + B_1^TQA_1 + B_1^TQA_2 + B_1^TQA_3 + B_1^TQB_1, \end{aligned}$$

or equivalently satisfying the linear matrix inequality (LMI):

$$\begin{pmatrix} A_0^TP + PA_0 + 2Q & PA_1 & PA_2 & PA_3 & PB_1 - C_1^T & A_0^T \\ \star & -(1-\sigma_1)Q & 0 & 0 & 0 & A_1^T \\ \star & \star & -(1-\sigma_2)Q & 0 & 0 & A_2^T \\ \star & \star & \star & -(1-\sigma_3)Q & 0 & A_3^T \\ \star & \star & \star & \star & -(D_{11}+D_{11}^T) & B_1^T \\ \star & \star & \star & \star & \star & -Q^{-1} \end{pmatrix} < 0. \tag{6}$$

Then the systems (4) is asymptotically stable and passive for all time-varying state delays $\tau_1(t)$, $\tau_2(t)$ and $\tau_3(t)$.

Proof Define a Lyapunov functional V(x(t)) as follows:

$$\begin{aligned} V(x(t)) &= x^T(t)Px(t) + \int_{t-\tau_1(t)}^{t} x^T(s)Qx(s)ds \\ &\quad + \int_{t-\tau_2(t)}^{t} \dot{x}^T(s)Q\dot{x}(s)ds + \int_{t-\tau_3(t)}^{t} x^T(s)Qx(s)ds. \end{aligned} \tag{7}$$

Calculating the derivative of the Lyapunov functional V(x(t)) along the solution of (4), it follows that

$$\begin{aligned} \dot{V}(x(t)) &= \dot{x}^T(t)Px(t) + x^T(t)P\dot{x}(t) \\ &\quad + x^T(t)Qx(t) - (1-\dot{\tau}_1(t))x^T(t-\tau_1(t))Qx(t-\tau_1(t)) \\ &\quad + \dot{x}^T(t)Q\dot{x}(t) - (1-\dot{\tau}_2(t))\dot{x}^T(t-\tau_2(t))Q\dot{x}(t-\tau_2(t)) \\ &\quad + x^T(t)Qx(t) - (1-\dot{\tau}_3(t))x^T(t-\tau_3(t))Qx(t-\tau_3(t)) \\ &\leq \dot{x}^T(t)Px(t) + x^T(t)P\dot{x}(t) \\ &\quad + 2x^T(t)Qx(t) - (1-\sigma_1)x^T(t-\tau_1(t))Qx(t-\tau_1(t)) \\ &\quad + \dot{x}^T(t)Q\dot{x}(t) - (1-\sigma_2)\dot{x}^T(t-\tau_2(t))Q\dot{x}(t-\tau_2(t)) \\ &\quad - (1-\dot{\tau}_3(t))x^T(t-\tau_3(t))Qx(t-\tau_3(t)) \\ &= x^T(t)\Big(A_0^TP + PA_0 + 2Q\Big)x(t) \\ &\quad + 2x^T(t)PA_1x(t-\tau_1(t)) + 2x^T(t)PA_2\dot{x}(t-\tau_2(t)) \\ &\quad + 2x^T(t)PA_3x(t-\tau_3(t)) + 2x^T(t)PB_1w(t) \\ &\quad - (1-\sigma_1)x^T(t-\tau_1(t))Qx(t-\tau_1(t)) \\ &\quad + \dot{x}^T(t)Q\dot{x}(t) - (1-\sigma_2)\dot{x}^T(t-\tau_2(t))Q\dot{x}(t-\tau_2(t)) \\ &\quad - (1-\sigma_3)x^T(t-\tau_3(t))Qx(t-\tau_3(t)). \end{aligned}$$

So we can obtain that

$$\begin{aligned} \dot{V}(x(t)) - 2z^T(t)w(t) &= x^T(t)(A_0^TP + PA_0 + 2Q)x(t) \\ &\quad + 2x^T(t)PA_1x(t-\tau_1(t)) + 2x^T(t)PA_2\dot{x}(t-\tau_2(t)) \\ &\quad + 2x^T(t)PA_3x(t-\tau_3(t)) + 2x^T(t)(PB_1 - C_1^T)w(t) \\ &\quad - w^T(t)(D_{11} + D_{11}^T)w(t) + \dot{x}^T(t)Q\dot{x}(t) \\ &\quad - (1-\sigma_1)x^T(t-\tau_1(t))Qx(t-\tau_1(t)) \\ &\quad - (1-\sigma_2)\dot{x}^T(t-\tau_2(t))Q\dot{x}(t-\tau_2(t)) \\ &\quad - (1-\sigma_3)x^T(t-\tau_3(t))Qx(t-\tau_3(t)) \\ &= \eta^T(t)\Omega\eta(t), \end{aligned} \tag{8}$$

where

$$\eta(t) = \Big[x(t)\ x(t-\tau_1(t))\ \dot{x}(t-\tau_2(t))\ x(t-\tau_3(t))\ w(t)\Big]^T,$$

$$\Omega = \left(\begin{array}{ccc} A_0^TP + PA_0 + 2Q & PA_1 & PA_2 \\ \star & -(1-\sigma_1)Q & 0 \\ \star & \star & -(1-\sigma_2)Q \\ \star & \star & \star \\ \star & \star & \star \end{array} \right.$$

$$\begin{pmatrix} \cdots & PA_3 & PB_1 - C_1^T \\ \cdots & 0 & 0 \\ \cdots & 0 & 0 \\ \cdots & -(1-\sigma_3)Q & 0 \\ \cdots & \star & -(D_{11}+D_{11}^T) \end{pmatrix} + \begin{pmatrix} A_0 \\ A_1^T \\ A_2^T \\ A_3^T \\ B_1^T \end{pmatrix} Q \begin{pmatrix} A_0 & A_1 & A_2 & A_3 & B_1 \end{pmatrix}.$$

From Schur complement, it easily follows that (5) and (6) hold. Hence,

$$\dot{V}(x(t)) \le 2z^T(t)w(t). \tag{9}$$

Integrating (9) from t_0 to t_1, we have

$$\int_{t_0}^{t_1} z^T(t)w(t)dt > \frac{1}{2}\Big[V(x(t_1)) - V(x(t_0))\Big].$$

Since $V(x(t)) > 0$ for $x \neq 0$ and $V(x(t)) = 0$ for $x = 0$, it follows that as $t_0 = 0$ and $t_1 \to \infty$ that the system (4) with $w = 0$ is asymptotically stable and passive. □

Remark 3.1 In this section, we provide a method of solving the synthesis problem for neutral systems with time-varying delays. In Section 4 and Section 5, a state feedback passive controller and an output feedback passive controller for neutral systems with time-varying delays in state and control input are proposed.

4 State-Feedback Passive Controller

On the basis of Theorem 1, we now want to construct the state feedback controller

$$u(t) = Kx(t), \tag{10}$$

such that the input-state-delay neutral system (1) is asymptotically stable and passive. Then the transformed systems become

$$\begin{cases} \dot{x}(t) = A_0x(t) + A_1x(t-\tau_1(t)) + A_2\dot{x}(t-\tau_2(t)) + B_1w(t) + B_2Kx(t-\tau_3(t)), \\ z(t) = (C_1 + D_1K)x(t) + D_{11}w(t), \\ y(t) = C_2x(t) + D_2w(t), \\ x(t) = \phi(t), \ \ t \ge 0. \end{cases} \tag{11}$$

Theorem 4.1 *Consider a state-delay neutral system (11), if there exist positive definite matrices P which satisfy the following inequality:*

$$\begin{pmatrix} A_0^TP + PA_0 + 2Q & PA_1 & PA_2 & PB_2K & PB_1 - (C_1+D_1K)^T & A_0^T \\ \star & -(1-\sigma_1)Q & 0 & 0 & 0 & A_1^T \\ \star & \star & -(1-\sigma_2)Q & 0 & 0 & A_2^T \\ \star & \star & \star & -(1-\sigma_3)Q & 0 & A_3^T \\ \star & \star & \star & \star & -(D_{11}+D_{11}^T) & B_1^T \\ \star & \star & \star & \star & \star & -Q^{-1} \end{pmatrix} < 0, \tag{12}$$

and

$$D_1K = B_1^TP - C_1, \tag{13}$$

then the system (11) is passive by the state-feedback passive controller (10).

Proof The closed form of (11) is similar to (4). Therefore, by Theorem 3.1, given positive definite matrix Q, if there exits positive definite symmetric matrix P which satisfies the following inequality

$$\begin{pmatrix} A_0^TP+PA_0+2Q & PA_1 & PA_2 & PB_2K & PB_1-(C_1+D_1K)^T & A_0^T \\ \star & -(1-\sigma_1)Q & 0 & 0 & 0 & A_1^T \\ \star & \star & -(1-\sigma_2)Q & 0 & 0 & A_2^T \\ \star & \star & \star & -(1-\sigma_3)Q & 0 & A_3^T \\ \star & \star & \star & \star & -(D_{11}+D_{11}^T) & B_1^T \\ \star & \star & \star & \star & \star & -Q^{-1} \end{pmatrix} < 0. \tag{14}$$

Since there are two unknown matrices P, K to be solved in (14), we can let the matrices P, K in (14) satisfy the following two conditions at the same time

$$\begin{pmatrix} A_0^TP+PA_0+2Q & PA_1 & PA_2 & PB_2K & PB_1 & A_0^T \\ \star & -(1-\sigma_1)Q & 0 & 0 & 0 & A_1^T \\ \star & \star & -(1-\sigma_2)Q & 0 & 0 & A_2^T \\ \star & \star & \star & -(1-\sigma_3)Q & 0 & K^TB_2^T \\ \star & \star & \star & \star & -(D_{11}+D_{11}^T) & B_1^T \\ \star & \star & \star & \star & \star & -Q^{-1} \end{pmatrix} < 0, \tag{15}$$

$$\begin{aligned} &-PB_1(D_{11}+D_{11}^T)^{-1}(C_1+D_1K) - (C_1+D_1K)^T)(D_{11}+D_{11}^T)^{-1}B_1^TP \\ &+(C_1+D_1K)^T(D_{11}+D_{11}^T)^{-1}(C_1+D_1K) < 0. \end{aligned} \tag{16}$$

Then the controller (10) can make system (11) be asymptotically stable and passive. From (16), we observe that if we choose

$$D_1K = B_1^TP - C_1, \tag{17}$$

then the inequality (16) is satisfied. In order to satisfied (15), we let

$$A_0^TP + PA_0 + 2Q + (1-\sigma_1)^{-1}PA_1Q^{-1}A_1^TP + (1-\sigma_2)^{-1}PA_2Q^{-1}A_2^TP$$

$$+(1-\sigma_3)^{-1}PA_3Q^{-1}A_3^TP+(PB_1-C_1^T)(D_{11}+D_{11}^T)^{-1}(B_1^TP-C_1)+M=-Q. \quad (18)$$

Therefore, we can say that the P in (15) is the solution satisfying the following modified algebraic Riccati equation shown as follows:

$$A_0^TP+PA_0+3Q+(1-\sigma_1)^{-1}PA_1Q^{-1}A_1^TP+(1-\sigma_2)^{-1}PA_2Q^{-1}A_2^TP$$

$$+(1-\sigma_3)^{-1}PA_3Q^{-1}A_3^TP+(PB_1-C_1^T)(D_{11}+D_{11}^T)^{-1}(B_1^TP-C_1)+M=0. \quad (19)$$

The existence of solution K in (17) can be seen in the following:

(i) If D_1 is square matrix and $det(D_1)\neq 0$, the unique solution $K=D_1^{-1}(B_1^TP-C_1)$ is presented.

(ii) Suppose the size of D_1 is $n\times m$ $(n>m)$ and $rank[D_1\ \ B_1^TP-C_1]=r$. Then if $r=m$, the unique solution K in (17) exists; if $r<m$, there are many solutions; if $r>m$ and $det(D_1^TD_1)\neq 0$, a least square approximation solution of K in (17) is shown as follows:

$$K=(D_1^TD_1)^{-1}D_1^T(B_1^TP-C_1). \quad (20)$$

□

5 Output Feedback Passive Controller

When state variable are not available for the feedback, it is necessary to construct a output feedback passive controller. If the state in (1) is not available, we propose the following dynamic output feedback controller in order to stabilize system (1):

$$\begin{cases} \dot{\eta}(t)=G\eta(t)+Ly(t), \\ u(t)=K\eta(t),\ \ \eta(0)=0, \end{cases} \quad (21)$$

where $\eta(t)\in R^n$ is the controller state vector, and G,L,K are gain matrices with appropriate dimensions to be determined later. Applying this controller (21) to system (1) results in the closed-loop system

$$\begin{cases} \dot{\overline{x}}(t)=\overline{A}_0\overline{x}(t)+\overline{A}_1\overline{x}(t-\tau_1(t))+\overline{A}_2\dot{\overline{x}}(t-\tau_2(t))+\overline{A}_3\overline{x}(t-\tau_3(t))+\overline{B}_1w(t), \\ z(t)=\overline{C}_1\overline{x}(t)+D_{11}w(t), \end{cases} \quad (22)$$

where

$$\overline{x}(t)=\begin{pmatrix} x(t) \\ \eta(t) \end{pmatrix},\ \overline{A}_0=\begin{pmatrix} A_0 & 0 \\ LC_2 & G \end{pmatrix},\ \overline{A}_1=\begin{pmatrix} A_1 & 0 \\ 0 & 0 \end{pmatrix},$$

$$\overline{A}_2=\begin{pmatrix} A_2 & 0 \\ 0 & 0 \end{pmatrix},\ \overline{A}_3=\begin{pmatrix} 0 & B_2K \\ 0 & 0 \end{pmatrix},\ \overline{B}_1=\begin{pmatrix} B_1 \\ LD_2 \end{pmatrix},\ \overline{C}_1=\begin{pmatrix} C_1 & D_1K \end{pmatrix}.$$

Theorem 5.1 *For a given symmetric positive Q, if there exist positive definite matrices P and gain matrices G, L, K such that the following linear matrix inequality (LMI):*

$$\left(\begin{array}{ccccccccccc}
A_0^T P + PA_0 + 2Q & C_2^T L^T & PA_1 & 0 & PA_2 & 0 & 0 & PB_2K & PB_1 - C^T & A_0^T & C_2^T L^T \\
LC_2 & G^T + G + 2Q & 0 & 0 & 0 & 0 & 0 & 0 & LD_2 - K^T D_1^T & 0 & G^T \\
\star & \star & (\sigma_1 - 1)Q & 0 & 0 & 0 & 0 & 0 & 0 & A_1^T & 0 \\
\star & \star & \star & (\sigma_1 - 1)Q & 0 & 0 & 0 & 0 & 0 & 0 & 0 \\
\star & \star & \star & \star & (\sigma_2 - 1)Q & 0 & 0 & 0 & 0 & A_2^T & 0 \\
\star & \star & \star & \star & \star & (\sigma_2 - 1)Q & 0 & 0 & 0 & 0 & 0 \\
\star & \star & \star & \star & \star & \star & (\sigma_3 - 1)Q & 0 & 0 & 0 & 0 \\
\star & \star & \star & \star & \star & \star & \star & (\sigma_3 - 1)Q & 0 & K^T B_2^T & 0 \\
\star & \star & \star & \star & \star & \star & \star & \star & -(D_{11} + D_{11}^T) & B_1^T & D_2^T L^T \\
\star & \star & \star & \star & \star & \star & \star & \star & \star & -Q^{-1} & 0 \\
\star & \star & \star & \star & \star & \star & \star & \star & \star & 0 & -Q^{-1}
\end{array}\right) < 0, \tag{23}$$

then the time-varying input-state-delay neutral system (1) is passive by the output feedback passive controller (21).

Proof Define positive symmetric matrices $\overline{P} > 0$ and $\overline{Q} > 0$ by

$$\overline{P} = \begin{pmatrix} P & 0 \\ 0 & I \end{pmatrix}, \quad \overline{Q} = \begin{pmatrix} Q & 0 \\ 0 & Q \end{pmatrix}.$$

Similar to the proof of Theorem 1, we can easily get that if the following LMI

$$\begin{pmatrix}
\overline{A}_0^T \overline{P} + \overline{PA}_0 + 2\overline{Q} & \overline{PA}_1 & \overline{PA}_2 & \overline{PA}_3 & \overline{PB}_1 - \overline{C}_1^T & \overline{A}_0^T \\
\star & (\sigma_1 - 1)\overline{Q} & 0 & 0 & 0 & \overline{A}_1^T \\
\star & \star & (\sigma_2 - 1)\overline{Q} & 0 & 0 & \overline{A}_2^T \\
\star & \star & \star & (\sigma_3 - 1)\overline{Q} & 0 & \overline{A}_3^T \\
\star & \star & \star & \star & -D_{11} - D_{11}^T & \overline{B}_1^T \\
\star & \star & \star & \star & \star & -\overline{Q}^{-1}
\end{pmatrix} < 0, \tag{24}$$

holds, then the time-varying input-state-delay neutral system (1) is passive by the output feedback passive controller (21).

Now, substitute the expressions of $\overline{A}_0, \overline{A}_1, \overline{A}_2, \overline{A}_3, \overline{B}_1, \overline{C}_1, \overline{P}, \overline{Q}$ into (24), it easily follows that (23) holds. This completes the proof. □

6 An Illustrative Example

In this section, the expanded theoretical results are illustrated through a numerical example. Consider the differential system of neutral type (1) under supposing

$$A_0 = \begin{pmatrix} 0 & 1 \\ -1 & -2 \end{pmatrix}, \ A_1 = \begin{pmatrix} 0 & 0 \\ 0.2 & 0.1 \end{pmatrix}, \ A_2 = \begin{pmatrix} 0 & 0 \\ 0.3 & 0.2 \end{pmatrix}, \ B_1 = \begin{pmatrix} 0 \\ 0.1 \end{pmatrix},$$

$$B_2 = \begin{pmatrix} 0 \\ 1 \end{pmatrix}, \ C_1 = \begin{pmatrix} 1 & 1 \end{pmatrix}, \ C_2 = \begin{pmatrix} 1 & 1 \end{pmatrix}, \ D_1 = 1, \ D_2 = 1, \ D_{11} = 1,$$

$$\tau_1(t) = 2.0 + 0.3\sin(t), \ \ \tau_2(t) = 3.5 + 0.4\cos(t), \ \ \tau_3(t) = 4.0 + 0.2\sin(t).$$

Hence we have $\sigma_1 = 0.3, \sigma_2 = 0.4, \sigma_3 = 0.2$. In order to solve the solution simply, we select $Q = \begin{pmatrix} 0.2 & 0 \\ 0 & 0.2 \end{pmatrix}$. So using MATLAB LMI Toolbox we solve the condition (12) and (13) and obtain that

$$K = \begin{pmatrix} -0.9427 & -0.8289 \end{pmatrix}, \quad P = \begin{pmatrix} 1.4530 & 0.5734 \\ 0.5734 & 1.7115 \end{pmatrix} > 0.$$

Hence, the system (1) is passive by the state-feedback passive controller (10).

7 Conclusions

In this paper, the passivity analysis and passive controllers' designs for the neutral systems with time-varying delays in state and control input are investigated by the Lyapunov functional method. The results are presented in terms of LMIs or Riccati equation, which can be solved easily by using the effective interior-point algorithm [24]. A numerical example is worked through to illustrate the effectiveness of results.

Acknowledgements

This work was supported by NSFC (No. 60674026), the Jiangsu Provincial Natural Science Foundation of China (No. BK2007016), the Jiangsu Provincial Program for Postgraduate Scientific Innovative Research of Jiangnan University (No. CX07B_116z) and PIRTJiangnan.

References

[1] Ju, H.P. Robust guaranteed cost control for uncertain linear differential systems of neutral type. *Applied Mathematics and Computation* **140** (2003) 523–535.

[2] Kolmanovskii, V. and Myshkis, A. *Applied Theory of Functional Differential Equations.* Kluwer Academic Publishers, Dordrecht, 1992.

[3] Gopalsamy, K. *Stability and Oscillations in Delay Differential Equations of Population Dynamics.* Kluwer Academic Publishers, Boston, 1992.

[4] Lou, X.Y. and Cui, B.T. Stochastic stability analysis for delayed neural networks of neutral type with Markovian jump parameters. *Chaos, Solitons and Fractals*, doi:10.1016/j.chaos.2007.06.114.

[5] Lou, X.Y. and Cui, B.T. Passive analysis and synthesis of Markovian jump systems of neutral type. *Int. J. Information and Systems Sciences* **3**(2) (2007) 231–242.

[6] Fan, K.K., Chen, J.D., Lien, C.H. and Hsieh, J.G. Delay-dependent stability criterion for neutral time-delay systems via linear matrix inequality approach. *J. Math. Anal. Appl.* **273** (2002) 580–589.

[7] Park, J.H. Stability criterion for neutral differential systems with mixed multiple time-varying delay arguments. *Mathematics and Computers in Simulation* **59** (2002) 401–412.

[8] Cui, B.T. and Lou, X.Y. Robust stability analysis of neutral stochastic neural networks with delay: an LMI approach *ICCA 2007: IEEE International Conference on Control and Automation.* Guangzhou, China, May 30–June 1, 2007, 117–122.

[9] Yue, D., Won, S. and Kwon, O. Delay-dependent stability of neutral systems with time delay: an LMI approach. *IEEE Proceedings Control Theory and Applications* **150** (2003) 23–27.

[10] Hai-Long Xing, Xiao-Zhu Zhong, Yan Shi, Jing-Cui Liang and Dong-Hua Wang. Stability of nonautonomous neutral variable delay difference equation. *Nonlinear Dynamics and Systems Theory* **5** (3) (2005) 299–314.

[11] Lin, S.Z. and Yu, Y.H. On the oscillations solutions of parabolic differential equations of neutral type. *Demonstratio Mathematica* **3** (1996) 603–614.

[12] Mishiev, D.P. and Bainov, D.D. Oscillation of the solution of parabolic differential equations of neutral type. *Appl. Math. Comput.* **28** (1988) 97–111.

[13] Wang, P.G. and Feng, C.H. Oscillation of parabolic equations of neutral type. *Journal of Computational and Applied Mathematics* **126** (2000) 111–120.

[14] Mahmoud, S. Robust H∞ control of linear neutral systems. *Automatica* **36** (2000) 757–764.

[15] Belevich, V. *Classical Network Synthesis.* New York: Van Nostrand, 1968.

[16] Brune, O. Synthesis of a finite two terminal network whose driving point impedance is a prescribed function of frequency. *J. Math. Physics* **10** (1931) 191–236.

[17] Hill, P. and Moylan, P. The stability of nonlinear dissipative systems. *IEEE Trans. Automat. Contr.* **AC-21** (1976) 708–711.

[18] Lozano, R. and Joshi, S. Strictly positive real transfer functions revisited. *IEEE Trans. Automat. Contr.* **35** (1990) 1243–1245.

[19] Willems, J. Dissipative dynamical systems-Part I: General theory. *Arch. Ration Mech. Anal.* **45** (1972) 321–351.

[20] Willems, J. Dissipative dynamical systems-Part II: Linear systems with quadratic supply rates. *Arch. Ration Mech. Anal.* **45** (1972) 352–393.

[21] Niculescu, S. and Lozano, R. On the passivity of linear delay systems. *IEEE Trans. Automat. Contr.* **46** (3) (2001) 460–464.

[22] Mahmoud, S. and Zribi, M. Passive control synthesis for uncertain systems with multiple-state delays. *Computers and Electrical Engineering* **28** (2002) 195–216.

[23] Fridman, E. and Shaked, U. On delay-dependent passivity. *IEEE Trans. Automat. Contr.* **47**(4) (2002) 664–669.

[24] Suplin, V. and Shaked, U. Robust H_∞ output-feedback control of systems with time-delay. *Systems & Control Letters* **57** (3) (2008) 193–199.

[25] Karimi, H. R. Robust dynamic parameter-dependent output feedback control of uncertain parameter-dependent state-delayed systems. *Nonlinear Dynamics and Systems Theory* **6** (2) (2006) 143–158.

[26] Zhou, J., Wen, C.Y. and Zhang, Y. Adaptive output control of a class of time-varying uncertain nonlinear systems. *Nonlinear Dynamics and Systems Theory* **5** (3) (2005) 285–298.

Nonlinear Dynamics and Systems Theory, 8 (2) (2008) 205–211

Optimization of Transfers to Neptune

C.R.H. Solórzano [1], A.A. Sukhanov [2] and A.F.B.A. Prado [1*]

[1] *Instituto Nacional de Pesquisas Espaciais (INPE)*
12227-010 - São José dos Campos, Brazil
[2] *Space Research Institute (IKI) of the Russian Academy of Sciences*
84/32 Profsoyuznaya St., 117810 Moscow, Russia

Received: November 7, 2006; Revised: December 12, 2007

Abstract: Here a mission to Neptune for the mid-term 2008–2020 is proposed. A direct transfer to Neptune is considered and also Venus, Earth, Jupiter and Saturn gravity assists are used for the trip to Neptune. Several mission options are analyzed, such as: Earth–Neptune, Earth–Jupiter–Neptune, Earth–Saturn–Neptune, Earth–Jupiter–Saturn–Neptune, Earth–Venus–Earth–Jupiter–Neptune, Earth–Venus–Earth–Jupiter–Saturn–Neptune. All the transfers are optimized in terms of the ΔV. The goal of this study is to compare the mission options in order to find a good compromise between the ΔV and time of flight to Neptune.

Keywords: *Neptune's system; swing-by; interplanetary mission.*

Mathematics Subject Classification (2000): 70F99, 70M20, 78M50.

1 Introduction

On August 20, 1977, the Voyager 2 was launched towards the exploration of our solar system. On August 25, 1989, it passed by Neptune. The gravity assist is a proven technique in interplanetary exploration, as exemplified by the missions Voyager, Galileo, Cassini etc. NASA's Solar System Exploration (Hammel et al. [1]) theme listed a Neptune mission as one of its top priorities for the mid-term (2008–2013). The interplanetary trajectory of the spacecraft is represented by a series of segments of undisturbed Keplerian motion in the gravispheres of relevant celestial bodies, while on the boundaries of these segments, the trajectory passes from the gravisphere into the heliosphere and vice versa. Studies of the interplanetary flight with gravity assist maneuvers are known to deal with cases where the spacecraft, on its way from one celestial body to another, approaches

* Corresponding author: prado@dem.inpe.br

a third attracting body which causes a significant change in the spacecraft trajectory. Ordinarily, this planetary maneuver provides a non-propulsive change in the spacecraft's heliocentric energy which can reduce the amount of propellant needed to complete an interplanetary mission (Labunsky et al. [2]). The heliocentric energy may be increased or decreased, depending upon the geometric details of the encounters (turn of velocity vector over the sphere of influence of the planet). Several interplanetary's missions used this tecnique. For example Sukhanov [3] proposed a mission to Sun using gravity assist of the inner planets.

2 The Mission Options

Earth and Venus are the inner planets that have a gravity field large enough to be used. Jupiter and Saturn show optimum opportunities for flights to Neptune using the energy gained during the close approach. However, to approach Neptune closely, the spacecraft should have low excess velocity to reduce the braking cost. The optimal launches dates in the time interval 2008–2020 are considered. The following transfer schemes are analyzed:

- Direct Earth to Neptune (EN) transfer.
- Earth - Jupiter - Neptune (EJN) transfer.
- Earth - Saturn - Neptune (ESN) transfer.
- Earth - Jupiter - Saturn - Neptune (EJSN) transfer.
- Earth - Venus - Earth - Jupiter - Neptune (EVEJN) transfer.
- Earth - Venus - Earth - Jupiter - Saturn - Neptune (EVEJSN) transfer.

Transfer Scheme	Launch Date	ExcessVelocity $V_\infty(km/s)$	MinimumTotal $\Delta V(km/s)$
EN	13.04.2012	9.436	8.992
EJN	14.01.2018	11.728	6.506
ESN	13.02.2017	12.955	7.775
EJSN	18.11.2015	15.757	6.719
EVEJN	24.08.2016	14.578	6.646
EVEJSN	09.06.2015	17.275	7.206

Table 2.1: Optimal transfer schemes for flight time of 12 years.

As it is seen from the Table 2.1, the minimum total ΔV is 6.506 km/s for the scheme EJN , with a flyby altitude of 0.2x10^3 km (Earth) and 1.2x10^3 km (Neptune). The excess velocity near Neptune is 11.728 km/s. Other scheme with low ΔV (minimum total) is EVEJN, however the excess velocity near Neptune is higher than in the EJN option.

Figures 2.1-2.2 shows the configuration for the transfer scheme EJN and EVEJN. Table 2.2 shows the optimal launch date for several transfers. The minimum total ΔV is 5.441 km/s for the scheme EVEJSN and the total flight duration is 23.69 years, with flyby altitude of 0.2x10^3 km (Earth) and 1.2x10^3 km (Neptune). The excess velocity near Neptune is 5.083 km/s, however the EVEJN scheme have minor excess velocity near Neptune (3.748 km/s) for the optimal transfer time of 29.95 years.

Figure 2.3 shows the planetary configuration and the transfer trajectory for the scheme EVEJSN. It is a typical 2015 Earth–Venus–Earth–Jupiter–Saturn–Neptune flight path projected on the plane of the ecliptic. It is possible that all the trajectories after Neptune (depending on the targeting conditions selected) have energy enough to escape from the solar system.

Figure 2.4 shows several transfer schemes from Earth to Neptune. Looking the curves of minimum total ΔV as function of the time of the transfer, the EJN, EJSN EVEJN, and EVEJSN schemes are most acceptables if the transfer duration is limited by the time of 12 years.

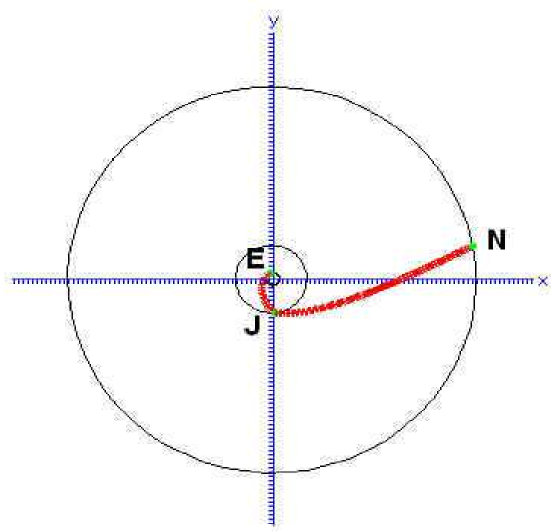

Figure 2.1: Planetary configuration and transfer trajectory for 2018 Earth–Jupiter–Neptune.

Transfer Scheme	Optimal Launch Date	ExcessVelocity $V_\infty(km/s)$	MinimumTotal $\Delta V(km/s)$
EN	09.04.2009	6.258	8.691
EJN	13.01.2018	7.050	6.367
ESN	17.01.2014	7.468	7.273
EJSN	26.11.2015	4.124	6.428
EVEJN	28.05.2013	3.748	5.642
EVEJSN	30.05.2015	5.083	5.441

Table 2.2: Optimal launch date for several transfers.

The EVEJSN scheme has several minimum total ΔV equal to the EJN, EJSN, EVEJN schemes. For a time of transfer larger than 14 years, the EVEJSN scheme is optimal, in terms of minimum total ΔV. Figure 2.5 shows the excess velocity near Neptune. The

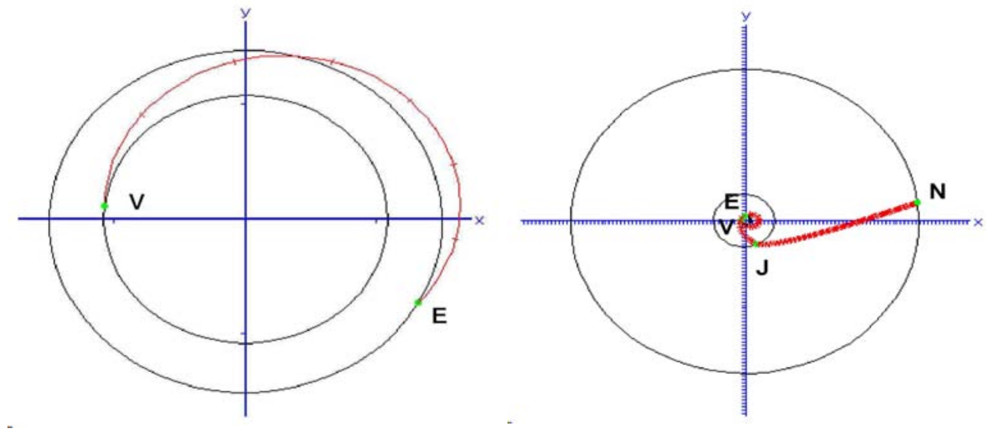

Figure 2.2: Planetary configuration and transfer trajectory for 2016 Earth–Venus–Earth–Jupiter–Neptune.

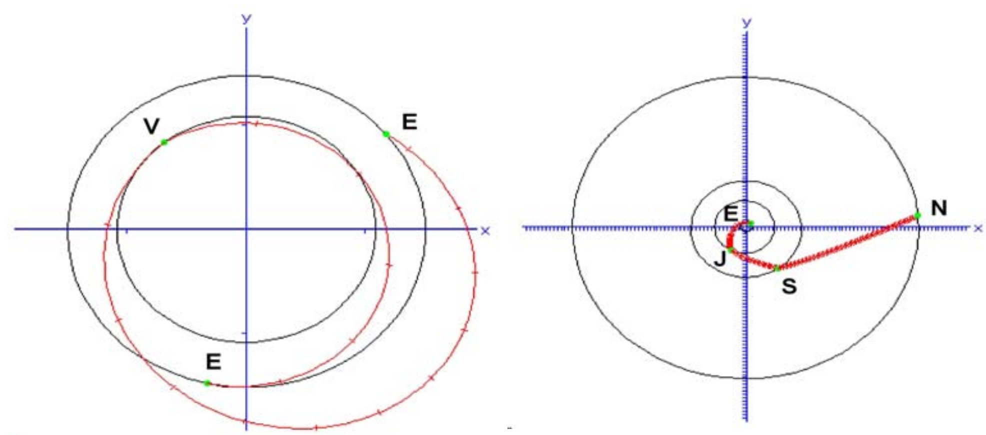

Figure 2.3: Planetary configuration and transfer trajectory for 2015 Earth–Venus–Earth–Jupiter–Saturn–Neptune.

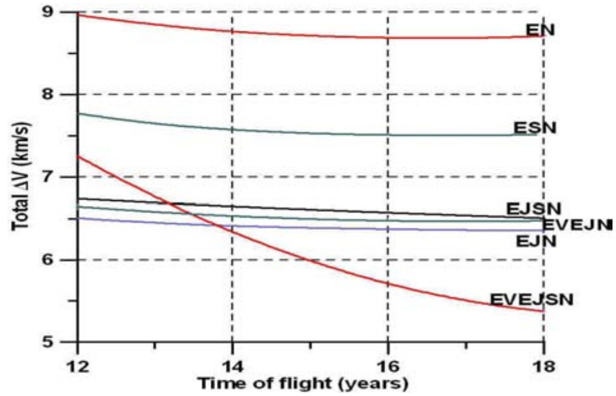

Figure 2.4: Total ΔV vs. time of flight for the spacecraft.

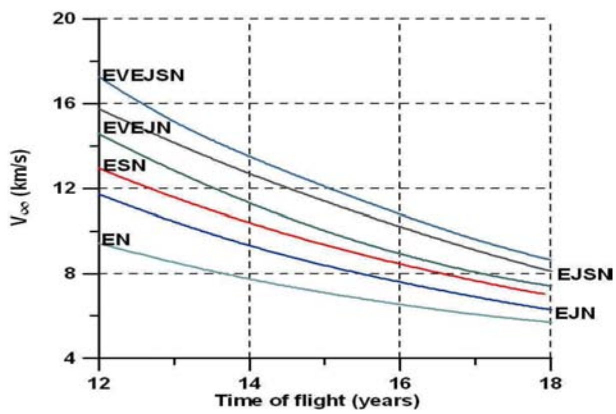

Figure 2.5: V_∞ vs. time of flight of the spacecraft.

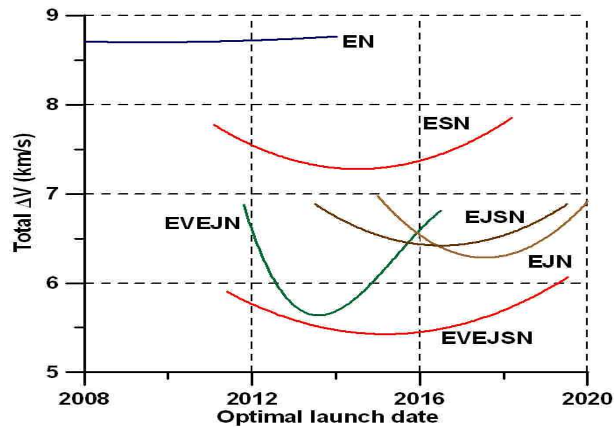

Figure 2.6: Optimal launch date for several transfer schemes.

EVEJSN scheme is optimal in terms of minimum total ΔV, however excess velocity near Neptune is very high in this scheme. The EJN and EVEJN schemes are more efficients for low excess velocity near Neptune and for minimum of ΔV.

Figure 2.6 shows the minimum total ΔV as a function of the optimal launch date for several transfer schemes in the time interval 2008–2020. The results are shown in Table 2.2. The gravity assists maneuvers with Jupiter and Saturn has enormous potential to reduce the total ΔV for trajectories to Neptune, however for the time interval considered Mars and Uranus are not in good positions.

Remember that it is also possible to use Earth gravity assists and Venus flybys as another way to increase the heliocentric energy of the trajectory to reach Jupiter. Besides the synodic period between Earth and Venus is 1.6 years, and the synodic period between Earth and Jupiter is 1.09 years.

For an initial Venus flyby (EVEJN, EVEJSN), we considered that the minimum flyby altitude at Venus is $0.3 \times 10^3 km$. When the launch ΔV decreases, the V_∞ at Venus also decreases.

Considering an initial Jupiter flyby, look that when the spacecraft have a flyby altitude at Jupiter of $4.22 \times 10^5 km$ (EJN scheme and time of flight of 12 years), the launch ΔV decreases, but the excess velocity in Jupiter increases.

For an Earth–Neptune direct transfer, when the launch ΔV decreases, the V_∞ at Neptune also decreases. This is the result of low energy launch, however, this is sufficient for arrival at Neptune. For the Earth–Jupiter–Neptune scheme, the transfer angle E-J undergoes to a decrease in the time interval considered. This is possible for the planetary configuration and for the initial conditions, however Jupiter is capable of the largest transfer angles for a given excess velocity due to its great mass. Following an initial Jupiter flyby (Earth-Jupiter-Saturn-Neptune), the transfer angle is too high and it decreases in the time interval considered. The others transfer angles are quasi-constant (J-N, J-S, S-N).

The launch ΔV for the Earth–Saturn–Neptune option also decreases, and the transfer angle E-S also decreases. This angle have the largest value for the excess velocity. The Saturn–Neptune angle is quasi-constant. For the Earth–Venus–Earth–Jupiter–Neptune and Earth–Venus–Earth–Jupiter–Saturn–Neptune schemes, the transfer angle E-V decreases, however the others transfer angles are quasi-constant. The transfer angle of V-E is high. The exploration of our outer solar system can also be increased by taking advantage of asteroid flyby opportunities, when the spacecraft passes through the asteroid belt. To incorporate an asteroid flyby, we first need to optimize a trajectory to Neptune with planetary flybys and then search for asteroids that pass close to this trajectory, to finally reoptimize the trajectory including one or more asteroid flybys.

3 Conclusions

In this paper, two important parameters, namely the minimum total ΔV and the excess velocity near Neptune V_∞ were obtained as functions of the launch date and flight duration. These two parameters determine the fuel consumption to launch from LEO, midcourse and to brake the spacecraft near Neptune, respectively. However, the braking near Neptune, in principle, can be performed using an aerobraking maneuver, so the launch ΔV was considered the most important parameter. Remember that in this paper an active braking was not used. The EJN scheme provides minimum total ΔV for the transfer duration with less than 14 years. This scheme also gives relatively low V_∞. For longer transfers the EVEJSN scheme is optimal in terms of minimum total ΔV, however V_∞ is high in this scheme. The EJN and EVEJSN schemes are most acceptables. If the transfer duration is limited by the time of 14 years or less, the EJN scheme is preferable in all respects. The EVEJSN scheme is getting preferable for transfers longer than 14 years.

Acknowledgments

The authors are grateful to CAPES (Coordenação de Aperfeiçoamento de Pessoal de Nível Superior), to the São Paulo State Science Foundation (FAPESP) for the research grant received under Contract 2003/03262-4 and 2007/04232-2, to the CNPq (Brazilian National Council for Scientific and Technological Development) for the contract 300221/95-9 and 308294/2004-1.

References

[1] Hammel, H.B. et al. Exploration of the Neptune System 2003-2013. *The Future of Solar System Exploration ASP Conference Series*, **272** (2002).

[2] Labunsky, A.V., Papkov, O.V., Sukhanov, K.G. *Multiple Gravity Assist Interplanetary Trajectories.* Earth Space Institute book series, 1998.

[3] Sukhanov, A.A. Close approach to Sun using gravity assists of the inner planets. *Acta Astronautica* **45** (1999) 175–185.

Nonlinear Dynamics and Systems Theory, 8 (2) (2008) 213–216

A Note on a Generalization of Sturm's Comparison Theorem

J. Tyagi * and V. Raghavendra

Department of Mathematics and Statistics, Indian Institute of Technology Kanpur, Kanpur - 208016, India

Received: February 25, 2007; Revised: November 30, 2007

Abstract: In this note, an attempt is made to generalize the Sturm's comparison theorem. Let t_1 and t_2 be two consecutive zeros of a solution y of an implicit equation

$$g_1(y''(t)) + r(t)g_2(y(t)) = 0$$

and x be a solution of

$$f_1(x''(t)) + q(t)f_2(x(t)) = 0.$$

Under certain conditions stated on the given functions f_1, f_2, g_1, g_2, q and r, we show that x has a zero between t_1 and t_2. Sturm's comparison theorem turns out to be a consequence of the established result.

Keywords: *Implicit differential equations; comparison theory.*

Mathematics Subject Classification (2000): 34C10, 34A09.

1 Introduction

Sturm's comparison theorem plays an important role in the theory of oscillations. In this note an attempt is made to generalize the Sturm's comparison theorem. Let f_1, f_2, g_1 and $g_2 \in C(\Re, \Re)$ and $q, r \in C(\Re^+, \Re)$ be given functions. Let x and y be solutions of the implicit second order equations

$$f_1(x''(t)) + q(t)f_2(x(t)) = 0, \tag{1.1}$$

$$g_1(y''(t)) + r(t)g_2(y(t)) = 0. \tag{1.2}$$

In this note, we assume the existence of solutions x and y of (1.1) and (1.2) on $J = [0, \alpha]$, $\alpha > 0$. Under certain conditions on f_1, f_2, g_1, g_2, q and r, we establish that between any two consecutive zeros t_1, t_2 of y, there is a zero of x, where $[t_1, t_2] \subseteq J$. Hypotheses along with the main result are stated in Section 2. Section 3 is devoted to a few consequences and examples of this result.

* Corresponding author: jagmohan.iitk@gmail.com

2 Main Result

This section deals with the main result. Let $f_1,\ f_2,\ g_1$ and $g_2 \in C(\Re, \Re)$ and $q, r \in C(\Re^+, \Re)$. We need the following hypotheses for further study

$$\mathbf{H_1}: \qquad \min_{0\neq u\in\Re} \frac{g_1(u)}{u} \geq \max_{0\neq u\in\Re} \frac{f_1(u)}{u},$$

$$\mathbf{H_2}: \qquad \min_{0\neq u\in\Re} \frac{f_2(u)}{u} \geq \max_{0\neq u\in\Re} \frac{g_2(u)}{u},$$

$$\mathbf{H_3}: \quad uf_1(u) > 0, \ \ ug_2(u) > 0, \ \ \forall\, 0 \neq u \in \Re.$$

Theorem 2.1 *Let x and y be nontrivial solutions of (2.1) and (2.2) respectively.*

$$f_1(x''(t)) + q(t)f_2(x(t)) = 0. \tag{2.1}$$

$$g_1(y''(t)) + r(t)g_2(y(t)) = 0. \tag{2.2}$$

Assume that the hypotheses $H_1 - H_3$ hold. Let t_1, t_2 be consecutive zeros of y and $q(t) > r(t) > 0$ for $t \in I = (t_1, t_2)$. Then, x vanishes at least once on I.

Proof By hypothesis, $y(t_1) = 0 = y(t_2)$ and $y(t) \neq 0$, $\forall\, t \in I$. Suppose $x(t) \neq 0$, $\forall\, t \in I$. Suppose if, $y''(t) = 0$ for some $t \in I$, then from H_1, H_3 and (2.2), we have $g_2(y(t)) = 0$ as well, but this contradicts the non vanishing of $y(t)$ in I. So $y''(t) \neq 0$, $\forall\, t \in I$. Similarly $x''(t) \neq 0$, $\forall\, t \in I$. From H_1–H_3, we have

$$g_1(y''(t))/y''(t) \geq f_1(x''(t))/x''(t) > 0, \quad \forall\, t \in I$$
$$\text{and} \quad f_2(x(t))/x(t) \geq g_2(y(t))/y(t) > 0, \quad \forall\, t \in I.$$

From the above two inequalities and since $1/r(t) > 1/q(t) > 0$, for all $t \in I$, we have

$$\frac{y(t)g_1(y''(t))}{g_2(y(t))r(t)y''(t)} > \frac{x(t)f_1(x''(t))}{q(t)f_2(x(t))x''(t)}. \tag{2.3}$$

Define $m(t) = x(t)y'(t) - x'(t)y(t),\ t \in I$. Then, $m'(t) = x(t)y''(t) - x''(t)y(t)$.

Case 1. $x(t) > 0,\ y(t) > 0$ on I.

In this case, $m(t_1) > 0,\ m(t_2) < 0$. This implies that

$$m(t_2) - m(t_1) < 0. \tag{2.4}$$

From (2.1) we have,

$$f_1(x''(t)) < 0, \quad t \in I.$$

The sector condition H_3 on f_1 now implies $x''(t) < 0$ for all $t \in I$. Similarly $y''(t) < 0$ for all $t \in I$. We notice that

$$m'(t) = -\frac{x(t)f_1(x''(t))y''(t)}{q(t)f_2(x(t))} + \frac{y(t)g_1(y''(t))x''(t)}{g_2(y(t))r(t)} \quad \forall\, t \in I. \tag{2.5}$$

By (2.3), we have $m'(t) > 0,\ t \in I$,

$$m(t_2) - m(t_1) > 0. \tag{2.6}$$

Inequalities (2.4) and (2.6) lead to a contradiction. Thus, x vanishes at least once between t_1 and t_2. The cases when $x(t) > 0,\ y(t) < 0;\ x(t) < 0,\ y(t) > 0;\ x(t) < 0,\ y(t) < 0$ are similarly dealt. These proofs are omitted for brevity. ☐

Remark 2.1 When f_1, f_2, g_1 and g_2 are identity functions, the celebrated Sturm's comparison theorem is a particular case of Theorem 2.1, see [3, 4]. Theorem 2.1 can also be viewed as a nonlinear version of the Sturm's comparison theorem.

3 A Few Consequences

This section primarily deals with consequences concerning Theorem 2.1. We observe that the hypotheses H_1 and H_2 can be relaxed. Let $S_1 = \{x(t) : \ t \in I\}, \ S_2 = \{y(t) : \ t \in I\}$ and $S \supseteq S_1 \cup S_2$. Then the condition in H_1 and H_2, we can replace $u \in \Re$ by $u \in S$. In practice it is hard to figure out what S is? For nonlinear equations these conditions could be impracticable unless we have a prior bounds on the solutions. Secondly, none of the condition have monotonicity criteria, see [1, 2] but sector condition is a part and parcel of it. Thirdly, we can derive results by comparing the implicit equations with an explicit equation for nonoscillation also, as shown below,

Proposition 3.1 *Let y be any nontrivial solution of*

$$y''(t) + f(y''(t)) + \frac{1}{5t^2}y(t) = 0, \ \ t > 0, \tag{3.1}$$

where, $f : \Re \to \Re$ be any continuous function satisfying $uf(u) > 0, \forall \ 0 \neq u \in \Re$. Then (3.1) is non oscillatory.

Proof Consider the differential equation

$$x''(t) + \frac{1}{4t^2}x(t) = 0. \tag{3.2}$$

(3.1) and (3.2) can be identified as (2.2) and (2.1) respectively, with $f_1(u) = u = f_2(u) = u, \ \ q(t) = \frac{1}{4t^2}, \quad g_1(u) = u + f(u), \ uf(u) > 0, \ \ \forall \ 0 \neq u \in \Re, \ g_2(u) = u, \ \ r(t) = \frac{1}{5t^2}$. Equation (3.2) is nonoscillatory, as $y(t) = t^{\frac{1}{2}}$ is a solution of (3.2). It is easy to see that f_1, f_2, g_1 and g_2 satisfy the hypotheses $H_1 - H_3$. So, Theorem 2.1 implies that (3.1) is nonoscillatory.

Proposition 3.2 *Let x be any nontrivial solution of*

$$x''(t) + 2(k^2x(t) + f(x(t))) = 0, \tag{3.3}$$

where, $f : \ \Re \to \Re$ be any continuous function satisfying $uf(u) > 0$ for all $0 \neq u \in \Re$, $k > 0$. Then (3.3) is oscillatory.

Proof Consider the differential equation

$$y''(t) + \frac{k^2}{4}y(t) = 0. \tag{3.4}$$

With $f_1(u) = u, \ f_2(u) = k^2u + f(u), \ uf(u) > 0, \forall\, 0 \neq u \in \Re, \ g_1(u) = u, \ g_2(u) = \frac{k^2}{4}u$, $q(t) = 2, \ r(t) = 1$ (3.3) and (3.4) can be identified as (2.1) and (2.2). It is easy to see that f_1, f_2, g_1 and g_2 satisfy the hypotheses H_1–H_3. So, Theorem 2.1 implies that x vanishes between any two consecutive zeros of $y(t) = \sin \frac{k}{2}t$. Since (3.4) is oscillatory. So, by Theorem 2.1, (3.3) is oscillatory. □

Remark 3.1 In proving (3.3) is oscillatory, we are using conditions different from what has been used in [1, Remark 1] and [2].

Example 3.1 Consider the differential equations

$$f_1(x''(t)) + q(t)f_2(x(t)) = 0, \tag{3.5}$$
$$g_1(y''(t)) + r(t)g_2(y(t)) = 0, \tag{3.6}$$

where, $f_1(u) = ue^{-|u|}$, $f_2(u) = u$, $q(t) = e^{-|\sin t|}$, $g_1(u) = u = g_2(u)$, $r(t) = e^{-1}$. Then, $x(t) = \sin t$ satisfies (3.5). Compare this with the equation

$$y''(t) + r(t)y(t) = 0,$$

with the solution $y(t) = \sin(t/\sqrt{e})$ on $[0, \pi\sqrt{e}]$. It is trivial to check that f_1, f_2, g_1 and g_2 satisfy the hypotheses $H_1 - H_3$. Also $q(t) > r(t) > 0$. Theorem 2.1 implies that not only must $\sin t$ vanish in $[0, \pi\sqrt{e}]$, which is clear, but also so must every other nontrivial solution of (3.5).

Example 3.2 Consider the differential equations

$$f_1(x''(t)) + q(t)f_2(x(t)) = 0, \tag{3.7}$$
$$g_1(y''(t)) + r(t)g_2(y(t)) = 0, \tag{3.8}$$

where $f_1(u) = u$, $f_2(u) = ue^{|u|}$, $q(t) = 2$, $g_1(u) = u = g_2(u)$, $r(t) = 1$. Here f_1, f_2, g_1 and g_2 satisfy the hypotheses H_1–H_3. Also $q(t) > r(t) > 0$. Let x be a nontrivial solution of (3.7). Then, Theorem 2.1 implies that x vanishes at least once between any two consecutive zeros of $y(t) = \sin t$. Since (3.8) is oscillatory, so (3.7) is oscillatory.

Acknowledgement

The first author is thankful to Council of the Scientific and Industrial Research, India, for providing him financial assistance to pursue his research.

References

[1] Man Kam Kwong and Wong, J.S.W. An application of integral inequality to second order nonlinear oscillation. *J. Diff. Eqns* **46** (1982) 63–77.

[2] Wong, P.J.Y. and Agarwal, R.P. Oscillatory behavior of solution of certain second order nonlinear differential equations. *J. Math. Anal. Appl.* **198** (1996) 337–354.

[3] Lakshmikantham, V., Deo, S.G. and Raghavendra, V. *Ordinary Differential Equations.* TMH, India, 1997.

[4] Simmons, G.F. *Differential Equations with Applications and Historical Notes.* TMH, 1974.

Cambridge Scientific Publishers

An International Book Series

Stability, Oscillations and Optimization of Systems

Modern stability theory, oscillations and optimization of nonlinear systems developed in respond to the practical problems of celestial mechanics and engineering has become an integral part of human activity at the end of XX century.

If, for a process or a phenomenon, for example, atom oscillations or a supernova explosion, a mathematical model is constructed in the form of a system of differential equations, the investigation of the latter is possible either by a direct (numerical as a rule) integration of the equations or by its analysis by qualitative methods.

In XX century the fundamental works by Euler (1707 – 1783), Lagrange (1736 – 1813), Poincaré (1854 – 1912), Lyapunov (1857 – 1918) and others have been thoroughly developed and applied in stability and oscillations investigation of nature phenomena and solution of many problems of technical progress.

In particular, the problems of piloted space flights and those of astrodynamics were solved due to modern achievements of stability theory and motion control. The Poincaré and Lyapunov methods of qualitative investigation of solutions to nonlinear systems of differential equations in macro-world study have been refined to a great extend though not completed. On the other hand modeling and establishing stability conditions for micro-processes are still on the stage of accumulating ideas and facts and forming the principles. One of the examples is the fact that the stability problem of thermonuclear synthesis has not been solved yet.

Obviously, this is one of the areas for application of stability and control theory in XXI century. For the development of efficient methods and algorithms in this area the interaction and spreading of the ideas and results of various mathematical theories will be necessary as well as the co-operation of scientists specializing in different fields.

The mathematical theory of optimal control (of moving objects, water resources, global process in world economy, etc.) is being developed in terms of basic ideas and results obtained in 1956 – 1961 and formulated in the Pontryagin's principle of optimality and Bellman's principle of dynamical programming. Considering manufacturing and production engineering activities, due to the difficulties of description of discrete events and hybrid processes, various heuristic and soft computing approaches have been developed for solving optimization problems. The efforts of many scholars and engineers in the framework of these ideas resulted in the efficient methods of control for many concrete systems and technological processes.

Thus, the development of classical ideas and results of stability and control theory remains the principle direction for the scholars and experts at modern stage of the mathematical theories. This fact will be demonstrated in the International Series **Stability, Oscillations and Optimization of Systems** by Cambridge Scientific Publishers Ltd.

Stability, Oscillations and Optimization of Systems provides a medium for the publication of high quality original monographs in the following areas:

Development of the theory and methods of stability analysis:

A. Stability Theory (ordinary differential equations, partial differential equations, stochastic differential equations, functional differential equations, integral equations, difference equations, etc.)
B. Dynamical Systems and Ergodic Theory (bifurcations and singularity, critical point theory, polystability, etc.)

Development of methods of the theory of nonlinear oscillations:
A. Analytical methods.
B. Qualitative methods.
C. Topological methods.
D. Numerical and computational methods, etc.

Development of the theory and methods of optimization of systems:
A. Optimal control of systems involving ODE, PDE, integral equations, equations with retarded argument, etc.
B. Minimax problems and nonsmooth analysis.
C. Necessary and sufficient conditions for optimality.
D. Hamilton-Jacobi theories.
E. Methods of successive approximations, etc.
F. Heuristics and metaheuristics for the optimization of ill defined and complex systems.

Applications:
A. Physical sciences (classical mechanics, including fluid and solid mechanics, quantum and statistical mechanics, plasma physics, astrophysics, etc.).
B. Engineering (mechanical engineering, aeronautical engineering, electrical engineering, chemical engineering).
C. Mathematical biology and life sciences (molecular biology, population dynamics, theoretical ecology).
D. Complex systems (synchronization, information and self-organization, collective dynamics, spatiotemporal chaos, biological and neural networks).
E. Manufacturing and production engineering.
F. Social sciences (economics, philosophy, sociology).

In the forthcoming publications of the series the readers will find fundamental results and survey papers by the experts from the worldwide which sum up the results of investigations in many directions of stability and control theory including uncertain and hybrid systems and systems with chaotic behavior of trajectories.

It is in this spirit that we see the importance of the **Stability, Oscillations and Optimization of Systems** series, and we are immensely thankful to Cambridge Scientific Publishers, Ltd. for their interest and cooperation in publishing this series.